B2.IV Nuclear and Particle Physics

A.J. Barr

February 13, 2014

Contents

Chapter 1

Introduction

When the great American physicist and bongo-drums player, Richard Feynman, was asked to think of a single sentence that would convey the most important scientific knowledge, he answered simply: 'Everything is made of atoms.'

Richard Feynman having fun.

Our understanding of matter at the atomic scale has made possible much of modern life, with its the mobile phones, computers and communications technology. Technologies from semiconductors, lasers, displays, and materials developments all require knowledge of how atoms behave and interact. The fundamentals of chemistry, drug development and biochemistry all rely on that fundamental insight. But we also know that atoms are not fundamental, and not indivisible; smaller structures exist inside.

The discovery of the atomic nucleus within the atom had profound consequences. The implications were not initially obvious; indeed the pioneering New Zealand nuclear physicist, Ernst Rutherford, reportedly said that the idea of getting practical energy out of the atomic nucleus was 'moonshine'.[1] Later in the 20^{th} century, theory and experiment on nuclear structure allowed us to understand the energy source of stars (including the sun), the most violent supernovae, the heating of the earth, and even the method of formation of the chemical elements around us. More immediately, fission power stations continue to provide the greatest contribution to low-carbon electricity in the UK, generating 18% of electricity in the UK and as much as 75% in France.

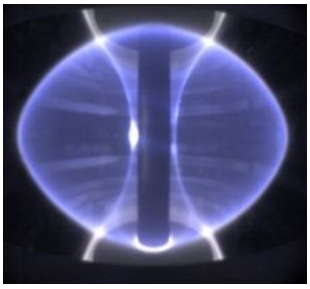

The plasma inside the MAST tokamak reactor runs at temperatures of up to 3,000,000 K.

Like fission, the physics of nuclear fusion (combining nuclei) has been understood for decades. The nuclear physics is not an area of current research in the field of nuclear physics, but future developments in controlling the plasma in which fusion occurs will be needed if we are to unlock the potential of this almost inexhaustible source of energy. Large-scale experimental facilities at the Culham Laboratory in Oxfordshire and the ITER fusion prototype plant in France are investigating ways to control high-energy plasmas for long times.

Today the physics questions about the fundamental make-up of forces and matter

[1] He turned out to be right, in a way, since the moonlight has since been understood to originate from fusion of hydrogen to helium inside the sun. It's perhaps unlikely that this is what he intended.

have moved on. We observe the most basic building blocks of nature to be point-like constituents . the quarks, leptons, making up matter, and with gauge bosons as the force-carrying particles. The experimental observations are described to amazing accuracy by the Standard Model of particle physics, a theoretical triumph of relativistic quantum field theory that correctly predicts the gyromagnetic ratio of the electron to an accuracy of one part in a trillion.

Laboratory measurements, together with a mathematical formalism, let us enquire into the nature of the vacuum, and into the dense and hot conditions of the universe a fraction of a second after its birth. They are also providing insights into the reasons why matter dominates over anti-matter, and the origins of mass. Performing experiments length scales and higher energies than ever before requires the invention of new technologies. The technologies of the future will, no doubt, grow out of our current areas of research. At the same time, spin-offs are already affecting the wider world. Perhaps the most remarkable invention of our era, the World Wide Web, was developed by Queens college graduate Tim Berners Lee when working at CERN in order to help physicists collaborate on designing and building the LHC. The technologies developed for current particle physics experiments have been used in medical imaging, climate forecasting, decoding the human genome, nuclear anti-proliferation, cancer treatment, information analysis and drug development.

The first web server. When Tim Berners Lee wrote his proposal for the World Wide Web it was annotated by his manager 'vague but interesting'.

Recently the LHC has opened up a new field by discovering a completely new type of particle. Observations suggest it is remarkably similar to the 'Higgs boson' of the Standard Model. This apparently fundamental spin-0 particles, and is only just starting to be investigated and understood. It is almost certainly the manifestation of entirely new fundamental force of nature, different from all of the others observed until now. Much about that force has not yet been investigated. To understand the properties of that force will require a long programme at a high-energy LHC and most likely new facilities and new ideas.

Many other experimental and theoretical questions remain open. The properties of neutrinos, are only now starting to be probed with precision. Soon we may know whether or not neutrinos are their own anti-particles. Other crucial differences between matter and anti-matter, differences essential to our existence, are being studied with ever greater detail in the decays of hadrons.

Not dark matter.

The 'Dark Matter' particle, believed to be responsible for the missing 80% of the matter in the universe, is being hunted by astroparticle and underground direct detection experiments. And it is hoped that future theories or experiments may throw light onto the enormous difference in strength between the forces.

New theories exist which can solve these problems. All predict the existence of new particles or phenomena, often within reach of either operating or proposed facilities. The close interplay of theory with experiment at the cutting edge of knowledge will be required if these new phenomena are to be predicted, measured and added to the canon of human knowledge.

Chapter 2

Nuclear physics and decays

2.1 Structure of matter and energy scales

Subatomic physics deals with objects of the size of the atomic nucleus and smaller. We cannot see subatomic particles directly, but we may obtain knowledge of their structures by observing the effect of projectiles that are scattered from them. The resolution any such probe is limited to of order the de Broglie wavelength,

$$\lambda = \frac{h}{p} \tag{2.1}$$

where h is Planck's constant, and p is the momentum of the projectile. If we wish to resolve small distances, smaller than the size of the atom, we will need to do so with probes with high momenta. Smaller objects also tend to have larger binding energies holding them together, so require larger energies to excite their internal components. Some typical sizes of objects are given below, together with the momementum of the projectile required to resolve their size, and typical binding energies in electron-volt (eV) units.

keV	10^3 eV
MeV	10^6 eV
GeV	10^9 eV
TeV	10^{12} eV

Object	Size	$p = \frac{h}{\lambda}$	Binding energy
Atom	10^{-10} m	$10\,\mathrm{keV}/c$	$\sim$ eV
Nucleus	$\sim 10^{-15}$ m	$1\,\mathrm{GeV}/c$	$\sim$ MeV
Quark	$< 10^{-19}$ m	$>$ TeV$/c$	$>$ TeV

We can see that small objects also tend to have high binding energies, and hence probes of large energy will be required in order to excite them or break them up. The momenta are indicated in units of eV$/c$ where c is the speed of light. These units make it easy to compare the momentum of the projetile to its corresponding energy $E = pc$ for the case of a massless probe such as a photon. The most convenient unit for describing the size of nuclei is the femtometer 10^{-15} m.[1] No sub-structure has yet been found for quarks even when using very high energy (TeV) probes.

[1] The unit of 10^{-15} m or femtometer is sometimes called the 'fermi' reflecting the many seminal contributions of the Italian physicist Enrico Fermi to the field of nuclear physics.

2.2 The Nuclear Periodic Table and Binding Energy

Nuclei are found to be made out of two constituents: protons and neutrons. We label nuclei by their **atomic number** Z which is the number of protons they contain, by their neutron number N, and by their **mass number** $A = Z + N$.

The symbol used to identify a nucleus is

$$^{\mathrm{A}}_{\mathrm{Z}}\mathrm{X}_{\mathrm{N}}$$

where X is the name of the chemical element. For example the Carbon-14 nucleus, which contains 8 neutrons and 6 protons is denoted $^{14}_{6}\mathrm{C}_{8}$. Since the element's name specifies the number of electrons, and hence the atomic number Z, and since $A = N + Z$, we can fully specify the nucleus by just the symbol for the chemical and the mass number,

$$^{\mathrm{A}}\mathrm{X} \quad \text{e.g.} \quad ^{14}\mathrm{C}.$$

Isotopes	Same Z
Isotones	Same N
Isobars	Same A

Notation for related nuclei

Most nuclei are spherical in shape. The nuclear radius r can be measured in scattering experiments, and follows the general rule

$$\boxed{r = r_0 A^{1/3}} \tag{2.2}$$

where the constant r_0 is the characteristic nuclear size and is about 1.2×10^{-15} m. The fact that r is proportional to $A^{1/3}$ indicates that the volume of the nucleus $V \propto r^3$ is proportional to the mass number A. Each proton or neutron is therefore making an equal contribution to the overall nuclear volume.

2.2.1 Binding energy and the semi-empirical mass formula

The mass $m(A, Z)$ of the nucleus containing Z protons and $A - Z$ neutrons should be given by the mass of its consituents, less the mass associated with the binding energy. The mass-energy is therefore

$$m(A, Z)c^2 = Zm_p c^2 + (A - Z)m_n c^2 - B(A, Z), \tag{2.3}$$

where $m_p \approx 938.3\,\mathrm{MeV}/c^2$ and $m_n \approx 939.6\,\mathrm{MeV}$ are the masses of the proton and neutron respectively. In nuclear physics it is convenient to measure energies in units of MeV and masses in units of MeV/c^2. Using these units makes it easy for us to convert from mass to mass-energy and vice versa. By assuming such units, we can omit the factors of c^2 in what follows. [2]

We can build up a functional form for the binding energy $B(A, Z)$ by considering the forces between the nuclear constituents. To find the full quantum mechanical ground state for all of the protons and neutrons would be a very difficult problem. However we can understand a great deal about nuclear behaviour by building up a model of the mass which encapsulates its key features. This we will do over the rest of the section, building up towards the **semi-empirical mass formula** of equation (2.5). The 'semi-empirical' means that the model is built partly partly by demanding agreement with data, and partly from our understanding of the underlying theory.

[2] For more on 'natural units' see appendix 2.A.

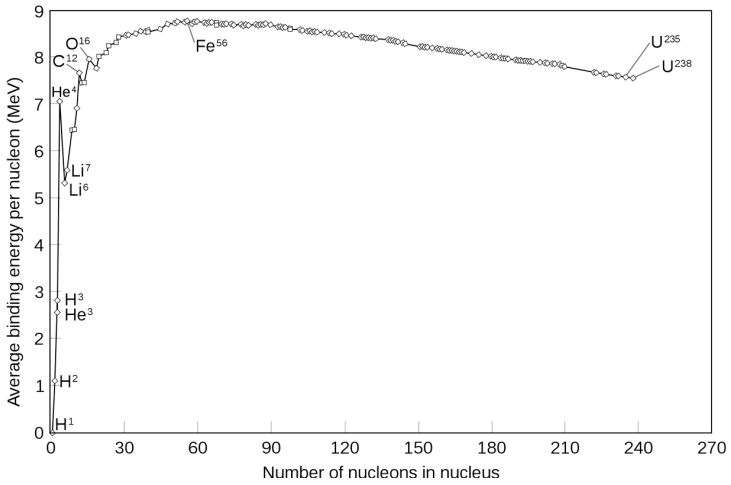

Figure 2.1: Binding energy per nucleon (B/A) as a function of A for some common nuclei. Data taken from [5]. Plot from [source].

Firstly, we will need an attractive force in order to hold the nucleus together against the mutual electrostatic replusion of its constituent protons. That force must be very strong, since the Coulomb electrostatic repulsion between a pair of protons, each of charge e and separated by distance $d \approx 1\,\text{fm}$, is

$$\begin{aligned} F &= \frac{e^2}{4\pi\epsilon_0\, d^2} \\ &\approx 230\,\text{N} \end{aligned}$$

which is macroscopic – comparable to the weight of a child.

What form should that nucleon-nucleon attractive force take? We can get clues about the force by looking at the binding energy per nucleon B/A is shown for some common nuclei, shown in Figure 2.1. For nuclei this binding energy is typically of order 8 MeV per nucleon. It can be seen that the most stable nuclei are found around ^{56}Fe. Different behaviours can be seen in different regions. There is a broad flattish plateau for the central region $30 < A < 200$ for which $B/A \approx 8\,\text{MeV}$. For A below about 30 the binding energy per nucleon is smaller than the plateau value and is spiky. There is a systematic drop in B/A for large A, particularly for $A > 200$.

To obtain a value of B/A that is rather flat, we cannot permit strong attractions between each of the constituent nucleons and every one of the others. If every nucleon felt an attraction to each of the others, then the binding energy would be expected to grow as approximately $B \propto A(A-1) \sim A^2$, and hence B/A would be approximately proportional to A. Such a linear growth in B/A is ruled out by the data (Figure 2.1).

To obtain the flat B/A found in nature we must assume that the strongly attractive force acts only between **nearest neighbour** nucleons. In this way, each nucleon binds to the same number of nearest neighbours, independently of the size of the nucleus, and hence the binding energy per nucleon is the same regardless of the

nuclear size,

$$B \approx \alpha A$$

where α is a constant with units of energy. The use of nearest-neighbour interactions indicates that the force must either be short-range, or screened from long-range interactions by the effects of the nucleons in between.

In modelling a nearest-neighbour force we ought to make a correction for the fact that those nucleons on the surface have fewer neighbours. To correct for the reduced number of binding opportunities on the surface we reduce the binding energy by an amount proportional to the surface area, leading to the corrected formula

$$B \approx \alpha A - \beta A^{\frac{2}{3}}. \tag{2.4}$$

The new contribution is negative since it reduces the binding energy. We have made use of the observation (2.2) that since the volume of the nucleus scales as $r^3 \propto A$, the surface area scales as $r^2 \propto A^{2/3}$.

These two terms (2.4) in this first approximation to the binding energy are known as the **volume term** and the **surface term** respectively. Together they form what is known as the **liquid drop model**, since a similar result would be found for a drop of fluid with nearest neighbour interactions and a surface tension parameterised by β. The liquid drop model is consistent with the observation that each nucleon requires the same volume of space, in agreement with equation (2.2).

So far, so good. However there is nothing in this liquid drop model to prevent the growth of arbitrarily large nuclei. Such large nuclei are not observed in nature, so we must be missing something. The obvious candidate is the **Coulomb repulsion**, which interacts over long distances, and so will tend to push larger nuclei apart. This electrostatic repulsion between protons will reduce the binding energy by an amount proportional to $Z(Z-1) \approx Z^2$ because every proton feels the repulsion from all of the other protons (not just nearest neighbours). The binding energy will be reduced by the electrostatic binding energy which can be parameterised by

$$\epsilon \frac{Z^2}{A^{\frac{1}{3}}}.$$

Here ϵ is a another constant with dimensions of energy, which we will calculate a value for in the examples. The Coulomb repulsion energy is inversely proportional to the radius of the nucleus, and hence to $A^{\frac{1}{3}}$, since the potential energy of a uniform sphere of charge Q is proportional to Q^2/r.

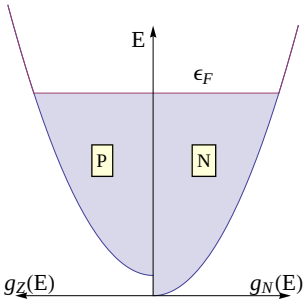

The density of states $g(E)$ for protons and neutrons as a function of energy E.

Two further terms are required to give a good match between our model and the data. Both of them are quantum mechanical in origin.

Firstly there is an **asymmetry term**. The origin of this term is as follows. Since protons are identical fermions, the Pauli exclusion principal states that no two of them may exist in the same state. Nor may any neutron occupy the same state as any other neutron. However it is possible for a proton and a neutron to exist in the same state since the two particles are not identical. The allowed states are therefore distinct, and are separately filled for the protons compared to the neutrons.

We can work out the size of the asymmetry effect by calculating the number of states available. Neutrons and protons are both fermions, and so obey Fermi-Dirac

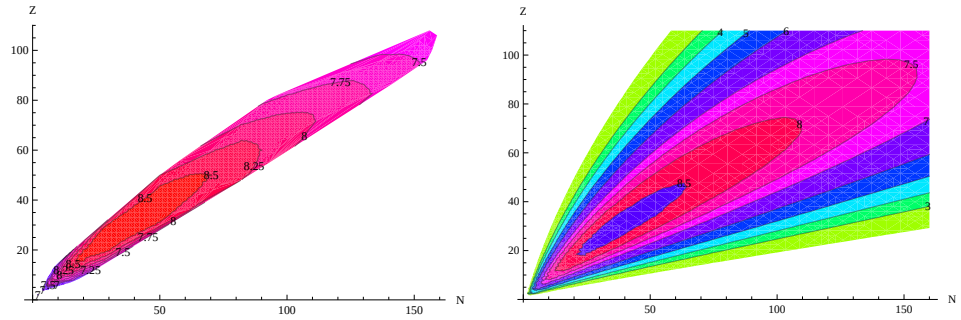

(a) **(a)**

Figure 2.2: Diagram showing binding energies as a function of proton and neutron number for **(a)** data [5] and **(b)** the Semi-Empirical Mass Formula.

statistics. The temperatures we are interested in are small compared to the chemical potential ($k_BT \ll \mu$). Under these circumstances the Fermi-Dirac distribution tends towards a step function — all levels are filled up to some energy level, known as the **Fermi Energy** ϵ_F, with all states with energy above ϵ_F left vacant.

$$p(E_i) = \frac{1}{e^{(E_i-\mu)/k_BT}+1}$$

The Fermi-Dirac function gives the probability $p(E_i)$ of filling a state with energy E_i for a system at temperature T and with chemical potential μ. k_B is the Boltzmann constant.

At large mass number A the Coloumb repulsion term would tend to favour larger N and smaller Z, since neutrons do not suffer from the Coulomb repulsion as protons do. However this energic advantage of neutrons over protons will be partially cancelled out by the fact that the additional neutrons must (on average) be placed in higher energy levels than additional protons, since all of the lower-energy neutron states will already be filled.

The density of available states is found to be proportional to $E^{\frac{1}{2}}$. In the examples we show that this leads to an energy equation of the form

$$\gamma\frac{(N-Z)^2}{A}.$$

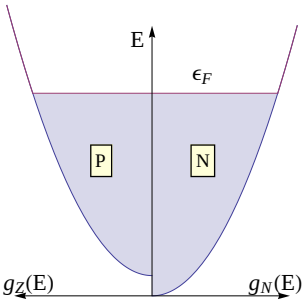

The density of states $g(E)$ for protons and neutrons as a function of energy E.

This **asymmetry term** reduces the binding energy, doing so most when the difference between the number of protons and of neutrons is largest.

Finally there is a **pairing term** which accounts for the observation that nuclei with either even numbers of protons (Z even) or with even numbers of neutrons (N even) tend to be more stable than those with odd nuclei. The pairing term is zero for odd-A nuclei. Even A nuclei have two possibilities. If both Z and N are even then the nucleus is more tightly bound and have an extra binding contribution, so B is increased by δ. If both Z and N are odd then the nucleus is less tightly bound and so B is decreased by δ.

N	Z	pairing term
even	even	δ
even	odd	0
odd	even	0
odd	odd	$-\delta$

Putting all five terms together we obtain a formula for the binding energy,

$$B(A,Z) = \alpha A - \beta A^{\frac{2}{3}} - \gamma\frac{(A-2Z)^2}{A} - \epsilon\frac{Z^2}{A^{\frac{1}{3}}} + \delta(A,Z),$$

having eliminated N in favour of A. Substituting this into the formula defining the

Volume	Surface	Asymmetry	Coulomb	Pairing
α	β	γ	ϵ	δ
15.835	18.33	23.2	0.71	$11.2/\sqrt{A}$

Figure 2.3: Typical values of the SEMF parameters (in MeV). From Bowler.

binding energy (2.3) we obtain the **semi-empirical mass formula** (SEMF)

$$M(A,Z) = Zm_p + (A-Z)m_n - \alpha A + \beta A^{\frac{2}{3}} + \gamma\frac{(N-Z)^2}{A} + \epsilon\frac{Z^2}{A^{\frac{1}{3}}} - \delta(N,Z). \tag{2.5}$$

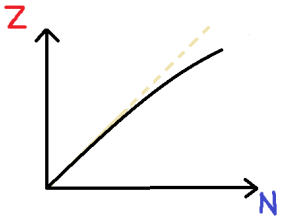

Sketch of the shape of the valley of stability.

Other than for $A < 30$, where our approximations are less valid, the SEMF gives a rather good description of the binding energies of the observed nuclei (Figure 2.2). In particular the SEMF correctly predicts the shape of the curved **valley of stability** in the Z, N plane within which the stable nuclei are found. The relative numbers of protons and neutrons along this valley reflects a trade-off between the Coulomb and asymmetry terms. At low A the asymmetry term favours $N = Z$. At larger A the Coulomb term starts to compete with the asymmetry term, reducing the ratio of protons to neutrons.

It is energetically favourable for nuclei far from that valley to migrate towards it by nuclear decay, in the ways we describe in the following section.

2.3 Decays and reactions

A table of the nuclides can be found in Figure 2.4. The stable long-lived nuclides lie along the valley of stability where the binding energy per nucleon is largest. The valley lies along $N \approx Z$ for light nuclei but has $N > Z$ for heavier nuclei. Nuclei far from that valley, and very heavy nuclei, tend to be unstable against nuclear decay.

While unstable nuclei will decay spontaneously, other reactions can be initiated by firing projectiles at a nucleus. Reactions are said to be **elastic** if the final state contains the same set of particles e.g. the elastic scattering of a photon from a nucleus, via an excited intermediate state:

$$X + \gamma \longrightarrow X^* \longrightarrow X + \gamma.$$

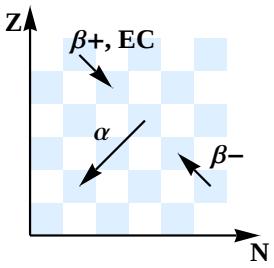

The changes in (Z, A) induced by various decays.

Reactions are **inelastic** if there is a change in particle content during the reaction e.g. radiative capture of a neutron

$$^{\mathrm{A}}\mathrm{X} + n \longrightarrow {}^{\mathrm{A+1}}\mathrm{X}^* \longrightarrow {}^{\mathrm{A+1}}\mathrm{X} + \gamma.$$

For all nuclear decays and reactions we define the Q value to be amount of energy 'released' by the decay,

$$Q = \sum M_i - \sum M_f$$

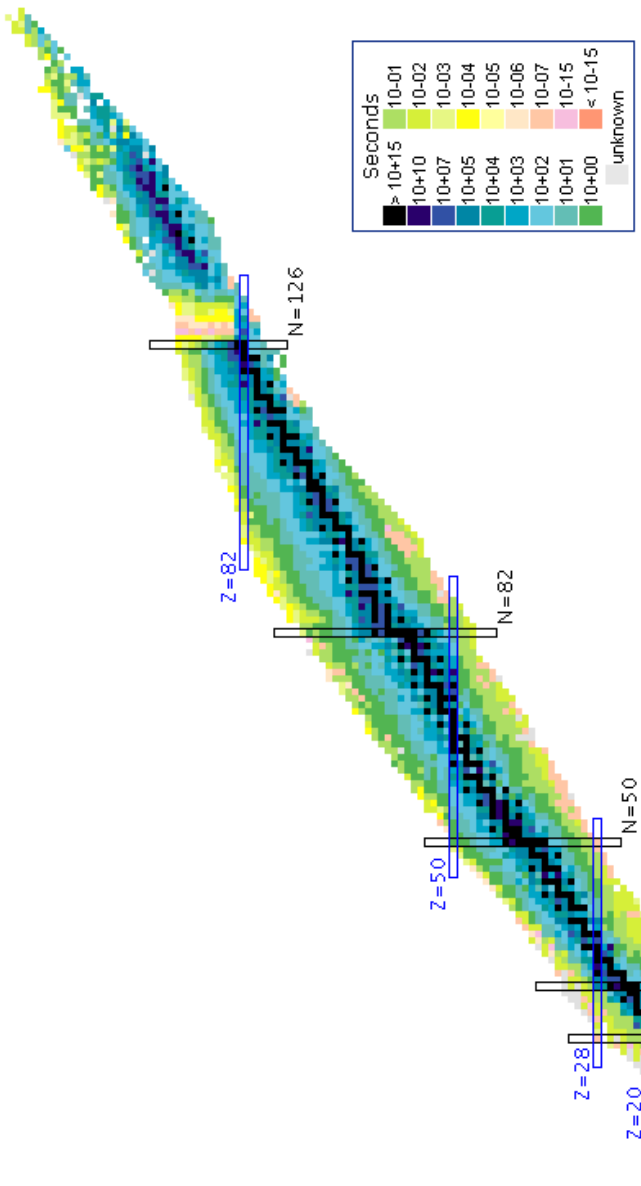

Figure 2.4: Table of the nuclides as a function of the number of neutrons (N, on the x-axis) and the number of protons (Z on the y-axis). Darker colours represent longer-lived nuclides, which can be found in the 'valley of stability'. The 'Magic Numbers' indicate particularly stable nuclei and are described in the shell model (see appendix 2.C). From http://www.nndc.bnl.gov/nudat2/.

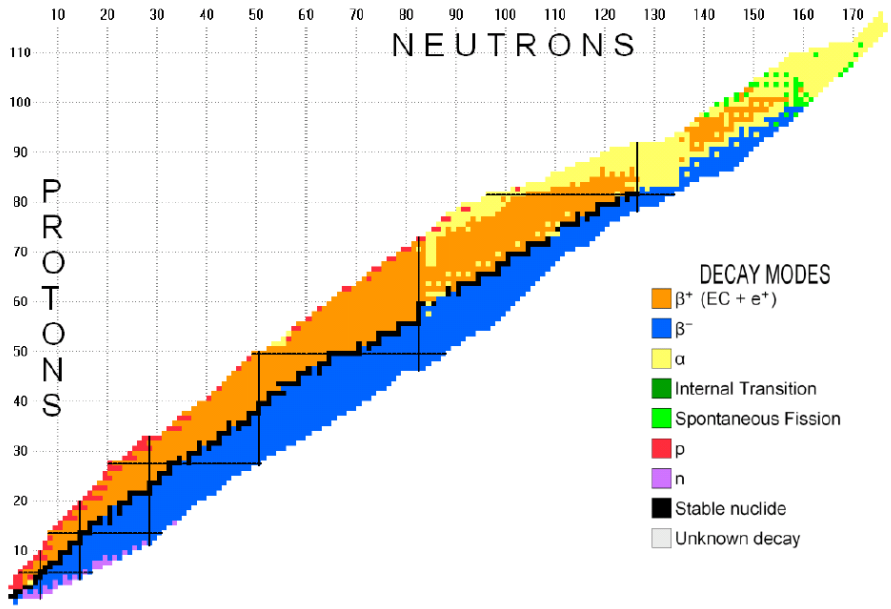

Figure 2.5: Decay modes of the nuclei. From [5].

The first sum is over the masses of the initial particles in the decay (including their binding energies), while the second sum is over the masses of the final-state particles (including their binding energies). A positive Q value shows that a reaction is energetically favourable.

2.3.1 Alpha Decays

Alpha decays occur when (usually heavy) nuclei eject an 'α particle', that is a helium nucleus containing two protons and two neutrons. The decay is

$$\boxed{{}^{\mathrm{A}}_{\mathrm{Z}}\mathrm{X} \longrightarrow {}^{\mathrm{A}-4}_{\mathrm{Z}-2}\mathrm{Y} + {}^{4}_{2}\mathrm{He}.}$$

The change of mass number of the heavy nucleus is $\Delta A = -4$ and the change in its atomic number is -2.

The process of decay of heavy nuclei is often via sequential chains involving both alpha and beta decays. Since $\Delta A = -4$ for α decays and $\Delta A = 0$ for β and γ decays we see that for any nucleus starting with mass number A (and if it only decays via alpha, beta or gamma decay processes) all other nuclei in that chain must have some other set of mass numbers $A' = A - 4m$, where m is an integer indicating the number of alpha decays that have occured.

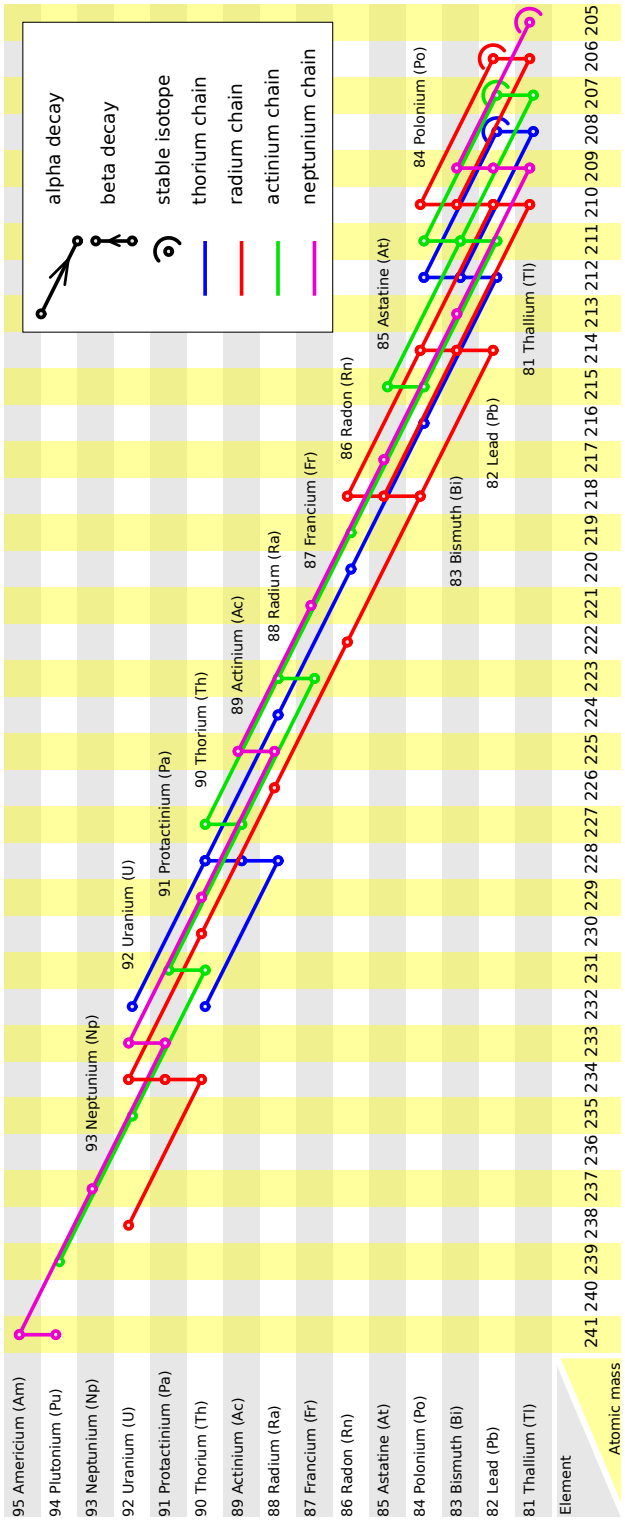

Figure 2.6: There are therefore *four* non-overlapping decay chains for the heavy elements, corresponding to $A = n$, $A = n+1$, $A = n+2$, and $A = n+3$ respectively, where n is an integer.

Rate calculation for α decays

We can model the α decay as a process in which 'proto α particles' are pre-formed inside the nucleus. Each is assumed to have a large number of collisions with the edge of the nucleus, but a small probability on each collision of **tunnelling** through the Coulomb barrier and escaping.

If the Q value of the decay is positive, then the decay is energetically favourable, but it may still be suppressed by a large tunnelling factor. Let us try to model the probability of tunnelling through the barrier. We will assume that the large exponential in the quantum tunnelling factor will dominate the calculation of the rate of decay, so we will neglect differences in the probability of formation of the proto-alpha particle, and its rates of hitting the barrier.

The time independent Schrödinger equation defines the energy eigenstate $|\Psi\rangle$,

$$E|\Psi\rangle = \left(\frac{p^2}{2m} + V\right)|\Psi\rangle.$$

where E is the energy of the alpha particle, p is the momentum operator, m is its mass, and V is the potential in which it moves.

For simplicity, we will ignore the spherical geometry and treat the problem as one-dimensional in the radial direction r so that for a state with energy Q,

$$Q\langle r|\Psi\rangle = \left(-\frac{1}{2m}\frac{\partial^2}{\partial r^2} + V(r)\right)\langle r|\Psi\rangle, \tag{2.6}$$

where we use natural units such that $\hbar = \frac{h}{2\pi} = c = 1$ (see appendix 2.A). In the Dirac notation $\langle r|\Psi\rangle$ represents the wave function — that is the amplitude to find the alpha particle located between r and $r + dr$. Without losing any generality we can write the wave function as the exponential of some other function $\eta(r)$,

$$\langle r|\Psi\rangle = \exp[\eta(r)]. \tag{2.7}$$

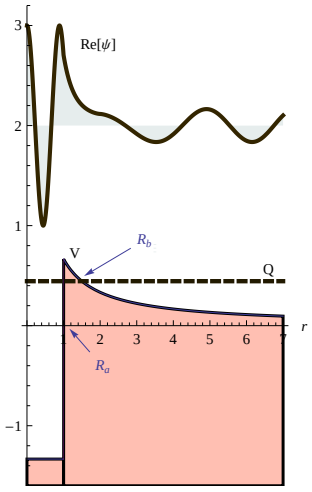

Real part of $\langle r|\Psi\rangle$ (as calculated in the WKBJ approximation) and $V(r)$ for a thin Coulomb potential barrier.

After inserting (2.7) into (2.6) and dividing by $\exp(\eta)$ we find

$$Q = -\frac{1}{2m}\left[\eta'' + (\eta')^2\right] + V(r),$$

where the primes indicate derivatives by r. We can model the potential $V(r)$ felt by any α particle by the function

$$V(r) = \begin{cases} \text{const} & r < R_a \\ \frac{zZ\alpha_{\text{EM}}}{r} & r > R_a \end{cases}$$

where inside the nucleus V is large and negative, and outside the nucleus it is given by the Coulomb potential and hence characterised by the charges z and Z of the α-particle and the daughter nucleus respectively. The constant α_{EM} in the Coulomb potential is the dimensionless electromagnetic fine structure constant

$$\alpha_{\text{EM}} = \frac{e^2}{4\pi\epsilon_0\hbar c} \approx \frac{1}{137}.$$

Within the barrier the potential is smoothly varying, so η should be a smoothly varying function of (r). We then expect $\eta'' \ll (\eta')^2$, and we can safely neglect the η'' term compared to the $(\eta')^2$.[3]

The tunnelling probability can be found from the ratio of the mod-squared amplitudes:

$$P = \frac{|\langle R_b|\Psi\rangle|^2}{|\langle R_a|\Psi\rangle|^2} = e^{-2G}.$$

where G (> 0) is given by

$$-G = \eta(R_b) - \eta(R_a) = -\sqrt{2m}\int_{R_a}^{R_b} dr\,\sqrt{V(r) - Q}.$$

The minus sign before the radical ensures that we select the exponentially falling solution. The inner limit of the integration is the radius of the nucleus

$$R_a \approx r_0 A^{\frac{1}{3}},$$

and the outer limit

$$R_b = \frac{Z_1 Z_2 \alpha_{\rm EM}}{Q},$$

the radius for which $Q > V$, i.e. where the α particle enters the classically allowed region.

2.3.2 Beta decays, electron capture

There are three related nuclear decay processes which are all mediated by the **weak nuclear interaction**. Neutron-rich isotopes can decay through the emission of an electron e and an anti-neutrino $\bar{\nu}_e$ in the **beta decay** a process:

$${}^{\rm A}_{\rm Z}{\rm X} \longrightarrow {}^{\rm A}_{\rm Z+1}{\rm Y} + e^- + \bar{\nu}_e. \tag{2.8}$$

The effect is to increase the atomic number by one, but to leave the mass number unchanged. At the level of the individual nucleons the reaction is

$$n \longrightarrow p + e^- + \bar{\nu}_e. \tag{2.9}$$

The emitted electron can be observed and its energy measured. The associated anti-neutrino has a very small interaction probability, and so is expected to escape unobserved. Long before neutrinos were observed, Wolfgang Pauli realised that an additional, invisible, massless particle was required in order to conserve energy and momentum in the decay (2.8). His arguments ran as follows. The emitted electrons are observed to have a variety of different kinetic energies, up to Q. Meanwhile the mass difference between the parent and daughter nucleus is fixed to a single value. The energy given to the recoiling daughter nucleus is small and is fixed by momentum conservation, so it can't be responsible for the deficit observed when the electron has energy less than Q. Energy conservation is then only possible if

[3] This is known as the WKBJ approximation. It is a good approximation if many wave-lengths (or in the classically forbidden regions, as here, many factors of $1/e$) of the wave-function occur before the potential changes significantly.

the total energy Q can be shared between the electron and some other unobserved partice – the (anti-)neutrino.

Pauli also argued that without the neutrino the reaction (2.9) would violate angular momentum conservation. Adding the angular momenta of just the two observed final state spin-half particles – the electron and the proton – according to the rules of quantum mechanical angular momentum addition we would find

$$\frac{1}{2} \oplus \frac{1}{2} = 0 \text{ or } 1.$$

Neither of the possibilities of total angular momentum $s = 0$ or $s = 1$ match the spin of the initial neutron, which has $s = \frac{1}{2}$. However by adding a third spin-half particle to the final state – the $s = \frac{1}{2}$ anti-neutrino – we can reconstruct a state which has total angular momentum equal to that of the proton ($s = \frac{1}{2}$) since

$$\frac{1}{2} \oplus \frac{1}{2} \oplus \frac{1}{2} = \frac{1}{2} \text{ or } \frac{3}{2}.$$

Isotopes which have a surplus of protons can proceed via one of two processes. The first is the emission of a positively charge anti-electron. This is known as **positron emission** or β^+ decay

$$^{\mathrm{A}}_{\mathrm{Z}}\mathrm{X} \longrightarrow {}^{\mathrm{A}}_{\mathrm{Z-1}}\mathrm{Z} + e^+ + \nu_e \tag{2.10}$$

The positron is the anti-particle of the electron. It has the same mass as the electron, but positive charge.

The second method of decay of proton-rich nuclei is by the nucleus removing one of the atomic electrons, the **electron capture** process:

$$^{\mathrm{A}}_{\mathrm{Z}}\mathrm{X} + e^- \longrightarrow {}^{\mathrm{A}}_{\mathrm{Z-1}}\mathrm{Z} + \nu_e \tag{2.11}$$

These two processes ((2.10) and (2.11)) result in the same change to the nucleus, and so compete with one another to reduce the Z number of proton-rich nuclei. When considering whether electron capture or β^+ decay will dominate we note that

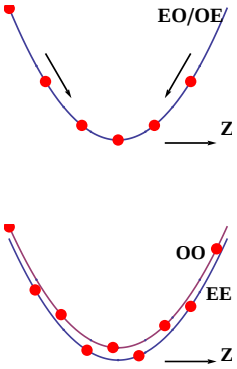

Mass as a function of Z for nuclides of the same A, for odd-A nuclei (above) and even-A nuclei (below). The even-A case has two curves separated by 2δ.

- The Q value for positron emission is $2 \times m_e c^2$ smaller than that for the corresponding electron capture.
- Electron capture relies on there being a substantial overlap of an electron wave-function with the nucleus.

When viewed at the level of the nuclear consitutents, all three of the interactions above — β decay (2.8), β^+ decay (2.10) and electron capture (2.11) — involve the interaction of four particles: a proton, a neutron, an (anti-)electron and an (anti-) neutrino.

$$n \longrightarrow p + e^- + \bar{\nu}_e \tag{2.12}$$
$$p \longrightarrow n + e^+ + \nu_e, \tag{2.13}$$
$$p + e^- \longrightarrow n + \nu_e. \tag{2.14}$$

We note that all of the reactions (2.12)–(2.14) are assumed to be occurring inside the complex environment of the nucleus. Of these three reactions, only neutron

decay (2.12) can occur in isolation, since it is the only one with $Q > 0$, (the neutron being about $1.3\,\text{MeV}/c^2$ heavier than the proton). The other two reactions (2.13)–(2.14) occur only within a nucleus, when the energy released from the rearrangement of the nuclear constituents is sufficient to compensate for the endothermic nature of the reaction at the level of the individual nucleon.

We note that all of three transitions — β^-, β^+, and e^- capture — leave the mass number A unchanged. The parent and daughter nuclei are isobars. The decay processes (2.12)–(2.14) allow transitions between isobars, and mean that for odd-A nuclei for any value of A there is usually only one stable isobar, that for which the mass of the system is minimum.

Even-A nuclei may have one stable isobar, but can also have two or very occasionally three. Multiple stable states are possible for A even because the binding curves for (even-Z, even-N) and (odd-Z odd-N) are separated by 2δ, where δ is the pairing energy in the SEMF. For an even-even nucleus, since all of the reactions (2.12)–(2.14) change both $|Z|$ and $|N|$ by one they result in an odd-odd nucleus, and so a transition to the higher of the two curves. None of the reactions permit a change in Z of two units, and the probability of two such reactions happening at once is extremely small, so an even-even nucleus with some Z can be stable provided that both the neighbouring nuclei with $Z + 1$ and $Z - 1$ have larger mass.

Fermi theory of beta decays

To understand the lifetimes of the nuclei, we wish to calculate the expected rates for $\beta^\pm$ decays. We follow the method and approximations of Enrico Fermi.

If we put the initial state particles on the left hand side of the diagram, and the final state particles on the right hand side, then we obtain the following three diagrams for the reactions (2.12)–(2.14).

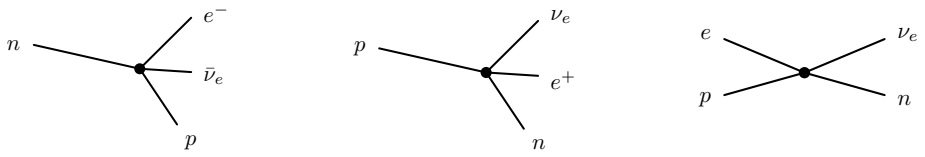

We shall assume that each of these four-particle interactions will happen at a single point in space. The amplitude for each reaction is given by the same constant — a four-body coupling constant which tells us the amplitude for each interaction at that point in space. For each of the three diagrams that coupling is the **Fermi constant**,

$$\boxed{G_F \approx 1.17 \times 10^{-5}\,\text{GeV}^{-2}}$$

which has units of inverse energy squared.

In using a single, constant factor, we implicitly make the simplifying assumption that the four-body interaction does not depend on the spins of the incoming or

outgoing particles. To simplfy calculations we will also follow Fermi in assuming that the wave-functions of the electron and the anti-neutrino can be represented by plane waves. This ignores the effect of the Coulomb attraction between the electron and the nucleus, and is a good approximation provided that the electron energy is sufficiently high.

We recall that in quantum mechanics, the rate of some a transition from an initial state to a final state characterised by a continuum of energy levels is given by the **Fermi Golden Rule**[4]

$$\Gamma = \frac{2\pi}{\hbar}|A_{fi}|^2 \frac{dN}{dE_f} \tag{2.15}$$

Here the transition rate Γ is given in terms of the amplitude A_{fi} connecting the initial and the final states, and the degeneracy $\frac{dN}{dE_f}$ of states at the final energy. It is the A_{fi} and $\frac{dN}{dE_f}$ that we shall have to calculate.

To be concrete, let us consider the beta decay reaction (2.12). We denote the initial nuclear wave-function by $\langle \mathbf{x}|\Psi_i\rangle$, the final nuclear wave-function by $\langle \mathbf{x}|\Psi_f\rangle$. The electron and anti-neutrino wave-functions are approximated as plane waves

$$\langle \mathbf{x}|\phi_e\rangle \equiv \phi_e = \exp\left(i\,\mathbf{p}_e \cdot \mathbf{x}\right) \tag{2.16}$$

$$\langle \mathbf{x}|\phi_\nu\rangle \equiv \phi_\nu = \exp\left(i\,\mathbf{p}_\nu \cdot \mathbf{x}\right). \tag{2.17}$$

We can now write down the initial state $|\Psi_i\rangle$, which is just that of the parent nucleus

$$|\Psi_i\rangle = |\psi_i\rangle,$$

and final state $|\Psi_f\rangle$, which is the product of the daughter nucleus state $|\psi_f\rangle$, the electron state $|\phi_e\rangle$ and the anti-neutrino state $|\phi_{\bar{\nu}_e}\rangle$

$$|\Psi_f\rangle = |\psi_f\rangle \times |\phi_e\rangle \times |\phi_{\bar{\nu}_e}\rangle.$$

The matrix element $\mathcal{A}_{fi}$ controls the transition from the initial to the final state

$$\mathcal{A}_{fi} = \langle \Psi_f|\mathcal{A}|\Psi_i\rangle$$

It can be obtained by working in the position representation and recognising that the amplitude G_F associated with the point-like interaction (2.12) should be integrated over the volume of the nucleus,

$$\mathcal{A}_{fi} = \int d^3x\; G_F\; \phi_e^*\, \phi_\nu^*\, \psi_f^*\, \psi_i.$$

The ϕ and ψ terms are the position representations (wave functions) of the four particles, and in the final state are found in complex conjugate form. The integral sums over the amplitudes for the point-like reaction to occur anywhere in the nucleus, since the reaction could have occurred anywhere within.

To perform the integral we first Taylor expand the exponentials in the plane wave functions (2.16)–(2.17) for the electron and the neutrino. The expansion is useful because the exponents $\mathbf{p}\cdot\mathbf{x}$ are small.[5] The product of ϕ_e^* and ϕ_ν^* can therefore be written

$$e^{-i(\mathbf{p}_e+\mathbf{p}_\nu)\cdot\mathbf{x}} \approx 1 - i(\mathbf{p}_e + \mathbf{p}_\nu)\cdot\mathbf{x} + \ldots \tag{2.18}$$

[4] For a refresher, see appendix 2.B.1

[5] The size of $\mathbf{x}$ is of order the typical nuclear size, i.e. $\sim 10\,\text{fm}$, which in natural units is $10\,\text{fm}/(197\,\text{MeV fm}) \sim 10^{-1}\,\text{MeV}^{-1}$. The typical momenta of the out-going particles are of order MeV, so the dot products in the exponents are of order 10^{-1}.

Provided that the first term in this expression does not vanish when performing the integral, it can be expected to dominate, and the whole integral can be approximated by

$$\begin{aligned}\mathcal{A}_{fi} &= G_F \int d^3x \; \psi_f^* \, \psi_i \\ &\equiv G_F \; M_{\rm nucl}\end{aligned}$$

where in the lower line $M_{\rm nucl}$ denotes the overlap integral between the neutron in the parent nucleus and the proton in the daughter nucleus. The size of the quantity $M_{\rm nucl}$ depends on the participating nuclei, and is known as the **nuclear matrix element**.

In some particularly simple cases $M_{\rm nucl}$ can be calculated analytically. In particular, if the initial-state neutron, and the final-state proton happen to inhabit the same state within a nucleus, the overlap integral is maximal, i.e. for those nuclei

$$|M_{\rm nucl}| = 1.$$

An example of a maximum overlap integral is found for the simplest case of the isolated neutron decay. [6]

To complete the job of calculating Γ we need to find the density of states factor $\frac{dN}{dE_f}$. The density of states for the outgoing electron can be calculated from the density of states inside a box[7],

$$dN = \frac{d^3\mathbf{p}}{(2\pi)^3}.$$

Assuming spherical symmetry the angular integrals yield 4π so

$$dN = \frac{4\pi \; p^2 dp}{(2\pi)^3}.$$

A similar result holds for the neutrino. The states allowed by the daughter nucleus are fixed by total momentum conservation, so provide no further contribution to the density of states. The recoil energy of the heavy daughter nucleus is negligible, so conservation of energy gives

$$E_e + E_\nu = Q,$$

where E_e is the kinetic energy of the electron. Hence the rate of decays that yield electrons with momenta between p_e and $p_e + dp_e$ is

$$d\Gamma(p_e) = G_F^2 |M_{\rm nucl}|^2 \frac{(Q - E_e)^2}{2\pi^3} p_e^2 dp_e.$$

In the relativistic limit where $E_e \gg m_e$ we can perform the integral and obtain the simple result

$$\boxed{\Gamma_\beta \propto Q^5.}$$

i.e. the rate depends on the fifth power of the available energy.

[6] Such decays are called 'super-allowed'.

[7] See appendix 2.B.2 for the source of this term.

'Forbidden' decays (*Non examinable*)

We have assumed that the first term in (2.18) will dominate, but it can vanish due to selection rules. For example, if the nuclear matrix element has odd parity the first term vanishes, since then we are integrating the product of an odd and an even function. In that case, the next term in the series is required, and the reaction rate is suppressed. Such decays are said to be 'first forbidden'. In general the larger the change in angular momentum required in the nuclear transition, the further along the series one will need to go to find a non-zero term, and the slower will be the decay.

We will later find that Beta decays are mediated at very small length scales ($\sim 10^{-18}\,\mathrm{m}$) by charged spin-1 force-carrying particles known as $W^{\pm}$ bosons.

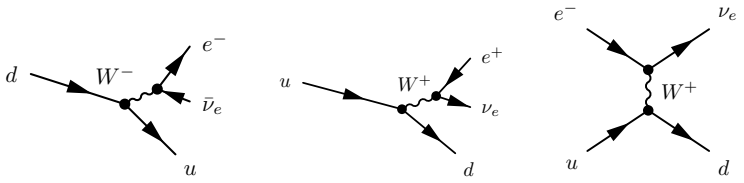

The Feynman diagrams above show the $W^{\pm}$ bosons responsible for β^- decay, β^+ decay, and electron capture. For probes with wavelength $\lambda \gg \lambda_{c,W}$, where

$$\lambda_{c,W} = \frac{\hbar}{m_W c}$$

is the W boson Compton wavelength, or equivalently for probes with momentum $p \ll m_W$, the small-distance behaviour of the interaction is not apparent. We do not resolve the W boson and instead we get what appears to be a single four-body interaction.

2.4 Nuclear Scattering

The structure of the nucleus can be probed by scattering projectiles from it. Those projectiles might be protons, electrons, muons, or indeed other nuclei.

2.4.1 Cross sections

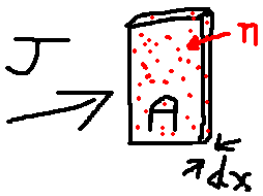

Many experiments take the form of scattering a beam of projectiles into a target.

Provided that the target is sufficiently thin that the flux is approximately constant within that target, the rate of any reaction W_i will be proportional to the flux of incoming projectiles J (number per unit time) the number density of scattering centres n in the target (number per unit volume), and the width δx of the target

$$W_i = \sigma_i \, n \, J \, \delta x. \tag{2.19}$$

The constant of proportionality σ_i has dimensions of area. It is known as the **cross**

As well as scattering experiments, the size of various nuclei can be determined by other methods, including:

- Shifts in the energy-levels of atomic electrons from the change of their Coulomb potential caused by the finite size of the nucleus.
- Muonic equivalents of the above. Muons are about 200 times heavier than electrons, so their "Bohr raduis" is about 200 times smaller. One observes the series of x-rays from the atomic (muonic) transitions

section for process i and is defined by

$$\boxed{\sigma_i = \frac{W_i}{n\,J\,\delta x}} \tag{2.20}$$

We can get some feeling for why this is a useful quantity if we rewrite (2.19) as

$$W_i = \underbrace{(n\,A\,\delta x)}_{N_{\text{target}}}\,J\,\underbrace{\frac{\sigma}{A}}_{P_{\text{scatt}}}$$

where A is the area of the target. Here N_{target} is the total number of targets illuminated by the projectile, and the cross section can be interpreted as the **effective area** presented to the beam per target for which a particular reaction can be expected to occur.

The total rate of loss of beam is given by $W = \Sigma W_i$, and the corresponding total cross section is therefore

$$\sigma = \sum_i \sigma_i.$$

We could choose to quote cross sections in units of e.g. fm^2 or in natural units of GeV^{-2}, however the most common unit used in nuclear and particle physics is the so-called **barn** (b) where

$$\boxed{1\,\text{barn} = 10^{-28}\,\text{m}^2}$$

We can convert the barn to natural units of MeV^{-2} using the $\hbar c$ conversion constant as follows

$$\begin{aligned} 1\,\text{barn} &= 10^{-28}\,\text{m}^2 \\ &= 100\,\text{fm}^2/(197\,\text{MeV fm})^2 \\ &= 0.00257\,\text{MeV}^{-2}. \end{aligned}$$

The 'differential cross section' $\frac{d\sigma}{d\Omega}$ is the cross section per unit solid angle of scattered particle. It is defined to be the rate of scattering per target per unit incoming flux density per unit solid angle ($d\Omega$) of deflected particle.

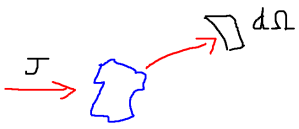

2.4.2 Resonances and the Breit-Wigner formula

Sometimes the projectile can be absorbed by the nucleus to form a compound state, then later reabsorbed. The time-energy uncertainty relationship of quantum

The decay width can be generalised to a particle which has many different decay modes. The rate of decay into mode i is given Γ_i. The total rate of decay is given by the sum over all possible decay modes

$$\Gamma = \sum_{i=1\ldots n} \Gamma_i.$$

The fraction of particles that decay into final state i, is known as the **branching ratio**

$$\mathcal{B} = \frac{\Gamma_i}{\Gamma}.$$

The quantity Γ_i is known as the **partial width** to final state i, whereas the sum of all partial widths is known as the **total width**.

mechanics tells us that if a state has only a finite lifetime (of order Δt), then it has an uncertaintity on its energy ΔE given by

$$\Delta E \Delta t \sim \hbar.$$

Using the fact that the decay rate $\Gamma = 1/\tau$, and using natural units to set $\hbar = 1$, we find that

$$\Delta E \sim \Gamma. \tag{2.21}$$

In these units, the uncertainty in the rest-energy of a particle is equal to the rate of its decay. This means that if we take a set of identical unstable particles, and measure the mass of each, we will expect to get a range of values with width of order Γ.

Long-lived intermediate states have small Γ and hence well-defined energies. We tend to think of these reasonably long-lived intermediate states as 'particles'. The neutron is an example of an unstable state that lives long enough for the word 'particle' to be meaningfully applied to it.

Short-lived intermediate states have large widths and less well defined energies. When the intermediate state is so short-lived that its width Γ is similar to its mass, then the decay is so rapid that it is no longer useful to think of it as a particle — it's really some transition through which the state happens to be momentarily passing.

We can develop these ideas more quantitatively by considering the general process

$$A + B \longrightarrow O \longrightarrow C + D. \tag{2.22}$$

The initial particles A and B collide to form an unstable intermediate O, which then decays to the final state C and D (which may or may not have the same particle content as the initial state). An example of a familiar process is the absorption and then emission of a photon by an atom, with an intermediate excited atomic state,

$$A + \gamma \longrightarrow A^* \longrightarrow A + \gamma.$$

Alternatively the reaction could represent an inelastic nuclear interaction, for example the nuclear absorption of a neutron to form a heavier isotope followed by its de-excitation

$$^{25}\mathrm{Mg} + n \longrightarrow {}^{26}\mathrm{Mg}^* \longrightarrow {}^{26}\mathrm{Mg} + \gamma.$$

Other reactions can create and annihilate other types of particle.

The reaction will proceed most rapidly when the energies of the incoming particles are correctly tuned to the mass of the intermediate. The reaction rate will be fastest when the energy of $A+B$ is equal to the rest-mass energy E_O of the intermediate state. The energy need only match E_O to within the uncertainty Γ in the energy of the intermediate.

Under the condition that the transition from $A+B$ to $C+D$ proceeds **exclusively** via the intermediate state '0', of mass m_0 and that the width of the intermediate is not too large ($\Gamma \ll m_0$), the probability for the scattering process, as a function of total energy E takes the familiar Lorentzian shape

$$p(E) \propto \frac{1}{(E-E_0)^2+\Gamma^2/4}. \tag{2.23}$$

This is the same peaked shape as seen in resonances in situations involving oscillators, and so the excited intermediate state is often called a **resonance**, and the process is known as resonant scattering.

Taking into account density of states and flux factors, and the possibilities of decay into multiple different final states, the overall cross-section for the process (2.22) is given by the famous **Breit-Wigner** formula

$$\boxed{\sigma_{i\to 0\to f} = \frac{\pi}{k^2}\frac{\Gamma_i\Gamma_f}{(E-E_0)^2+\Gamma^2/4}.} \tag{2.24}$$

Since excited states are very common, this is an important result not just in nuclear and particle physics, but also in any process where excitations are found. The terms in this equation are as follows:

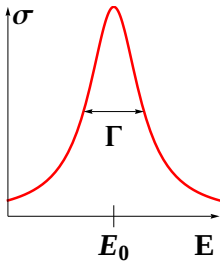

The Breit-Wigner line shape.

- Γ_i is the *partial width* of the resonance to decay to the initial state $A+B$
- Γ_f is the *partial width* of the resonance to decay to the final state $C+D$
- Γ is the *full width* of the resonance at half-maximum (and equal to the sum $\sum_j \Gamma_j$ over all possible decay modes)
- E is the centre-of-mass energy of the system
- E_0 is the characteristic rest mass energy of the resonance
- k is the wave-number of the incoming projectile in the centre-of-mass frame which is equal to its momentum in natural units.

The cross-section is non-zero at any energy, but has a sharp peak at energies E close to the rest-mass-energy E_0 of the intermediate particle. Longer lived intermediate particles have smaller Γ and hence sharper peaks.

Resonant scattering experiments can tell us about the excited states of nuclei, and hence provide further information about nuclear structure and interactions. All sorts of particles which are too short-lived to travel macroscopic distances can nevertheless be created as intermediate states and studied from the properties of their Breit-Wigner peaks.

2.4.3 Nuclear scattering and form factors

When a target only slightly perturbs the wave-function of the projectile, the resulting scattering behaves rather like optical diffraction.

In optics, the properties of a microscopic aperture can be understood from the pattern obtained when light, of wavelength similar to the size of the aperture, is diffracted by that apperture. Far from the aperture, the optical pattern observed is the two dimensional Fourier transformation of the aperture function. This is true even if the optical aperture is too small to observe directly.

Now consider scattering a wave from a three-dimensional projectile. Again, the observed diffraction pattern comes from a Fourier transform of the object, but now the aperture function is replaced with the potential $V(\mathbf{x})$.

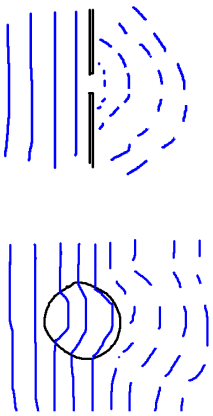

Diffractive scattering from a slit and from an object.

In the Born approximation, which is valid for weak potentials, the amplitude $f(\Delta\mathbf{k})$ for scattering a projectile such that its change in momentum is $\Delta\mathbf{k}$, is proportional to the 3D Fourier transform of the scattering potential V,

$$f(\Delta\mathbf{k}) = A \int d^3x \; V(\mathbf{x}) \; e^{-i\Delta\mathbf{k}\cdot\mathbf{x}} \tag{2.25}$$

where A is a normalising constant. The probability to scatter into some small angle $d\Omega$ is then proportional to $|f(\Delta\mathbf{k})|^2$.

Let us consider the scattering of a projectile of charge z from a nucleus with charge Z and spherically symmetric local charge density $\rho(r)$, centred at the origin. The potential at some point $\mathbf{x}'$ is given by summing over the Coulomb potentials from distributed charges at all other locations $\mathbf{x}''$,

$$\begin{aligned} V(\mathbf{x}') &= \frac{ze^2}{4\pi\epsilon_0} \int d^3x'' \, \frac{\rho(\mathbf{x}'')}{|\mathbf{x}' - \mathbf{x}''|} \\ &= z\alpha \int d^3x'' \, \frac{\rho(\mathbf{x}'')}{|\mathbf{x}' - \mathbf{x}''|} \end{aligned}$$

where in the second step we again use the relation (valid in natural units) that the electromagnetic fine structure constant $\alpha = \frac{e^2}{4\pi\epsilon_0}$.

Substituting this form of the potential into the Born relation (2.25) we find

$$f(\Delta\mathbf{k}) = z\alpha A \int d^3x' \int d^3x'' e^{-i(\Delta\mathbf{k})\cdot\mathbf{x}'} \frac{\rho(\mathbf{x}'')}{|\mathbf{x}' - \mathbf{x}''|}.$$

We may simplify this expression by defining a new variable $\mathbf{X} = \mathbf{x} - \mathbf{x}'$. This change of variables allows us to factorize the two integrals, giving the result

$$f(\Delta\mathbf{k}) = \underbrace{\left[\frac{1}{Z} \int d^3x' \rho(x') e^{-i\Delta\mathbf{k}\cdot\mathbf{x}'}\right]}_{\text{Form Factor}} \times \underbrace{Zz\alpha A \left[\int d^3X \frac{e^{-i\Delta\mathbf{k}\cdot\mathbf{X}}}{|\mathbf{X}|}\right]}_{\text{Rutherford}}. \tag{2.26}$$

The scattering amplitude from a distributed charge is therefore equal to the product of two terms. The second term can be recognised as the Rutherford scattering

amplitude – the amplitude that would be obtained from scattering from a point charge density $\rho(\mathbf{x}) = Z\delta(\mathbf{x})$. The second term therefore tells us nothing about the internal structure of the nucleus. All of the interesting information about the nuclear structure is encapsulated in the first term,

$$\boxed{F_{\rm nucl}(\Delta\mathbf{k}) = \int d^3x \; N(\mathbf{x}) \; e^{-i\Delta\mathbf{k}\cdot\mathbf{x}}}$$

which is known as the **nuclear form factor**. The form factor is the three-dimensional Fourier transform of the normalised charge density $N(\mathbf{x}) = \rho(\mathbf{x})/Z$. All of the interesting information about the size and structure of the nucleus is found in $F_{\rm nucl}(\Delta\mathbf{k})$. We will find interesting scattering — that is interesting 'diffraction patterns' — if the exponent is of order unity. For this to be true the de Broglie wave-length of the projectile must be of the same order as the nuclear size, as was noted in the introduction to this chapter.

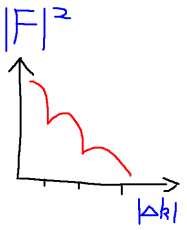

Sketch of a nuclear form factor diffraction pattern.

The mod-squared of the optical amplitude gives the intensity. Similarly it is $|F|^2$ which is important when considering the flux of scattered projectile particles. The rate at which particles are scattered into unit solid angle is given by

$$\frac{dN}{d\Omega} = |F_{\rm nucl}(|\Delta\mathbf{k}|)|^2 \left(\frac{dN}{d\Omega}\right)_{\rm Rutherford} . \tag{2.27}$$

This equation is more often written in terms of the differential cross section for scattering

$$\boxed{\frac{d\sigma}{d\Omega} = |F_{\rm nucl}(|\Delta\mathbf{k}|)|^2 \left(\frac{d\sigma}{d\Omega}\right)_{\rm Rutherford} .}$$

By examining the form factor for particles scattered with various changes in momentum $|\Delta\mathbf{k}|$ we can infer information about $N(\mathbf{x})$ and hence about the size and shape of the nuclear potential $V(\mathbf{x})$.

2.5 Key points

- In **natural units** (appendix 2.A), $\hbar = c = 1$ and

$$\boxed{[\text{Mass}] = [\text{Energy}] = [\text{Momentum}] = [\text{Time}]^{-1} = [\text{Distance}]^{-1}}$$

A useful conversion constant is

$$\boxed{\hbar c \approx 197 \text{ MeV fm}}$$

- The nuclear mass is well described by the **semi-empirical mass formula**

$$\boxed{M(A,Z) = Zm_p + (A-Z)m_n - \alpha A + \beta A^{\frac{2}{3}} + \gamma \frac{(A-2Z)^2}{A} + \epsilon \frac{Z^2}{A^{\frac{1}{3}}} - \delta(A,Z).}$$

- The binding energy leads to a **valley of stability** in the (A, Z) plane where the stable nuclei lie

- In a reaction or decay, the Q-value is the energy released in a decay

$$\boxed{Q = \sum M_i - \sum M_f}$$

If $Q > 0$ the reaction is **exothermic** – it gives out energy, whereas if $Q < 0$ the reaction is **endothermic**, and energy must be supplied for it to proceed.

- Alpha decay rates are dominated by quantum **tunnelling** through the Coulomb barrier.

- Beta decay rates and electron capture are governed by the **Fermi coupling constant**

$$\boxed{G_F \approx 1.17 \times 10^{-5} \text{ GeV}^{-2}}$$

- The **cross section** is defined by:

$$\boxed{\sigma_i = \frac{W_i}{n\, J\, \delta x}} \tag{2.28}$$

The **differential cross section** is the cross section per unit solid angle

$$\boxed{\frac{d\sigma_i}{d\Omega}}$$

- Cross sections for sub-atomic physics are often expressed in the unit of **barns**.

$$\boxed{1 \text{ barn} = 10^{-28} \text{ m}^2}$$

- The **Breit Wigner formula** for resonant scattering is

$$\boxed{\sigma_{i\to 0\to f} = \frac{\pi}{k^2} \frac{\Gamma_i \Gamma_f}{(E-E_0)^2 + \Gamma^2/4}.}$$

- In elastic nuclear scattering the **form factor**

$$\boxed{F(|\Delta k|) = \int d^3x \left(\frac{\rho(x)}{Z}\right) e^{-i\mathbf{\Delta k}\cdot\mathbf{x}},}$$

is the 3D Fourier transform of the normalised charge density, and is related to the Rutherford scattering differential cross section by

$$\boxed{\frac{d\sigma}{d\Omega} = |F_{\rm nucl}(|\mathbf{\Delta k}|)|^2 \left(\frac{d\sigma}{d\Omega}\right)_{\rm Rutherford}.}$$

2.A Natural units

In the S.I. system of units, times are measured in seconds and distances in meters. In those units the speed of light takes the value close to $3 \times 10^8\,\mathrm{ms}^{-1}$.

We could instead have chosen to use unit of time such that $c = 1$. For example we could have used units in which time is measured in seconds and distance in light-seconds. In those units the speed of light is one (one light-second per second). Using units in which $c = 1$ allows us to leave c out of our equations (provided we are careful to remember the units we are working in). Such units are useful in relativistic systems, since now the relativistic energy-momentum-mass relations are simplified to

$$E = \gamma m$$
$$p = \gamma m v$$
$$E^2 - p^2 = m^2.$$

So for a relativistic system setting $c = 1$ means that energy, mass and momentum all have the same dimensions.

Since we are interested in quantum systems, we can go further and look for units in which $\hbar$ is also equal to one. In such units the energy E of a photon will be equal to its angular frequency ω

$$E = \hbar\omega = \omega.$$

Setting $\hbar = 1$ therefore means that the units of energy are the same as the units of inverse time. Units with $\hbar = 1$ imply that time (and via $c = 1$ distance too) must have the same dimensions as inverse energy, E^{-1}.

So in our system **natural units** with $\hbar = c = 1$ we have have that all of the following dimensions are the same:

$$\boxed{[\mathrm{Mass}] = [\mathrm{Energy}] = [\mathrm{Momentum}] = [\mathrm{Time}]^{-1} = [\mathrm{Distance}]^{-1}}$$

We are still free to choose a convenient unit for all of these quantities. In subatomic physics it is common to use units of energy (or inverse energy). The nuclear energy levels have typical energies of the order of 10^6 electron-volts, so we shall measure

energies, momenta and masses in MeV, and lengths and times in MeV^{-1}. At the end of a calculation we might wish to recover, for example, a "real" length from one measured in our MeV^{-1} units. To do so we can make use of the conversion factor

$$\boxed{\hbar c \approx 197 \text{ MeV fm}}$$

which tells us that one of our MeV^{-1} length units corresponds to 197 fm where $1\,\text{fm} = 10^{-15}$ m.

2.B Tools for cross-section calculations

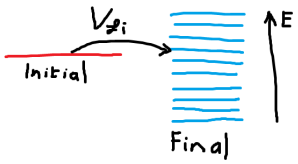

2.B.1 Decays and the Fermi Golden Rule

In subatomic physics we are interested in the decays of unstable particles, such as radioactive nuclei, muons from the atmosphere, or Higgs bosons. Using time-dependent perturbation theory in quantum mechanics it is possible to show that that the transition rate of an unstable state into a continuum of other states is given by the **Fermi Golden Rule**:

$$\boxed{\Gamma = \frac{2\pi}{\hbar} |V_{fi}|^2 \frac{dN}{dE_f},} \tag{2.29}$$

where

- Γ is the rate of the decay
- V_{fi} is the matrix element of the Hamiltonian coupling the initial and the final states
- $\frac{dN}{dE_f}$ is the density of final states.

2.B.2 Density of states

The density of states for a single particle within a cubic box with sides length a can be calculated as follows. The plane wave solution is of form

$$\langle \mathbf{x}|\Psi\rangle \propto \exp\left(i\mathbf{k}\cdot\mathbf{x}\right).$$

If we require periodic boundary conditions, with period a equal to the side of the box, then the values of the wavenumber k_x are constrained to $k_x = 2\pi n/a$ for integer n. Similar conditions hold for k_y and k_z. The number of momentum states within some range of momentum $d^3\mathbf{p} = d^3\mathbf{k}$ (for $\hbar = 1$) is therefore given by

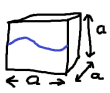

$$dN = \frac{d^3\mathbf{p}}{(2\pi)^3\hbar}\mathcal{V}$$

where $\mathcal{V} = a^3$ is the volume of the box.

2.B.3 Fermi G.R. example

Consider the isotropic decay of a neutral spin-0 particle A into two massless daughters, B and C

$$A \longrightarrow B + C.$$

The Fermi G.R. gives the decay rate (in natural units) of A as

$$\Gamma = 2\pi \left|V_{fi}\right|^2 \frac{dN}{dE_f}.$$

The density of final states can be found from the allowed momenta $\mathbf{p}_B$ of particle B.

$$dN = \frac{d^3\mathbf{p}_B}{(2\pi)^3}\mathcal{V}$$

When $\mathbf{p}_B$ is fixed there is no further freedom for $\mathbf{p}_C$ since the sum of the momenta of the two final state particles is fixed by total momentum conservation. This constraint means that for the two body final state there is no additional term in the density of states for $\mathbf{p}_C$.[8] Since all decay angles are equally probable, the integrals over the angles contribute 4π, leading to

$$\Gamma = 2\pi \left|V_{fi}\right|^2 \frac{4\pi\, p_B^2}{(2\pi)^3} \frac{dp_B}{dE_f}\mathcal{V}.$$

The relativistic decay products each have momentum $|\mathbf{p}_B| = E_f/2$ so $\frac{dp_B}{dE_f} = \frac{1}{2}$. Normalising to one unstable particle in our unit volume gives $\mathcal{V} = 1$, and results in a decay rate

$$\begin{aligned}\Gamma &= \frac{1}{2\pi}\left|V_{fi}\right|^2 p_B^2 \\ &= \frac{1}{8\pi}\left|V_{fi}\right|^2 m_A^2.\end{aligned}$$

2.B.4 Lifetimes and decays

The number of particles remaining at time t is governed by the decay law[9]

$$\frac{dN}{dt} = -\Gamma N,$$

where the constant Γ is the decay rate per nucleus. The equation is easily integrated to give

$$N(t) = N_0 \exp\left(-\Gamma t\right).$$

We can calculate the particles' average proper lifetime τ, using the probability that they decay between time t and $t + \delta t$

$$p(t)\,\delta t = -\frac{1}{N_0}\frac{dN}{dt}\,\delta t = \Gamma \exp\left(-\Gamma t\right)\,\delta t.$$

[8] For a three-body final state there would be terms in dN of the form $\frac{d^3p}{(2\pi)^3}$ for two of the three particles, the third again being fixed by momentum conservation.

[9] The decay law was discovered experimentally by Frederick Soddy (1877-1956). Soddy, who had been a scholar at Merton, was also first person to understand that radioactivity led to the transmutation of the elements — in effect making him the first true alchemist.

The mean lifetime is then

$$\begin{aligned} \tau &= \langle t \rangle \\ &= \frac{\int_0^\infty t\, p(t)\, dt}{\int_0^\infty p(t)\, dt} \\ &= \frac{1}{\Gamma} \end{aligned}$$

The decay law can be justified from precise experimental verification. In essence it represents a statement that the decay rate is independant of the history of the nucleus, its method of preparation and its environment. These are often excellent approximations, provided that the nucleus lives long enough that has mass $m \gg \Gamma$ where Γ is its decay width, and provided it it not bombarded with disruptive probes, such as high-energy strongly interacting particles.

2.B.5 The flux factor

When calculating a cross section σ from a rate Γ, we need to take into account that for scattering from a single fixed target

$$\sigma = \frac{W}{\mathcal{J}}$$

where $\mathcal{J}$ is the flux density of incoming particles. The flux density is itself given by

$$\mathcal{J} = n_p v$$

where n_p is the number density of projectiles and v is their speed. If we normalise to one incoming particle per unit volume, then $n_p = 1$ and the cross section is simply related to the rate by

$$\sigma = \frac{W}{v}$$

2.B.6 Luminosity

In a **collider** — a machine which collides opposing beams of particles — the rate of any particular reaction will be proportional to the cross section for that reaction and on various other parameters which depend on the machine set-up. Those parameters will include the number of particles in each collding bunch, their spatial distributions, and their frequency of bunch crossings.

We can define a parameter called the **luminosity** $\mathcal{L}$ which encapsulates all the relevant machine parameters. It is related to the rate W and the cross section σ by

$$\mathcal{L} = \frac{W}{\sigma}.$$

For any collider the luminosity tells us the instantaneous rate of reaction for any cross section. The product of the time-integrated luminosity and the cross section tell us the expected count of the events of that type

$$N_{\mathrm{events,\,i}} = \sigma_i \int \mathcal{L}\, dt\ .$$

For a machine colliding trains of counter-rotating bunches containing N_1 and N_2 particles respectively at a bunch-crossing rate f, we can show that the luminosity is

$$\boxed{\mathcal{L} = \frac{N_1 N_2 f}{A},}$$

where A is the cross-sectional area of each bunch (perpendicular to the beam direction).

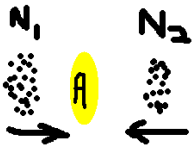

We have assumed above that the distributions of particles within each bunch is uniform. If that is not the case (e.g. in most real experiments the beams have approximately Gaussian profiles) then we will have to calculate the effective overlap area A of the bunches by performing an appropriate integral.

2.C Shell Model §

Non examinable

The SEMF provides a reasonable description of the binding energies of the nuclei for $A > 30$ but only the overall structure, not the finer details.

Differences at small A (e.g. the tightly bound isotopes $^4_2\mathrm{He}$ and $^{16}_8\mathrm{O}$) are already obvious in Figure 2.1. Figure 2.7 shows in more detail the difference between the measured binding energy (per nucleon) and the SEMF prediction. Islands of particularly high stability — that is with anomalously large B/A — are clearly visible near some special values of N or Z:

$$\{2, 8, 20, 28, 50, 82, 126\}.$$

These are known as the **magic numbers**. They correspond to configurations of nuclear shells that are precisely filled with either protons or neutrons. Evidence for this shell structure can be found in the binding energies, excitation energies, abundances, spins, and magnetic moments. Some nuclei, such the Helium nucleus $^4_2\mathrm{He}$ have magic numbers both for N and for Z. This observation goes some way to explaining why it is that Helium nuclei are emitted by heavy particles in the process of alpha decay. The shell model gives further insight into a variety of nuclear properties, but is beyond the scope of this course.

2.D Gamma decays §

Non examinable

Gamma decays are electromagnetic transitions, and are found when excited nuclear states relax to their ground states.

Similarly to the beta decay case, one can work out the rate using the Fermi golden rule. If one represents the initial nuclear wave-function by Ψ_a and the final nuclear

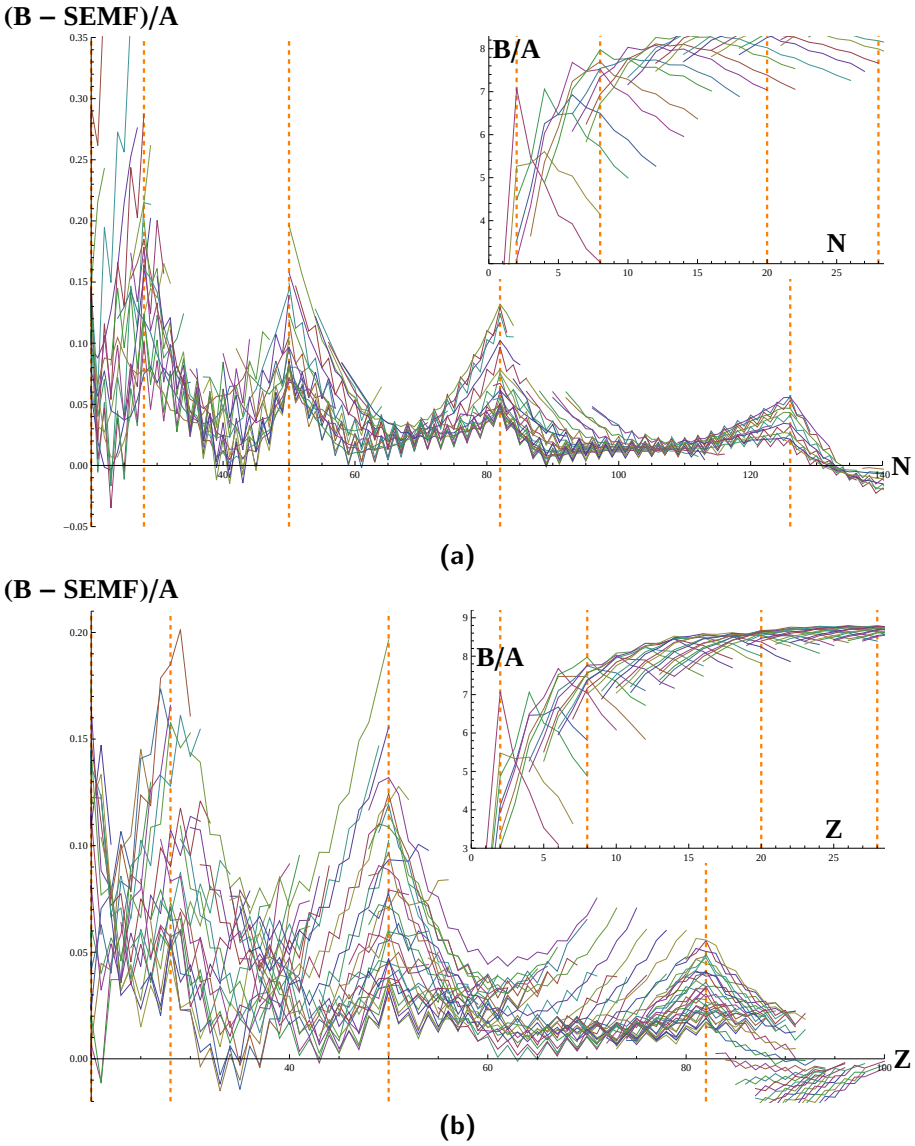

Figure 2.7: Difference between the measured binding energy (per nucleon) and the SEMF prediction. **(a)** The x-axis shows the number of neutrons in the nucleus; curves show isoto**p**es (same Z). **(b)** The x-axis shows the number of protons in the nucleus; curves show isoto**n**es (same N). In both cases the inset shows the binding energy per nucleon for the low-A nuclei. The magic numbers $\{2, 8, 20, 28, 50, 82, 126\}$ are marked with dashed lines.

wave-function by Ψ_b, then the appropriate matrix element is found to be

$$\langle \Psi_f | M | \Psi_i \rangle = \int d^3x \, \Psi_b^* (\mathsf{A} \cdot \hat{\mathsf{J}}) \, e^{-i\mathbf{k}\cdot\mathbf{x}} \Psi_a$$

where A represents the electromagnetic 4-potential and $\hat{\mathsf{J}} = q\hat{\mathsf{P}}/m$ is the electric 4-current operator. The electromagnetic selection rules and transitions are analogous to those of atomic physics.

Further Reading

- *"An Introduction to Nuclear Physics"*, W. N. Cottingham and D. A. Greenwood, 2001 for the basics
- *"Nuclear Physics"*, M.G. Bowler, Pergamon press, 1973
- *"Introductory Nuclear Physics"*, P.E. Hodgeson, E. Gadioli and E. Gadioli Erba, OUP, 2003
- The BNL table of the nuclides provides good reference data http://www.nndc.bnl.gov/nudat2/.

Bolwer and Hodgeson et. al. are good books which go well beyond this course.

Chapter 3

Hadrons

3.1 Symmetry, patterns and substructure

The proton and the neutron have rather similar masses. They are distinguished from one another by at least their different electromagnetic interactions, since the proton is charged, while the neutron is electrically neutral, but they have identical properties under the strong interaction. This provokes the question as to whether the proton and neutron might have some sort of common substructure. The substructure hypothesis can be investigated by searching for other similar patterns of multiplets of particles.

$$\begin{aligned} m_p &= 938.3\,\text{MeV}/c^2 \\ m_n &= 939.6\,\text{MeV}/c^2 \end{aligned}$$

There exists a zoo of other strongly-interacting particles. Exotic particles are observed coming from the upper atmosphere in cosmic rays. They can also be created in the labortatory, provided that we can create beams of sufficient energy. The Quark Model allows us to apply a classification to those many strongly interacting states, and to understand the constituents from which they are made.

3.1.1 Pions

The lightest strongly interacting particles are the *pions* (π). These can be produced by firing protons with energies of order GeV into material. Different pion creation interactions are observed to occur, such as

$$\begin{aligned} p + p &\rightarrow p + p + \pi^0 \\ p + p &\rightarrow p + p + \pi^+ + \pi^- \\ p + n &\rightarrow p + n + \pi^0 + \pi^+ + \pi^-. \end{aligned}$$

There are three different pions with charges, $+1$, 0 and -1 (π^+, π^0 and π^- respectively). In each of these pion production interactions electric charge is conserved. However some of the energy of the incident particle(s) is turned into creation of new pion particles.

The three pions have masses

$$m_{\pi^+} = m_{\pi^-} = 139.6\,\text{MeV}/c^2$$
$$m_{\pi^0} = 135.0\,\text{MeV}/c^2.$$

Again we see an interesting pattern – all three pions have similar masses, in this case that mass is about one seventh of that of the proton or neutron.

In fact the two charged pions have exactly the same mass. This is because the π^+ and π^- are anti-particles of one another. Anti-particles share the same mass, but have opposite charges. The π^0 has no charge, and is its own anti-particle.

Collisions also produce negatively charged anti-protons, $\bar{p}$.

$$p + p \rightarrow p + p + p + \bar{p}.$$

There is also an anti-neutron $\bar{n}$, with the same mass m_n as the neutron, and which which can also be produced in collisions e.g.

$$p + p \rightarrow p + p + n + \bar{n}.$$

Though the neutron has no charge it is *not* its own anti-particle. We can tell the two are different because the anti-neutron decays differently from the neutron:

$$\begin{aligned} n &\rightarrow p + e^- + \nu \\ \bar{n} &\rightarrow \bar{p} + e^+ + \bar{\nu}. \end{aligned}$$

Another piece of evidence that neutrons are not the same as anti-neutrons is that they do not annihilate against one another inside nuclei.

3.1.2 Baryon number conservation

In all of the reactions above, we observe that the total number of protons and neutrons less anti-protons and anti-neutrons

$$N(p) + N(n) - N(\bar{p}) - N(\bar{n})$$

is conserved. This rule is a special case of the conservation of **baryon number**, which is a quantum number carried by protons and neutrons, but not by pions. Protons and neutrons each have baryon number $+1$, while their anti-particles have baryon number -1.

Baryon number conservation keeps the proton stable, since it forbids the decay of the proton to e.g. a π^0 and a π^+ each of which have baryon number of zero. Experimental lower bound on the lifetime of the proton can be made by close observation of large tanks of water underground, yielding

$$\tau_p > 1.6 \times 10^{25}\,\text{years}.$$

This is very much longer than the lifetime of the universe ($\approx 1.4 \times 10^{10}$ years) so we would expect protons created in the early universe still to be around today. Thankfully they are – as you can easily verify experimentally.

Magnetic moments *Non examinable*

Hints about proton and neutron substructure can also be found in their magnetic dipole moments. It is a prediction of the Dirac theory that any fundamental spin-half fermion with charge $\mathcal{Q}$ and mass m should have a magnetic moment

$$\mu = \frac{\mathcal{Q}\hbar}{2m}.$$

This would predict that if the proton was a fundamental particle it would have magnetic moment equal to the nuclear magneton

$$\mu_N = \frac{e\hbar}{2m_p}$$

However the proton has a magnetic moment of 2.79 μ_N, in disagreement with the Dirac prediction for a fundamental particle. The neutron, which would have no magnetic moment in the Dirac theory, has magnetic moment equal to -1.91 μ_N. These observations suggest that protons and neutrons are not fundamental particles, but are made of something smaller.

3.1.3 Delta baryons

Other groups of strongly interacting particles are also observed. Charged pions live long enough to be made into beams, and so we can study their reactions with protons and neutrons. Examples of reactions observed include the production and decay of a the Δ multiplet of particles, which are observed as resonances in the cross-sections for processes such as

$$\begin{aligned}
\pi^- + n &\rightarrow \Delta^- \rightarrow \pi^- + n \\
\pi^- + p &\rightarrow \Delta^0 \rightarrow \pi^0 + n \\
\pi^+ + n &\rightarrow \Delta^+ \rightarrow \pi^0 + p \\
\pi^+ + p &\rightarrow \Delta^{++} \rightarrow \pi^+ + p
\end{aligned}$$

The four short-lived delta particles Δ have different charges ($+2, +1, 0, -1$), including a double-positively charged particle, Δ^{++}. All have rest-mass-energy close to 1232 MeV. All are produced in charge-conserving reactions. All have spin quantum number $s = 3/2$. They decay in a very short time — of order 10^{-22} s — so cannot be observed as propagating particles. Instead they are observed as resonances. From the width Γ of the resonance we can infer the lifetime of the corresponding particle.

From the reactions above we can see that all four deltas must have baryon number $+1$, in order to conserve baryon number throughout each reaction — these Δ particles are baryons. Conservation of baryon number implies that none of the Δ particles can be anti-particles of one another – they must have separate anti-particles, which would be created in reactions with anti-protons or anti-neutrons.

3.2 Accelerating protons – linear accelerators

We needed protons with kinetic energy of order GeV to perform these experiments. Unless we are willing to wait for the occasional high-energy cosmic ray coming from space, we'll need to accelerate them. Since the magnetic field changes only the direction of $\mathbf{p}$, it is the electrical field which is used to increase their energy of the particles.

$$\boxed{\frac{d\mathbf{p}}{dt} = \mathcal{Q}[\mathbf{E} + \mathbf{v} \times \mathbf{B}]}$$

Reminder of the Lorentz force law.

The problem we encounter if we try to use a constant electric field to do our acceleration is that to get these very high energies (of order GeV) we need to pass them through an enormous potential difference – of order 10^9 volts. Van der Graaff generators can reach potentials of order ten million volts, but then tend to break down because of electrical discharge (sparking) to nearby objects. For the particle creation reactions above, we're looking for about two orders of magnitude more energy than this.

We can get around the limitations of a static potential difference by realizing that only that only the local $\mathbb{E}$ field needs to be aligned along $\mathbf{v}$, and only during the period in which the particle is in that particular part of space.

We can use then use time-varying electric fields. In the margin is a picture of a **linear accelerator** or *linac*. In this device we have a series of cylindrical electrodes with holes through the middle of each which allow the beam to pass through. Electrodes are attached alternately to either pole of an alternating potential. The particles are accelerated in bunches. As each bunch travels along we reverse the potential while the bunch is inside electrode (where this is no field). We can then ensure that when the bunch is in the gap between the electrodes the field is always in the correct direction to keep it accelerating.

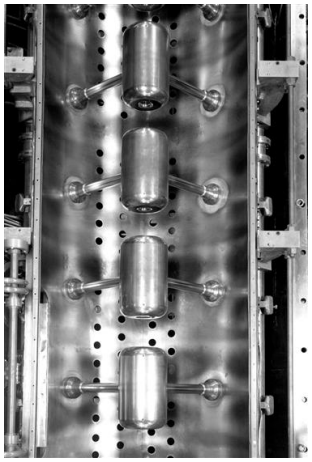

The linear accelerator injector to the CERN proton synchrotron. ©CERN

The oscillating potential on the electrodes may be created by connecting wires directly from the electrodes to an oscillator. For radio frequency AC oscillations we can instead bathe the whole system in an electromagnetic standing wave, such that the protons always 'surf' the wave and are continually accelerated.

3.3 Hadrons – symmetries as evidence for quarks

We have noted the existence of a variety of strongly-interacting particles coming in multiplets with similar masses. The generic name for all these strongly interacting particles is **hadrons**. There are many more of them than we have listed. We therefore need an organising principle – a model that can explain why the strongly interacting particles should come in these multiplets with similar properties. That model is the **quark model**.

3.3.1 Baryons

In the quark model, we can explain the properties of the nucleons, the delta particles, and other similar states as being composites — bound states of smaller, fundamental particles, called quarks. The quarks are spin-half fermions, and are point-like. No internal structure has ever been observed for a quark.

If we try to build a state out of two spin-half fermions, then quantum mechanical angular momentum addition formulae tell us that the four resulting states will be a spin-1 triplet and a spin-0 singlet. These are the wrong spins for our baryons, so baryons can not be made of pairs of spin-half constituents. However if we build a state out of **three** spin-half fermions, then the eight resulting states are two spin-$\frac{1}{2}$ doublets and a spin-$\frac{3}{2}$ quadruplet. These are the right spins for the the baryons we observe.

Baryons are made out of **triplets** of spin-half fermions called **quarks**.

If sets of three constituent quarks are to explain all of the charge states discussed above, then we will need them to come in two distinct types or **flavour**, with electric charges of $+2/3e$ and -1/3e. As shown in Table 3.1, the proton is made of two up-quarks and a down-quark. The neutron is made of two down-quarks and an up quark.

Particle	Quarks	Spin	Charge	Mass / MeV
p	uud	$\frac{1}{2}$	+1	938.3
n	udd	$\frac{1}{2}$	0	939.6
Δ^{++}	uuu	$\frac{3}{2}$	+2	~ 1232
Δ^{+}	uud	$\frac{3}{2}$	+1	~ 1232
Δ^{0}	udd	$\frac{3}{2}$	0	~ 1232
Δ^{-}	ddd	$\frac{3}{2}$	-1	~ 1232

Table 3.1: Properties of the nucleons and Δ baryons as explained by the quark model. The charges of the baryons are equal to the sum of the charges of their constituent quarks. The proton and neutron are the spin-half angular momentum combinations, while the heavier, unstable delta baryons form the spin-$\frac{3}{2}$ combinations.

	Charge	Spin	Parity
u	$+\frac{2}{3}e$	$\frac{1}{2}$	+
d	$-\frac{1}{3}e$	$\frac{1}{2}$	+
$\bar{u}$	$-\frac{2}{3}e$	$\frac{1}{2}$	−
$\bar{d}$	$+\frac{1}{3}e$	$\frac{1}{2}$	−

Up and down quarks, their antiparticles, and quantum numbers.

3.3.2 Mesons

The pions have spin zero. If they are made out of quarks, it must be from an even number of them. The simplest hypothesis is to use only two quarks. How can we build the triplet of pion charges $\{-1, 0, +1\}$ out of pairs quarks of charge $\mathcal{Q}_u = +\frac{2}{3}$ and $\mathcal{Q}_d = -\frac{1}{3}$? We can do so if we also use anti-quarks, which have the opposite charges to their respective quarks. The positively charged pion is composed of an up quark and an anti-down quark. The negatively charged pion is a anti-up quark and a down quark.

	Quarks	Spin	Charge	Mass / MeV
π^+	$u\bar{d}$	0	$+1$	139.6
π^0	$u\bar{u}$, $d\bar{d}$	0	0	135.0
π^-	$d\bar{u}$	0	-1	139.6

Table 3.2: Properties of the pions as explained in the quark model. The neutral pion exists in a superposition of the $u\bar{u}$ and $d\bar{d}$ states.

Composite hadrons formed from a quark and an anti-quark are known as **mesons**.

We have found that the pions are spin-0 states of u and d quark/anti-quark pairs. What happens to the spin-1 states? We would expect to see a set of mesons with spin-1, and indeed we do. The ρ^+, ρ^0 and ρ^- mesons are the equivalent spin-1 combinations. They all have mass of about 770 MeV.

The mesons and baryons are eigenstates of the parity operator, which inverts the spatial coordinates. The eigen-values be found as follows. The Dirac equation describing the relativistic propagation of spin-half particles requires that a particle and its anti-particles have opposite parity quantum numbers. The parity of the quark is set to be positive ($+1$) by convention, so the anti-quark has negative parity (-1). The parity of the meson state is therefore

$$P_{\text{meson}} = (+1)(-1)(-1)^L = (-1)^{L+1}$$

where the term $(-1)^L$ is the spatial parity for a state with orbital angular momentum quantum number L. The lowest-lying meson states for any quark content all have $L = 0$ so we can expect them to have negative parity – this is indeed what we observe for the pions.

The term symbol for the mesons is written J^P, where J is the angular momentum quantum number of the meson, and P is its parity quantum number. The pions have $J^P = 0^-$ and so are called pseudoscalars.

3.3.3 Quark flow diagrams

We're now in a position to understand the production and decay reactions of the Δ baryons at the quark level. Let us take the example of the Δ^0 and examine the reaction as a flow of quarks:

$$\begin{aligned} \pi^- + \quad p &\rightarrow \Delta^0 \rightarrow \pi^0 + \quad n \\ d\bar{u} + uud &\rightarrow udd \rightarrow d\bar{d} + udd \end{aligned}$$

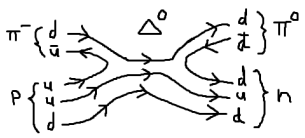

In the first part of the reaction a $\bar{u}$ antiquark in the pion annihilates against a u quark in the proton, leaving a udd state in the correct configuration to form a Δ^0 baryon. In the decay, a quark—anti-quark pair is created to form a neutral pion and a neutron. In the quark model, the conservation of baryon number is a consequence of the conservation of quark number. Each quark has baryon number of $\frac{1}{3}$, and each

anti-quark has baryon number of $-\frac{1}{3}$. This leads to the correct baryon numbers: $+1$ for qqq baryons, -1 for $\bar{q}\bar{q}\bar{q}$ anti-baryons, and 0 for $q\bar{q}$ mesons.

Since quarks can only annihilate against antiquarks of the same flavour, quark flavour is conserved throughout the strong reaction[1]. This is a characteristic property of all of the strong interactions:

Strong interactions conserve quark flavour

3.3.4 Strangeness

The up and down quarks are sufficient to describe the proton, neutron, pions and delta baryons. However the story does not stop there. Other particles are also created in strong interactions — particles which did not fit into the two-quark-flavour model and were called 'strange particles'. Bubble chamber experiments were used to examine the properties of beams of strange particles and demonstrated that the strange particles could travel macroscopic distances before decaying. Their stability could be explained if there was a new, almost-conserved, quantum number associated with these strange particles. This 'strangeness' quantum number is conserved in strong interaction. In order to decay the particles had to undergo a weak interaction, which changed the strangeness.

For example some strong interactions produce charged Kaon particles, $K^{\pm}$ with masses just less than $500\,\text{MeV}$, and which carry the strange quantum number

$$p + p \rightarrow p + p + K^{+} + K^{-}.$$

The positively charged Kaon is said to have strangeness $+1$, while the negatively charged particle has strangeness -1.

Each kaon can decay to a final state consisting only of pions (e.g. $K^{+} \rightarrow \pi^{0}\pi^{+}$). Considering the baryon number of the final state pions is zero, this tells us that kaons must also have zero baryon number and so must be mesons rather than baryons, since the pions carry no baryon number. Within the quark model we expect

The strangeness can then be transferred to other particles in other strong interactions. For example

$$\bar{K}^{0} + p \rightarrow \pi^{+} + \Lambda^{0}$$

or

$$K^{+} + n \rightarrow K^{0} + p$$

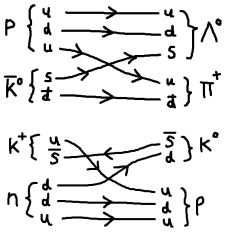

These various different interactions can be understood if we introduce a third quark s, to join u and d. This strange quark must have charge $-\frac{1}{3}$. Due to an accident of history the strange quark carries strangeness quantum number of -1 rather than $+1$. It's anti-particle, the anti-strange quark $\bar{s}$ has charge $+\frac{1}{3}$ and carries strangeness $+1$. We can now see that the positively charged kaon can be a $u\bar{s}$ meson, and the negatively charged kaon a $s\bar{u}$ meson.

[1] Quark flavour is conserved in strong and electromagnetic interactions, but not in weak interactions. For example the beta decay process $n \rightarrow p + e^{-} + \bar{\nu}$ does not conserve quark flavour number, so must be mediated by the weak interaction.

Drawing quark flow diagrams we see that the K^0 must be a $d\bar{s}$ meson – a neutral particle with strangeness $+1$. The Λ^0 must be a baryon with quark content uds.

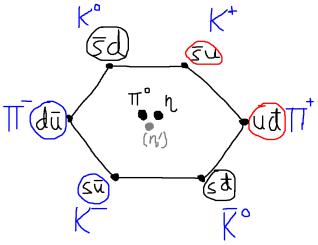

The octet of pseudoscalar mesons along with the η' singlet. All have $J^P = 0^-$. The mesons are positioned according to their strangeness (vertical) and the third component of their isospin (horizontal).

3.3.5 The light pseudoscalar octet

We can list the meson states it's possible form with three quarks, u, d and s and their anti-quarks. There are three flavours of quarks and three (anti-)flavours of anti-quarks so we should find 3×3 states. These states break down into an octet and a singlet ($3 \times 3 = 8 + 1$).

The octet contains three pions, four kaons, and the η meson. The singlet η' is largely a $s\bar{s}$ state, and is heavier than the other mesons.

The four kaons, K^+, K^-, K^0 and $\bar{K}^0$ are the lowest lying strange mesons, and therefore have $S = L = 0$. They must then have 'spin' $J = 0$ and negative parity ($J^P = 0^-$), just like the three pions we have already encountered.

The flavour content of the K mesons and the $\pi^\pm$ mesons is uniquely determined from their strangeness and charge. There are three uncharged mesons with zero strageness, which are mixtures of $u\bar{u}$, $d\bar{d}$ and $s\bar{s}$ states. That makes the full set of $S = 0$, $L = 0$, $J = 0$ mesons made from u, d, s quarks and their anti-quarks. All of these lightest states have orbital angular momentum $L = 0$, and so parity quantum number equal to the product of the quark and anti-quark parities, which according to the Dirac equation is -1.

We should expect another nine states, also with $L = 0$ but with $S = 1$ and hence $J = 1$. Those states are also observed, the ρ mesons mentioned above, being three of them. These states also have negative parity as expected from the value of L. These spin-1 states are known as the vector mesons.

3.3.6 The light baryon octet

Baryon parity

Using similar arguments to those used in calculating meson parity, we can calculate the spin and parity of the lightest baryons. The spin is $\frac{1}{2} \oplus \frac{1}{2} \oplus \frac{1}{2}$ which is either $\frac{1}{2}$ or $\frac{3}{2}$. The parity is $(+1)(+1)(+1) \times (-1)^L$ which is positive for the lightest $L = 0$ states. We therefore expect to have $J^P = \frac{3}{2}^+$ and $J^P = \frac{1}{2}^+$ states. The anti-baryon partners have the same spins and negative parity.

(Note J^P is a term symbol specifying both J and P. It should not be confused with an exponent and does not mean 'J to the power of P'.)

We also expect to be able to form various baryons using quark combinations that include strange quarks. Such baryons do indeed exist. If we examine the spin-half

baryons we find a triplet of strangeness -1 baryons:

$$\Sigma^+ = uus$$
$$\Sigma^0 = uds$$
$$\Sigma^- = dds$$

We also find a doublet of strangeness -2 baryons:

$$\Xi^0 = uss$$
$$\Xi^- = dss$$

The Λ_0 singlet is a uds state, so shares the same quark content as the Σ^0 but has a different internal organisation of those quarks. The light $J^P = \frac{1}{2}^+$ baryons are therefore organised into an octet comprising: two Ξ baryons, two nucleons, three Σ baryons and the Λ^0.

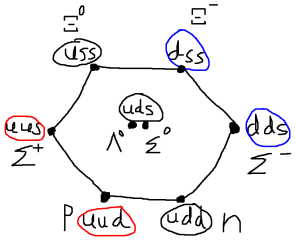

The $\frac{1}{2}^+$ octet of baryons made from triplets u, d and s quarks.

We can find out more about the masses of the constituent quarks by examining the masses of the composite baryons. The masses of the Σ baryons, with one strange quark, are around 1200 MeV. The masses of the Ξ baryons with two such quarks are about 1300 MeV. The proton and neutron have masses close to 940 MeV. The baryon masses lead us to the conclusion that the strange quark mass must be of the order of 100 to 150 MeV. The u and d quark masses are so small that they are in fact very hard to measure. Almost all the rest mass energy of their host hadrons is tied up in the energy of the strong interaction field in which they reside.

The $J^P = \frac{3}{2}^+$ multiplet of u, d and s baryons contains ten different states – it is a decuplet. It is noticable that, unlike the lighter $\frac{1}{2}^+$ baryons, the $\frac{3}{2}^+$ multiplet includes states with the triplets of quarks of the same flavours.

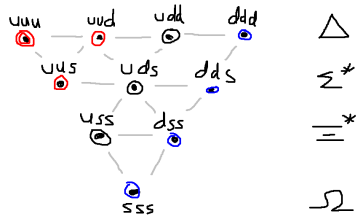

The $\frac{3}{2}^+$ baryon decuplet.

3.4 Colour

A closer investigation of the $J = \frac{3}{2}$ baryons shows an interesting problem when we consider the symmetry – under exchange of labels – of the three quarks in the uuu, ddd and sss baryons. The problem will be found to be resolved when we consider the 'charges' of the quarks under the strong force that bind them together.

The quarks in these baryons are identical fermions, so from the spin statistics theorem, the state-vector $|\psi\rangle$ should be antisymmetric under interchange of any pair of labels:

$$|\psi(1,2,3)\rangle = -|\psi(2,1,3)\rangle \quad \text{etc.}$$

Let's test this taking the Δ^{++} baryon as an example. The state vector must describe the spin, the spatial wave-function, and the flavour. If the separate parts of the state vector can be written as a direct product, then we might expect

$$|\psi_{\text{trial}}\rangle \stackrel{??}{=} |\psi_{\text{flavour}}\rangle \times |\psi_{\text{space}}\rangle \times |\psi_{\text{spin}}\rangle. \tag{3.1}$$

Let us examine the exchange symmetry of each part of (3.1) in turn, taking the example of the the Δ^{++} baryon.

Spin statistics

Given a system of particles, the state vector $|\psi\rangle$ must be symmetric under interchange of labels of any pair of identical bosons. It must be anti-symmetric under interchange of labels of any pair of identical fermions.

The Δ^{++} is composed of three up-type quarks, so we expect that

$$|\psi_{\rm flavour}\rangle = |u_1\rangle|u_2\rangle|u_3\rangle.$$

The flavour part of the state vector is symmetric under interchange of any pair of labels.

The spin of the Δ baryons is $\frac{3}{2}$, which means that the *spin part* of its state vector must also be symmetric under interchange of labels. For example the $m = \frac{3}{2}$ spin state can be written in terms of the quark spins as

$$|s = \frac{3}{2}, m_s = \frac{3}{2}\rangle \;=\; |\uparrow_1\rangle|\uparrow_2\rangle|\uparrow_3\rangle$$

which is symmetric under exchange of any pair of labels. The three other $s = \frac{3}{2}$ states (which have $m_s = \frac{1}{2}, -\frac{1}{2}$ and $-\frac{3}{2}$) can be created from $|\frac{3}{2}, \frac{3}{2}\rangle$ using the lowering operator

$$\hat{S}_- = \hat{S}_{1-} + \hat{S}_{2-} + \hat{S}_{3-}$$

which is also symmetric under interchange of any pair of labels. This means that all of the $s = \frac{3}{2}$ states have a spin part which is symmetric under interchange of any pair of labels.

The space part of the state vector is also symmetric under interchange of any pair of quark labels, since for this 'ground state' baryon all of the quarks are in the lowest-lying $l = 0$ state. The result is that $|\psi_{\rm trial}\rangle$ is overall symmetric under interchange of any pair of labels of quarks, and does *not* satisfy the spin statistics theorem. Something is wrong with equation (3.1).

The resolution to this dilemma is that there must be some other contribution to the state vector which is anti-symmetric under interchange of particles. What is missing is the description of the strongly interacting charges – also known as the 'colour'.

To describe the baryon state we need to extend the space of our quantum model to include a colour part $|\psi_{\rm colour}\rangle$ to the state vector,

$$\boxed{|\psi_{\rm baryon}\rangle = |\psi_{\rm flavour}\rangle \times |\psi_{\rm space}\rangle \times |\psi_{\rm spin}\rangle \times |\psi_{\rm colour}\rangle.} \tag{3.2}$$

The flavour, space and spin parts remain symmetric under interchange of any pair of labels, provided that the colour part is totally antisymmetric under interchange. We can arrange for total antisymmetry by using a determinant[2]

$$|\psi_{\rm colour}\rangle = \frac{1}{\sqrt{6}} \left|\left| \begin{pmatrix} r_1 & g_1 & b_1 \\ r_2 & g_2 & b_2 \\ r_3 & g_3 & b_3 \end{pmatrix} \right|\right|, \tag{3.3}$$

[2]This can be compared to the more familiar case of the two-particle spin state

$$|\psi(S=0)\rangle = \frac{1}{\sqrt{2}} \left|\left| \begin{pmatrix} \uparrow_1 & \downarrow_1 \\ \uparrow_2 & \downarrow_2 \end{pmatrix} \right|\right| = \frac{1}{\sqrt{2}} \left(|\uparrow_1\rangle|\downarrow_2\rangle - |\downarrow_1\rangle|\uparrow_2\rangle\right)$$

which has $S = 0$ and hence no net spin.

which will change sign under interchange of any two rows – a procedure equivalent to swapping the corresponding labels.

For us to be able to build such a determinant we require that there must be three different colour charges, which we have labelled 'r', 'g' and 'b', following the convention that they are known as red, green and blue. The need for three such colour 'charges' has since been proven in very many other experimental measurements. The antisymmetric colour combination (3.3) is the only combination of three quark states that has no net colour.

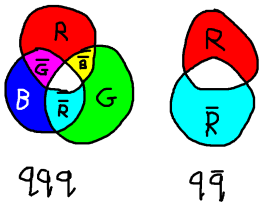

Baryon and mesons are both colourless states.

Quarks carry colour, while anti-quarks carry anti-colour. The colour in the mesons is contained in quark-antiquark combinations in the superposition

$$|\psi^{\text{meson}}_{\text{colour}}\rangle = \frac{1}{\sqrt{3}}\left(|r\bar{r}\rangle + |g\bar{g}\rangle + |b\bar{b}\rangle\right)$$

which is also colourless.

The strongly interacting particles observed – the qqq baryons and the $q\bar{q}$ mesons have no net colour. Quarks, which do have net colour have never been observed in isolation.

No coloured object has ever been observed in isolation.

Quarks only occur within the colourless combinations consisting of three quarks qqq for baryons and a quark and an anti-quark $q\bar{q}$ for mesons.

The quarks are **confined** within hadrons by the strong force, and are unable to exist as free particles. If we attempt to knock a u quark out of a proton (for example by hitting the proton with a high-energy electron, as we shall discuss on page 81) we do not observe a free u quark in the final state. Instead the struck u-quark uses part of its kinetic energy to create other $q\bar{q}$ pairs out of the vacuum, and joins together with them so that the final state contains only colour-neutral hadrons.

The particles that carry the strong force between quarks are known as **gluons**. Each gluon carries both colour and anti-colour. There are eight gluons, since of the nine possible othogonal colour–anti-colour combinations, one is colourless. We will later find (§6.3) that the fact that the gluon also carries colour charge itself makes the strong force very different from the electromagnetic force, which is mediated by neutral photons.

3.5 Heavier quarks

We have so far discussed hadrons made from three flavours of quarks, u, d and s. In fact these are only half of the total number which are found in nature. The full set of six quarks is as follows:

It's very difficult to obtain good values for the masses of the light quarks, since they are always bound up inside much heavier hadrons.

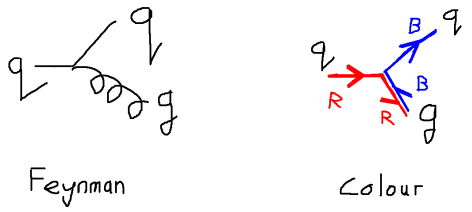

Figure 3.1: The diagram on the left shows the emission of a gluon from a quark. The right hand side shows a possible colour-flow. The gluon changes the colour of the quark, and itself carries both colour and anti-colour.

Name	Symbol	Charge	Mass [GeV]
down	d	$-\frac{1}{3}$	~0.005
up	u	$+\frac{2}{3}$	~0.003
strange	s	$-\frac{1}{3}$	0.1
charm	c	$+\frac{2}{3}$	1.2
bottom	b	$-\frac{1}{3}$	4.2
top	t	$+\frac{2}{3}$	172

It can be seen that the quarks only come in charges of $-\frac{1}{3}$ and $+\frac{2}{3}$. Their anti-quark partners have the opposite charges. It is useful to group the quarks into three generations, each containing a $+\frac{2}{3}$ and a $-\frac{1}{3}$ partner:

$$\begin{pmatrix} u \\ d \end{pmatrix} \quad \begin{pmatrix} c \\ s \end{pmatrix} \quad \begin{pmatrix} t \\ b \end{pmatrix} \qquad \begin{matrix} \leftarrow \mathcal{Q} = +\frac{2}{3} \\ \leftarrow \mathcal{Q} = -\frac{1}{3} \end{matrix}$$

where the up and down form the first generation, the strange and charm quarks the second, and the top and bottom quarks form the third generation. The pairings are those favoured by the weak interaction (§6.4), and mean that (for example) when a t quark decays it does so dominantly to a b quark.

What further hadrons may we expect from these additional quarks? All these quarks – other than the top quark – form hadrons in both meson ($q\bar{q}$) and baryon (qqq) combinations. The top quark is so heavy that it decays almost immediately, before it can form hadrons. An example of a charmed meson is the $c\bar{d}$ state with $J = 0$ known as the D^+ meson. Similarly there are mesons containing b quarks, such as the $b\bar{b}$ meson known as the Υ.

We can put these quarks and anti-quarks together to form colourless hadrons in any qqq or $q\bar{q}$ flavour combinations we choose, so long as we ensure that the final state-vector is antisymmetric with respect to exchange of labels of any identical quarks. So for example valid combinations are:

$$cds,\ b\bar{u},\ c\bar{c},\ uud, \quad \text{etc.}$$

3.6 Charmonium

The charm quark was first discovered in $c\bar{c}$ bound states. These 'charmonium' mesons are interesting because bound states of heavy quarks can tell us about the properties of the strong nuclear force which binds them.

The hadrons containing only the lightest quarks, u, d and s, have masses that tell us only a little about the mass of their constituent quarks. Most of the energy of the lightest baryons and mesons is stored in the strong-interaction field.

The charm quark (and to an even greater extent the bottom quark) is sufficiently heavy that mesons containing $c\bar{c}$ combinations are dominated by the mass of the constituent quarks. The energy in the field is now a relatively small correction to the rest mass energy of the baryons, and the whole two-particle system can be reasonably well described by non-relativistic quantum mechanics. If we model the system as a two-body quantum system, with reduced mass $\mu = m_c/2$ then we can write down the Schrödinger equation for the energy eigenstates of the system,

$$\left(\frac{P^2}{2\mu} + V\right)|\Psi\rangle = E|\psi\rangle.$$

The potential V due to the strong force between a quark and its anticolour partner is well described by the function

$$V(r) = -\frac{4}{3}\frac{\alpha_s}{r} + \frac{r}{a^2}, \tag{3.4}$$

The first term is the strong-force equivalent to the Coulomb potential. The electromagnetic fine structure constant (α) has replaced by the strong-force constant α_s, and the factor of $4/3$ has its origin in the three colour 'charges' rather than the single one electromagnetic charge. The term linear in r means that V continues growing as $r \to \infty$. It is this linear term that leads to quark confinement, since an infinite amount of energy would be required to separate the quarks to infinity.

For $c\bar{c}$ or 'charmonium' mesons, the typical separation r is rather smaller than a. In these states the linear term can be neglected, and the potential takes the $1/r$ form familiar from atomic physics. We then expect that the energy eigenstates should follow the pattern of the hydrogenic states.

$$E_n = -\frac{\mu\alpha^2}{2n^2}$$

Hydrogen atomic energy levels.

The energy levels should then be given by the strong-force equivalent of the hydrogenic energies:

$$E_n = -\frac{\mu}{2n^2}\left(\frac{4}{3}\alpha_s\right)^2. \tag{3.5}$$

Therefore we expect to see charmonium states with energies equal to $2m_c + E_n$. The observed charmonium spectrum bears out these predictions (Figure 3.2).

$n\,^{2S+1}L_J$	j^P	Name
1^1S_1	0^-	η_c
1^1L_1	1^+	h_c
1^3S_1	1^-	J/Ψ
2^3S_1	1^-	Ψ'

Some charmonium states and their quantum numbers

The lowest-lying state again has $L = S = 0$, and hence $J = 0$ and parity $(+1)(-1)(-1)^L = (-1)^{L+1} = -1$. This state is labelled η_C in Figure 3.2.

The first meson to be discovered was not the lightest one η but the slightly heavier J/Ψ. The J/Ψ has spin 1 and negative parity resulting from $S = 1$ and $L = 0$.

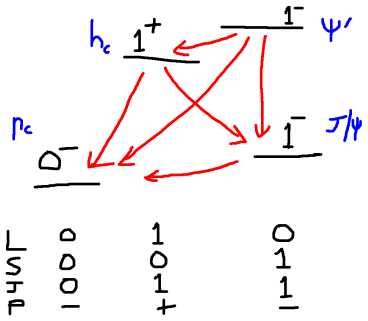

Figure 3.2: Some of the lowest-lying charmonium ($c\bar{c}$) states. Radiative transitions between states are indicated by arrows.

These are exactly the right quantum numbers to allow it to be made in electron-positron collisions, via an intermediate (virtual) photon, since the photon also has quantum numbers $J^P = 1^-$

$$e^- + e^+ \to \gamma^* \to J/\psi.$$

The transitions in the plot indicate possible electromagnetic transitions between charmonium states. Measurement of the gamma-ray photon energies allows us to make precision measurement of mass differences, and hence of the predictions of (3.5). Charmonium states which are heavier than $2m_D$ can decay rapidly via the strong force to either a D^0 and a $\bar{D}^0$ meson or to final state consisting of a D^+ and a D^- meson.

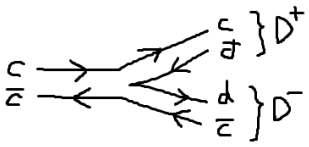

Those charmonium states which are lighter than $2m_D$ cannot decay to a pair of charmed D mesons. Instead the charm and anti-charm quarks must annihilate either via the electromagnetic force, or via a suppressed version of the strong interation. [3] This unusally suppressed strong decay is known as an 'OZI suppression' and is a feature of decays in which the intermediate state consists only of gluons. The $c\bar{c}$ states with $m < 2m_D$ are therefore unusually long-lived and are visible as very narrow resonances with masses close to 3 GeV.

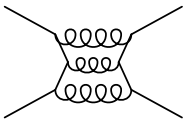

The 'OZI-suppressed' decay of the J/ψ proceeds via a-three gluon intermediate state.

We can go further and use the difference between the 1S and the 2S levels to find out the size of the strong 'fine structure constant'. It is found that α_s is much larger than for the electromagnetic case – in fact close to unity.

$$\boxed{\alpha_s \approx 1}$$

This much larger value of α_s compared the electromagnetic fine structure constant $\alpha \approx \frac{1}{137}$ is a reflection of the relative strengths of the two forces.

[3] The reason for this suppression is that a single-gluon intermediate state cannot be colourless, so is forbidden. A two-gluon final state has positive parity under the charge conjucation operator so is forbidden for any state, such as the J/ψ, which is negative under charge conjugation. Hence a three-gluon intermediate state is required.

The 'bottomonium' ($b\bar{b}$) system of mesons are the corresponding set of hydrogenic states for the bottom quark. They lead to sharp resonances close to $2m(b) \approx 10\,\text{GeV}$.

3.7 Hadron decays

The strong interaction allows reactions and decays in which quarks are interchanged between hadrons, but there is no change of net quark flavour. For example we saw in §3.3.3 that strong decays such as

$$\underset{udd}{\Delta^+} \to \underset{udd}{n} + \underset{u\bar{d}}{\pi^+},$$

conserve net quark content. The strong decays occur very rapidly, typically occur over lifetimes of order $10^{-22}\,\text{s}$.

Electromagnetic interactions do not change quark flavour either. Therefore if overall quark flavour is changed, for example in the strangeness-violating reactions,

$$\underset{u\bar{s}}{K^+} \to \underset{u\bar{d}}{\pi^+} + \underset{u\bar{u},d\bar{d}}{\pi^0} \qquad [\Delta S = -1]$$

$$\underset{dds}{\Sigma^-} \to \underset{ddu}{n} + \underset{u\bar{d}}{\pi^-} \qquad [\Delta S = +1]$$

a **weak** interaction must involved.

Only **weak** interactions can change quark flavour.

Weak decays are suppressed by the Fermi coupling constant, and so weakly decaying particles are characterised by much longer lifetimes, of order $10^{-10}\,\text{s}$. This may seem like a short life, but is twelve orders of magnitude much longer than typical strong decays.

Decay	Typical lifetime
Strong	$10^{-22}\,\text{s}$
EM	$10^{-18}\,\text{s}$
Weak	$10^{-10}\,\text{s}$

Examples of other weak decays include the decay of the charged pion to a muon[4] and an associated neutrino

$$\pi^- \to \mu^- + \bar{\nu}_\mu$$

and the beta decay of a neutron.

$$n \to p + e^- + \bar{\nu}_e$$

The neutron is unusually long-lived even for a weak decay ($\tau = 881\,\text{s}$). The long life is due to the closeness in mass between the neutron and the proton, which results in a small density of states for the decay products (recall the $\Gamma \propto Q^5$ rule in §2.3.2).

Electromagnetic decays have typical lifetimes intermediate between those of strong and weak decays. For example the electromagnetic decay

$$\pi^0 \to \gamma + \gamma$$

has a lifetime of $8 \times 10^{-17}\,\text{s}$.

[4] As we will see in §6.1 the muon is a fundamental particle with electric charge but no strong interactions – like an electron electron but heavier.

Hadron lifetimes

The lifetime of hadron states depends on the force by which they decay. Typical lifetimes are as follows:

Force	Typical lifetime	Example
Strong	10^{-22} s	$\Delta^- \rightarrow \pi^+ + p$
Electromagnetic	10^{-18} s	$\pi^0 \rightarrow \gamma + \gamma$
Weak	10^{-10} s	$K^+ \rightarrow \pi^0 + \pi^+$

Where more than one decay mode is possible, decay modes with much very small rates are often unobserved. For example consider the two baryons in the $J^P = \frac{1}{2}^+$ multiplet with quark content uds:

$$\Lambda^0 \quad (1115.7 \text{ MeV})$$
$$\Sigma^0 \quad (1192.6 \text{ MeV})$$

The Λ^0 is the lightest neutral strange baryon. Strangeness-conserving decays to other hadrons e.g. $p + K^-$ are kinematically forbidden, hence the only way the Λ^0 can decay is via the strangeness-violating weak decays:

$$\Lambda^0 \rightarrow p + \pi^- \quad (64\%)$$
$$\Lambda^0 \rightarrow n + \pi^0 \quad (36\%)$$

The lifetime of the Λ^0 is therefore relatively long by subatomic stanards – $\tau \approx 2.6 \times 10^{-10}$ s.

By contrast the heavier Σ^0 is decays electromagnetically to the Λ^0 with a lifetime of 7×10^{-20} s:

$$\Sigma^0 \rightarrow \Lambda^0 + \gamma$$

Since $\Gamma_{\text{EM}} \gg \Gamma_{\text{Weak}}$ the weak decay mode of the Σ^0 is not observed.

Key concepts

- Strongly interacting objects are composed of point-like spin-half objects called **quarks** q
- Quarks come in three strong-charges, r, g, b known as **colours**
- There are six different **flavours** of quark in three **generations**

$$\begin{pmatrix} u \\ d \end{pmatrix} \quad \begin{pmatrix} c \\ s \end{pmatrix} \quad \begin{pmatrix} t \\ b \end{pmatrix}$$

  each containing a $+2/3$ and a $-1/3$ charged partner.
- **Anti-quarks** $\bar{q}$ have the opposite charges and colours to their respective quarks
- The quarks are **confined** in the 'colourless' combinations called hadrons
- **Mesons** are colourless $q\bar{q}$ combinations
- **Baryons** are colourless qqq combinations

3.A Isospin §

Non-examinable

We can get extra insight into the meson and baryon combinations using the concept of **isospin**. The name 'isospin' is used in analogy to the spin, since the algebra of the isospin states has the same structures as the angular momentum states of quantum mechanics. However isospin is completely separate from angular momentum – it is simply an internal quantum number of the system that tells us about the quark content.

Let us consider the u and d quarks to be the isospin-up and isospin-down states of an isospin-half system.

The quantum number I is the total isospin quantum number, with $I = \frac{1}{2}$ for the nucleon doublet. The third component of isospin, I_3 distinguishes the proton with $I_3 = \frac{1}{2}$ from the neutron with $I_3 = -\frac{1}{2}$. These are analogous to the quantum numbers s and m_s which label the eigenstates of the angular momentum operators S^2 and S_z.

We can label the quark states with their quantum numbers $|I, I_3\rangle$. The $|u\rangle$ and $|d\rangle$ quarks form a $|\frac{1}{2}, \pm\frac{1}{2}\rangle$ isospin doublet:

$$\begin{pmatrix} |u\rangle \\ |d\rangle \end{pmatrix}$$

as do the the antiquarks

$$\begin{pmatrix} -|\bar{d}\rangle \\ |\bar{u}\rangle \end{pmatrix}.$$

The minus sign in front of the $|\bar{d}\rangle$ state ensures that the anti-quark doublet has the correct transformation properties.

The ladder operators $I_\pm$ change the third component of isosipin

$$I_- |u\rangle = |d\rangle$$
$$I_+ |d\rangle = |u\rangle$$

Similarly the ladder operators act on the anti-quarks

$$I_-|\bar{d}\rangle = -|\bar{u}\rangle$$
$$I_+|\bar{u}\rangle = -|\bar{d}\rangle.$$

Using the ladder operators we can generate the other pion states from the π^+:

$$\begin{aligned} I_-|\pi^+\rangle &= I_-|u\bar{d}\rangle \\ &= |d\bar{d}\rangle - |u\bar{u}\rangle = \sqrt{2}\,|\pi^0\rangle \end{aligned}$$

Operating again with I_- will generate the state $|\pi^-\rangle = |d\bar{u}\rangle$. The three pions $\{\pi^+, \pi^0, \pi^-\}$ form a $I = 1$ triplet with $I_3 = \{+1, 0, -1\}$.

The $|0, 0\rangle$ state is the linear combination of $|u\bar{u}\rangle$ and $|d\bar{d}\rangle$ that is othogonal to $|\pi^0\rangle$,

$$|0, 0\rangle = \tfrac{1}{\sqrt{2}}(|d\bar{d}\rangle + |u\bar{u}\rangle).$$

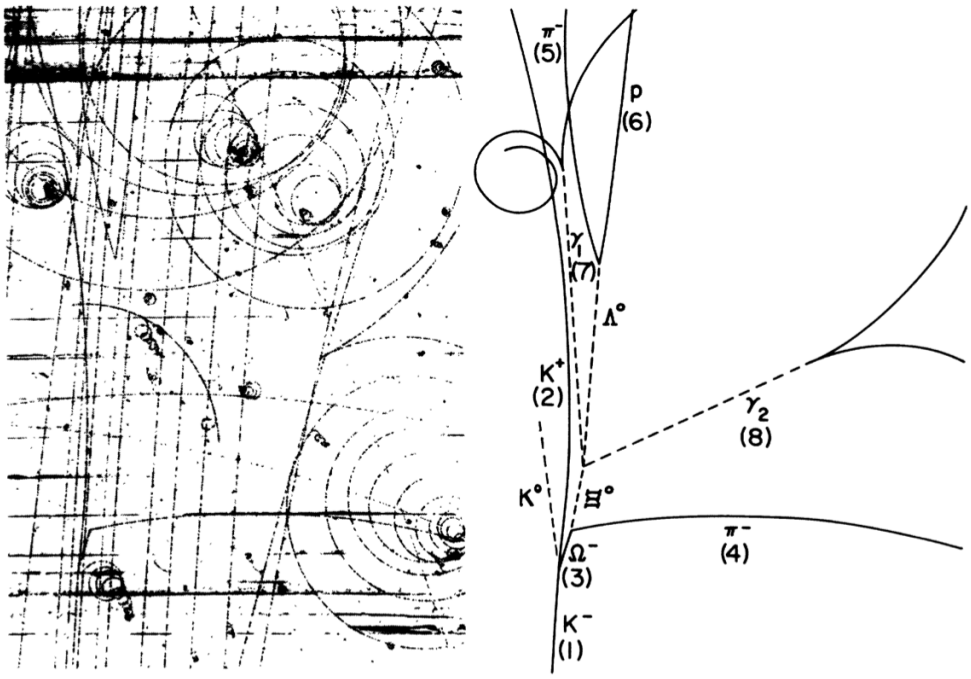

Figure 3.3: Bubble chamber photograph and line drawing showing the discovery of the Ω^- baryon. From [6].

This is the state of the η meson. Quarks other than the u and d do not carry isospin.

3.B Discovery of the Omega §

Non examinable

The triply strange Ω^- baryon was discovered in the set of decays shown in Figure 3.3.

The weak interaction is the only interaction that can change quark flavour, so strange hadrons can and do travel macroscopic distances before they decay.

In the figure the production of the Ω^- was from the interaction of a negatively charged beam of kaons onto the hydrogen target:

$$K^- + p \;\rightarrow\; \Omega^- + K^+ + K^0.$$

and found through its three sequential weak decays:

$$\begin{aligned} \Omega^- &\rightarrow \Xi^0 + \pi^- \\ \Xi^0 &\rightarrow \Lambda^0 + \pi^0 \\ \Lambda^0 &\rightarrow p + \pi^-. \end{aligned}$$

Only the charged particles create tracks of bubbles in the chamber. The presence of the neutral pion can be inferred due to a happy accident. The π^0 particle almost

always decays to a pair of photons $\pi^0 \rightarrow \gamma + \gamma$. Unusually, both of the photons produced in the pion decay have converted into $e^+ + e^-$ pairs $\gamma \rightarrow e^+ + e^-$ in the presence of the atomic nuclei, leaving vee-shaped bubble tracks.

Further reading

- B. Martin, *Nuclear and Particle Physics: An Introduction*
- W. S. C. Williams, *Nuclear and Particle Physics*
- K.S. Krane *Introductory Nuclear Physics*

Chapter 4

Non-relativistic scattering theory

4.1 Scattering theory

We are interested in a theory that can describe the scattering of a particle from a potential $V(\mathbf{x})$. Our Hamiltonian is

$$H = H_0 + V.$$

where H_0 is the free-particle kinetic energy operator

$$H_0 = \frac{p^2}{2m}.$$

In the absence of the potential V the solutions of the Hamiltonian could be written as the free-particle states satisfying

$$H_0|\phi\rangle = E|\phi\rangle.$$

These free-particle eigenstates could be written as momentum eigenstates $|\mathbf{p}\rangle$, but since that isn't the only possibility we hold off writing an explicit form for $|\phi\rangle$ for now. The full Schrödinger equation is

$$(H_0 + V)|\psi\rangle = E|\psi\rangle.$$

We define the eigenstates of H such that in the limit where the potential disappears ($V \to 0$), we have $|\psi\rangle \to |\phi\rangle$, where $|\phi\rangle$ and $|\psi\rangle$ are states with the same energy eigenvalue. (We are able to do this since the spectra of both H and $H + V$ are continuous.)

A possible solution is[1]

$$|\psi\rangle = \frac{1}{E - H_0} V|\psi\rangle + |\phi\rangle. \tag{4.1}$$

[1] Functions of operators are defined by $f(\hat{A}) = \sum_i f(a_i)|a_i\rangle\langle a_i|$. The reciprocal of an operator is well defined provided that its eigenvalues are non-zero.

By multiplying by $(E - H_0)$ we can show that this agrees with the definitions above. There is, however the problem of the operator $1/(E - H_0)$ being singular. The singular behaviour in (4.1) can be fixed by making E slightly complex and defining

$$\boxed{|\psi^{(\pm)}\rangle = |\phi\rangle + \frac{1}{E - H_0 \pm i\epsilon} V|\psi^{(\pm)}\rangle}. \tag{4.2}$$

This is the **Lippmann-Schwinger** equation. We will find the physical meeting of the $(\pm)$ in the $|\psi^{(\pm)}\rangle$ shortly.

4.1.1 Scattering amplitudes

To calculate scattering amplitudes we are going to have to use both the position and the momentum basis, the incoming beam is (almost) a momentum eigenstate, and V is a function of position $\mathbf{x}$. If $|\phi\rangle$ stands for a plane wave with momentum $\hbar\mathbf{k}$ then the wavefunction can be written

$$\langle \mathbf{x}|\phi\rangle = \frac{e^{i\mathbf{k}\cdot\mathbf{x}}}{(2\pi)^{\frac{3}{2}}}.$$

We can express (4.2) in the position basis by bra-ing through with $\langle\mathbf{x}|$ and inserting the identity operator $\int d^3x' \, |\mathbf{x}'\rangle\langle\mathbf{x}'|$

$$\langle \mathbf{x}|\psi^{(\pm)}\rangle = \langle \mathbf{x}|\phi\rangle + \int d^3x' \left\langle \mathbf{x}\right| \frac{1}{E - H_0 \pm i\epsilon} \left|\mathbf{x}'\right\rangle \langle \mathbf{x}'|V|\psi^{(\pm)}\rangle. \tag{4.3}$$

The solution to the Greens function defined by

$$G_\pm(\mathbf{x}, \mathbf{x}') \equiv \frac{\hbar^2}{2m} \left\langle \mathbf{x}\right| \frac{1}{E - H_0 \pm i\epsilon} \left|\mathbf{x}'\right\rangle$$

is

$$G_\pm(\mathbf{x}, \mathbf{x}') = -\frac{1}{4\pi} \frac{e^{\pm ik|\mathbf{x}-\mathbf{x}'|}}{|\mathbf{x} - \mathbf{x}'|}.$$

Using this result we can see that the amplitude of interest simplifies to

$$\langle \mathbf{x}|\psi^{(\pm)}\rangle = \langle \mathbf{x}|\phi\rangle - \frac{1}{4\pi}\frac{2m}{\hbar^2} \int d^3x' \frac{e^{\pm ik|\mathbf{x}-\mathbf{x}'|}}{|\mathbf{x} - \mathbf{x}'|} V(\mathbf{x}')\langle \mathbf{x}'|\psi^{(\pm)}\rangle \tag{4.4}$$

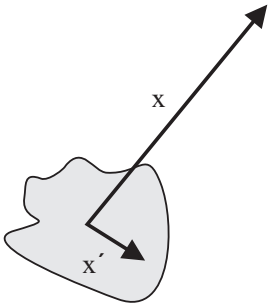

where we have also assumed that the potential is local in the sense that it can be written as

$$\langle \mathbf{x}'|V|\mathbf{x}''\rangle = V(\mathbf{x}')\delta^3(\mathbf{x}' - \mathbf{x}'').$$

The wave function (4.4) is a sum of two terms. The first is the incoming plane wave. For large $r = |\mathbf{x}|$ the spatial dependence of the second term is $e^{\pm ikr}/r$. We can now understand the physical meaning of the $|\psi^{(\pm)}\rangle$ states; they represent outgoing $(+)$ and incoming $(-)$ spherical waves respectively. We are interested in the outgoing $(+)$ spherical waves – the ones which have been scattered from the potential.

We want to know the amplitude of the outgoing wave at a point $\mathbf{x}$. For practical experiments the detector must be far from the scattering centre, so we may assume $|\mathbf{x}| \gg |\mathbf{x}'|$.

We define a unit vector $\hat{\mathbf{r}}$ in the direction of the observation point

$$\hat{\mathbf{r}} = \frac{\mathbf{x}}{|\mathbf{x}|}$$

and also a wave-vector $\mathbf{k}'$ for particles travelling in the direction $\hat{\mathbf{x}}$ of the observer,

$$\mathbf{k}' = k\hat{\mathbf{r}}.$$

Far from the scattering centre we can write

$$\begin{aligned} |\mathbf{x} - \mathbf{x}'| &= \sqrt{r^2 - 2rr'\cos\alpha + r'^2} \\ &= r\sqrt{1 - 2\frac{r'}{r}\cos\alpha + \frac{r'^2}{r^2}} \\ &\approx r - \hat{\mathbf{r}} \cdot \mathbf{x}' \end{aligned}$$

where α is the angle between the $\mathbf{x}$ and the $\mathbf{x}'$ directions.

It's safe to replace the $|\mathbf{x} - \mathbf{x}'|$ in the denominator in the integrand of (4.4) with just r, but the phase term will need to be replaced by $r - \hat{\mathbf{r}} \cdot \mathbf{x}'$. So we can simplify the wave function to

$$\langle \mathbf{x}|\psi^{(+)}\rangle \xrightarrow{r \text{ large}} \langle \mathbf{x}|\mathbf{k}\rangle - \frac{1}{4\pi}\frac{2m}{\hbar^2}\frac{e^{ikr}}{r}\int d^3x'\, e^{-i\mathbf{k}'\cdot\mathbf{x}'} V(\mathbf{x}')\langle \mathbf{x}'|\psi^{(+)}\rangle$$

which we can write as

$$\langle \mathbf{x}|\psi^{(+)}\rangle = \frac{1}{(2\pi)^{\frac{3}{2}}}\left[e^{i\mathbf{k}\cdot\mathbf{x}} + \frac{e^{ikr}}{r} f(\mathbf{k}', \mathbf{k})\right].$$

This makes it clear that we have a sum of an incoming plane wave and an outgoing spherical wave with amplitude $f(\mathbf{k}', \mathbf{k})$ given by

$$f(\mathbf{k}', \mathbf{k}) = -\frac{1}{4\pi}(2\pi)^3 \frac{2m}{\hbar^2}\langle \mathbf{k}'|V|\psi^{(\pm)}\rangle. \tag{4.5}$$

We will ignore the interference between the first term which represents the original 'plane' wave and the second term which represents the outgoing 'scattered' wave, which is equivalent to assuming that the incoming beam of particles is only approximately a plane wave over a region of dimension much smaller than r.

We then find that the partial cross-section $d\sigma$ — the number of particles scattered into a particular region of solid angle per unit time divided by the incident flux[2] — is given by

$$d\sigma = \frac{r^2|j_{\text{scatt}}|}{|j_{\text{incid}}|} d\Omega = |f(\mathbf{k}', \mathbf{k})|^2\, d\Omega.$$

[2]Remember that the flux density is given by $\mathbf{j} = \frac{\hbar}{2im}[\psi^*\nabla\psi - \psi\nabla\psi^*]$.

This means that the differential cross section is given by the simple result

$$\boxed{\frac{d\sigma}{d\Omega} = |f(\mathbf{k}', \mathbf{k})|^2.}$$

The differential cross section is simply the mod-squared value of the scattering amplitude.

4.1.2 The Born approximation

If the potential is weak we can assume that the eigenstates are only slightly modified by V, and so we can replace $|\psi^{(\pm)}\rangle$ in (4.5) by $|\mathbf{k}\rangle$.

$$f^{(1)}(\mathbf{k}', \mathbf{k}) = -\frac{1}{4\pi}(2\pi)^3 \frac{2m}{\hbar^2}\langle \mathbf{k}'|V|\mathbf{k}\rangle. \tag{4.6}$$

This is known as the **Born approximation**. Within this approximation we have the simple result that

$$\boxed{f^{(1)}(\mathbf{k}', \mathbf{k}) \propto \langle \mathbf{k}'|V|\mathbf{k}\rangle.}$$

Up to some constant factors, the scattering amplitude is found by squeezing the perturbing potential V between incoming and the outgoing momentum eigenstates of the free-particle Hamiltonian.

Expanding out (4.6) in the position representation (by insertion of a couple of completeness relations $\int d^3x' \, |\mathbf{x}'\rangle\langle\mathbf{x}'|$) we can write

$$f^{(1)}(\mathbf{k}', \mathbf{k}) = -\frac{1}{4\pi}\frac{2m}{\hbar^2}\int d^3x' e^{i(\mathbf{k}-\mathbf{k}')\cdot\mathbf{x}'} V(\mathbf{x}').$$

This result is telling us that scattering amplitude is proportional to the **3d Fourier transform** of the potential. By scattering particles from targets we can measure $\frac{d\sigma}{d\Omega}$, and hence infer the functional form of $V(r)$. This result is used, for example, in the nuclear form factor (Section 2.4.3).

4.2 Virtual Particles

One of the insights of subatomic physics is that at the microscopic level forces are caused by the exchange of force-carrying **particles**. For example the Coulomb force between two electrons is mediated by excitations of the electromagnetic field – i.e. photons. There is no real 'action at a distance'. Instead the force is transmitted between the two scattering particles by the exchange of some unobserved photon or photons. The mediating photons are emitted by one electron and absorbed by the other. It's generally not possible to tell which electron emitted and which absorbed the mediating photons – all one can observe is the net effect on the electrons.

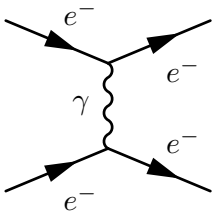

Other forces are mediated by other force-carrying particles. In each case the messenger particles are known as **virtual particles**. Virtual particles are not directly observed, and have properties different from 'real particles' which are free to propagate.

To illustrate why virtual particles have unusual properties, consider the elastic scattering of an electron from a nucleus, mediated by a single virtual photon. We can assume the nucleus to be much more massive than the electron so that it is approximately stationary. Let the incoming electron have momentum $\mathbf{p}$ and the outgoing, scattered electron have momentum $\mathbf{p}'$. For elastic scattering, the energy of the electron is unchanged $E' = E$. The electron has picked up a change of momentum $\Delta\mathbf{p} = \mathbf{p}' - \mathbf{p}$ from absorbing the virtual photon, but absorbed no energy. So the photon must have energy and momentum

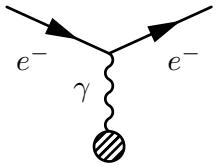

$$\begin{aligned} E_\gamma &= 0 \\ \mathbf{p}_\gamma &= \Delta\mathbf{p} = \mathbf{p}' - \mathbf{p}. \end{aligned}$$

The exchanged photon carries momentum, but no energy. This sounds odd, but is nevertheless correct. What we have found is that for this *virtual* photon, $E_\gamma^2 \neq p_\gamma^2$. The particular value $E_\gamma = 0$ is special to the case we have chosen, but the general result is that for *any virtual particle* there is an energy-momentum invariant[3] which is *not* equal to the square of its mass

$$\mathsf{P} \cdot \mathsf{P} = E^2 - \mathbf{p} \cdot \mathbf{p} \neq m^2.$$

Such virtual particles do *not* satisfy the usual energy-momentum invariant and are said to be '**off mass shell**'.

Note that we would not have been able to escape this conclusion if we had taken the alternative viewpoint that the electron had emitted the photon and the nucleus had absorbed it. In that case the photon's momentum would have been $\mathbf{p}_\gamma = -\Delta\mathbf{p}$. The square of the momentum would be the same, and the photon's energy would still have been zero.

These exchanged, virtual, photons are an equally valid solution to the (quantum) field equations as are the more familiar travelling-wave solutions of 'real' on-mass-shell photons. It is interesting to realise that all of classical electromagnetism is actually the result of very many photons being exchanged.

4.3 The Yukawa Potential

There is a type of potential that is of particular importance in subatomic scattering, which has the form (in natural units)

$$\boxed{V(r) = \frac{g^2}{4\pi}\frac{e^{-\mu r}}{r}.} \tag{4.7}$$

This is known as the **Yukawa potential**. The constant g^2 tells us about the depth of the potential, or the size of the force. When $\mu = 0$ (4.7) has the familiar $1/r$ dependence of the electrostatic and gravitational potentials. When μ is non-zero, the potential also falls off exponentially with r, with a characteristic length of $1/\mu$.

[3] We used sans serif capitals P to indicate Lorentz four-vectors $\mathsf{P} = (E, p_x, p_y, p_z)$. The dot product of two Lorentz vectors $\mathsf{A} \cdot \mathsf{B} = a_0 b_0 - a_1 b_1 - a_2 b_2 - a_3 b_3$ is a Lorentz invariant scalar.

The Yukawa potential and the range of forces

The electromagnetic force is mediated by excitations of the electromagnetic force, i.e. photons. The photon is massless so the electrostatic potential falls as $1/r$. The exponential fall-off of (4.7) is removed since $\mu = 0$, and so electromagnetism is effective even at large distances.

By contrast, the weak nuclear force, which is mediated by particles with μ close to 100 GeV is feeble at distances larger than about $1/(100\,\text{GeV}) \approx (197\,\text{MeV fm})/(100\,\text{GeV}) \sim 10^{-18}\,\text{m}$. This makes it short-range in nature, and so it appears to be weak. (In fact the coupling constant g for the so-called 'weak' force is actually larger than that for the electromagnetic force.)

To understand the meaning of the μ term it is useful to consider the relativistic wave equation known as the Klein-Gordan equation

$$\left(\frac{\partial^2}{\partial t^2} - \nabla^2 + \mu^2\right)\varphi(\mathbf{r}, t) = 0. \tag{4.8}$$

This is the relativistic wave equation for spin-0 particles. The plane-wave solutions to (9.5) are

$$\begin{aligned}\phi(\mathsf{X}) &= A\exp\left(-i\mathsf{P}\cdot X\right)\\ &= A\exp\left(-iEt + i\mathbf{p}\cdot\mathbf{x}\right).\end{aligned}$$

These solutions require the propagating particles to be of mass $\mu = \sqrt{E^2 - p^2}$. The Klein-Gordon equation is therefore describing excitations of a field of particles each of mass μ. The Yukawa potential is another solution to the field equation (9.5). The difference is that the Yukawa potential describes the *static* solution due to virtual particles of mass μ created by some source at the origin.

The scattering amplitude of a particle bouncing off a Yukawa potential is found to be

$$\langle\mathbf{k}'|V_{\text{Yukawa}}|\mathbf{k}\rangle = -\frac{g^2}{4\pi\,(2\pi)^3}\frac{1}{\mu^2 + |\Delta\mathbf{k}|^2}. \tag{4.9}$$

We can go some way towards interpreting this result as the exchange of a virtual particle as follows. We justify the two factors of g as coming from the points where a virtual photon is either created or annihilated. This **vertex factor** g is a measure of the interaction or 'coupling' of the exchanged particle with the other objects. There is one factor of g the point of creation of the virtual particle, and another one at the point where it is absorbed.

The other important factor in the scattering amplitude (4.9) is associated with the momentum and mass of the exchanged particle:

$$-\frac{1}{\mu^2 + |\Delta\mathbf{k}|^2}$$

In general it is found that if a virtual particle of mass μ and four-momentum P is exchanged, there is a **propagator factor**

$$\boxed{\frac{1}{\mathsf{P}\cdot\mathsf{P} - \mu^2}} \tag{4.10}$$

Vertex factors in electromagnetism

In electromagnetism we require that at a vertex where a photon interacts with a particle, the vertex factor g should to be proportional to the charge of the particle $\mathcal{Q}e$. For a particle of charge $\mathcal{Q}_1 e$ scattering from a field generated by another particle of charge $\mathcal{Q}_2 e$, we seek a ($\mu = 0$) Yukawa potential of the form

$$V_{\rm EM} = \frac{(\mathcal{Q}_1 e)(\mathcal{Q}_2 e)}{4\pi\epsilon_0 r}.$$

For scattering from a Coulomb potential we can therefore use the Yukawa result (4.9) by making the substitution

$$\frac{g^2}{4\pi} \Rightarrow \frac{\mathcal{Q}_1\mathcal{Q}_2 e^2}{4\pi\epsilon_0}.$$

This identification shows that the vertex factors g are just dimensionless measures of the charges of the particle. The vertex factor for a charge $\mathcal{Q}e$ is $\mathcal{Q}g_{\rm EM}$ where

$$\frac{g_{\rm EM}^2}{4\pi} = \alpha_{\rm EM} \approx \frac{1}{137}.$$

in the scattering amplitude. This relativistically invariant expression is consistent with our electron-scattering example, where the denominator was:

$$\begin{aligned} \mathsf{P}\cdot\mathsf{P} - \mu^2 &= E^2 - p^2 - \mu^2 \\ &= 0 - |\Delta\mathbf{k}|^2 - \mu^2 \\ &= -\left(\mu^2 + |\Delta\mathbf{k}|^2\right) \end{aligned}$$

Note that the propagator (4.13) becomes singular as the particle gets close to its mass shell. i.e. as $\mathsf{P}\cdot\mathsf{P} \to \mu^2$. It is only because the exchanged particles are *off* their mass-shells that the result is finite.

The identification of the vertex factors and propagators will turn out to be very useful when we later try to construct more complicated scattering processes. In those cases we will be able to construct the most important features of the scattering amplitude by writing down:

- an appropriate vertex factor each time a particle is either created or annihilated and
- a propagator factor for each virtual particle.

By multiplying together these factors we get the scattering amplitude.

Key concepts

- The amplitude for scattering from a potential can be solved iteratively, using the **Lippman-Schwinger** equation:

$$\boxed{|\psi^{(\pm)}\rangle = |\phi\rangle + \frac{1}{E - H_0 \pm i\epsilon} V|\psi^{(\pm)}\rangle}$$

- The leading **Born approximation** to the scattering amplitude is

$$\boxed{f^{(1)}(\mathbf{k}', \mathbf{k}) \propto \langle \mathbf{k}'|V|\mathbf{k}\rangle}$$

- The differential cross-section is given in terms of the scattering amplitude by

$$\boxed{\frac{d\sigma}{d\Omega} = |f(\mathbf{k}', \mathbf{k})|^2}$$

- Forces are transmitted by **virtual** mediating particles which are off-mass-shell:

$$\mathsf{P} \cdot \mathsf{P} = E^2 - \mathbf{p} \cdot \mathbf{p} \neq m^2$$

- The **Yukawa potential** for an exchanged particle of mass μ and coupling g is

$$\boxed{V(r) = \frac{g^2}{4\pi} \frac{e^{-\mu r}}{r}} \tag{4.11}$$

- The scattering amplitude contains a **vertex factors** g for any point where particles are created or annihilated

- The relativistic **propagator** factor is

$$\boxed{\frac{1}{\mathsf{P} \cdot \mathsf{P} - \mu^2}}$$

  for each virtual particle.

4.A Beyond Born: non-relativistic propagators §

Non examinable

To see how things develop if we don't want to rashly assume that $|\psi^{\pm}\rangle \approx |\phi\rangle$ it is useful to define a **transition operator** T such that

$$V|\psi^{(+)}\rangle = T|\phi\rangle$$

Multiplying the Lippmann-Schwinger equation (4.2) by V we get an expression for T

$$T|\phi\rangle = V|\phi\rangle + V\frac{1}{E - H_0 + i\epsilon}T|\phi\rangle.$$

Since this is to be true for any $|\phi\rangle$, the corresponding operator equation must also be true:

$$T = V + V\frac{1}{E - H_0 + i\epsilon}T.$$

This operator is defined recursively. It is exactly what we need to find the scattering amplitude, since from (4.5), the amplitude is given by

$$f(\mathbf{k}', \mathbf{k}) = -\frac{1}{4\pi}\frac{2m}{\hbar^2}(2\pi)^3\langle \mathbf{k}'|T|\mathbf{k}\rangle.$$

We can now find an iterative solution for T:

$$T = V + V\frac{1}{E - H_0 + i\epsilon}V + V\frac{1}{E - H_0 + i\epsilon}V\frac{1}{E - H_0 + i\epsilon}V + \dots \qquad (4.12)$$

We can interpret this series of terms as a sequence of the operators corresponding to the particle interacting with the potential (operated on by V) and propagating along for some distance (evolving as it goes according to $\frac{1}{E-H_0+i\epsilon}$).

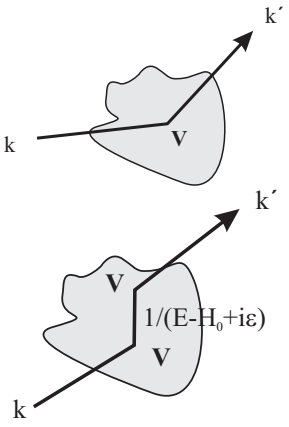

The operator

$$\boxed{\frac{1}{E - H_0 + i\epsilon}} \qquad (4.13)$$

is the non-relativistic **propagator**. Propagators are central to much of what we will do later on, so it is a good idea to try to work out what they mean. Physically the propagator can be thought of as a term in the expansion (4.12) which is giving a contribution the amplitude for a particle moving from an interaction at point A to another at point B. Mathematically it is a Greens function solution to the Lippmann-Schwinger equation in the position representation (4.3).

We are now in a position to quantify what we meant by a 'weak' potential earlier on. From the expansion (4.12) we can see that the first Born approximation (4.6) will be useful if the matrix elements of T can be well approximated by its first term V.

When is this condition likely to hold? Remember that the Yukawa potential was proportional to the square of a dimensionless coupling constant $\propto g^2$. If $g^2 \ll 1$ then successive applications of V introducing higher and higher powers of g and can

usually be neglected. This will be true for electromagnetism, since the dimensionless coupling relevant for electromagnetism is related to the fine structure constant

$$\frac{g^2}{4\pi} = \alpha = \frac{e^2}{4\pi\epsilon_0\hbar c} \approx \frac{1}{137}.$$

Since $\alpha \ll 1$, we can usually get away with just the first term of (4.12) for electric interactions (i.e. we can use the Born approximation).

Chapter 5

Feynman diagrams

5.1 Aim of the game

To calculate the probabilities for *relativistic* scattering processes we need to find out the Lorentz-invariant scattering amplitude which connects an initial state $|\Psi_i\rangle$ containing some particles with well defined momenta to a final state $|\Psi_f\rangle$ containing other (often different) particles also with well defined momenta.

We make use of a graphical technique popularised by Richard Feynman[1]. Each graph – known as a **Feynman Diagram** – represents a contribution to $\mathcal{M}_{fi}$. This means that each diagram actually represents a **complex number** (more generally a complex function of the external momenta). The diagrams give a pictorial way to represent the contributions to the amplitude.

In Feynman diagrams, spin-$\frac{1}{2}$ particles such as electrons are indicated with a straight line with an arrow.

Fermion line

The arrow follows the direction of particle flow, in the same was as in quark-flow diagrams (§3.3.3).

Diagrams consist of **lines** representing particles and **vertices** where particles are created or annihilated. I will place the incoming state on the left side and the outgoing state on the right side. Since the diagrams represent transitions between well-defined states in 4-momentum they already include the contributions from **all possible paths in both time and space** through which the intermediate particles might possibly have passed. This means that it is not meaningful to ask about the time-ordering of any of the internal events, since all possible time-orderings are necessarily included.

Photon line

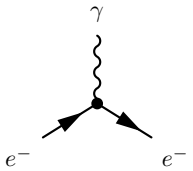

Vertex

[1] American physicist (1918-1988).

5.2 Rules for calculating diagrams

It turns out that are simple rules for calculating the complex number represented by each diagram. These are called the **Feynman rules**. In quantum field theory we can derive these rules from the Lagrangian density, but in this course we will simply quote the rules relevant for the Standard Model.

5.2.1 Vertices

Vertices are places where particles are created or annihilated. In the case of the electromagnetic interaction there is only **one** basic vertex which couples a photon to a charged particle with strength proportional to its charge.

To calculate the contribution to $\mathcal{M}_{fi}$, for each vertex we associate a **vertex factor**. For interactions of photons with electrons the vertex factor is of size $\boxed{-g_{\rm EM}}$ where $g_{\rm EM}$ is a dimensionless charge or **coupling constant**.[2] The coupling constant is a number which represents the strength of the interaction between the particle and the force carrier at that vertex. For the electromagnetic force the coupling strength must be proportional to the electric charge of the particle. So for the electromagnetic vertex we need a dimensionless quantity proportional to the charge. Recall that for the electromagnetic fine structure constant:

$$\alpha_{\rm EM} \equiv \frac{e^2}{4\pi\epsilon_0\hbar c} \approx \frac{1}{137}.$$

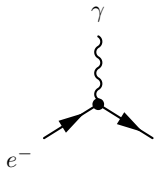

The electromagnetic vertex. The vertex factor is $-g_{\rm EM}$.

is dimensionless. It is convenient to choose $g_{\rm EM}$ such that

$$\alpha_{\rm EM} = \frac{g_{\rm EM}^2}{4\pi}.$$

In other words the coupling constant $g_{\rm EM}$ is a dimensionless measure of the $|e|$ where e is the charge of the electron. The size of the coupling between the photon and the electron is

$$-g_{\rm EM} = -\sqrt{4\pi\alpha_{\rm EM}}.$$

The electromagnetic vertex factor for any other charged particle f with charge $\mathcal{Q}_f$ times that of the proton is then

$$\boxed{g_{\rm EM}\mathcal{Q}_f}$$

So, for example, the electromagnetic vertex factor for an electron is of size $-g_{\rm EM}$ while for the up quark it is of size $+\frac{2}{3}g_{\rm EM}$.

[2] We are simplifying the situation by ignoring the spin of the electron. If spin is included the vertex factor becomes $-g_{\rm EM}$ times a matrix, in fact a Dirac gamma matrix, allowing the spin direction of the electron as represented by a 4-component spinor. For now we will ignore this complication and for the purpose of Feynman diagrams treat all spin $\frac{1}{2}$ fermions, such as electrons, muons, or quarks, as spinless. The Dirac matrices also distinguish electrons from anti-electrons. The sign of the vertex factor is well defined when the Dirac representations are used for the particles.

5.2.2 Anti-particles

An anti-particle has the same mass as its corresponding particle cousin, but his charge is the opposite to that of the particle.[3] The Feynman diagram for an anti-particle shows the arrow going the 'wrong' way (here right to left), since the particle flow is opposite to that of anti-particle.

Anti-fermion.

The same basic electromagnetic vertex is responsible for many different reactions. Consider each of the partial reactions

$$\begin{aligned} e^- &\rightarrow e^- + \gamma \\ e^- + \gamma &\rightarrow e^- \\ e^+ &\rightarrow e^+ + \gamma \\ e^+ + \gamma &\rightarrow e^+ \\ e^- + e^+ &\rightarrow \gamma \\ \gamma &\rightarrow e^- + e^+. \end{aligned} \tag{5.1}$$

Each of these is just a different time ordering of the same fundamental vertex that couples an electron to a photon.

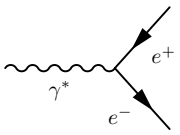

The electromagnetic vertex with particle-antiparticle final state

5.2.3 Distinct diagrams

A Feynman diagram represents all possible time orderings of the possible vertices, so the positions of the vertices within the graph are arbitrary. Consider the following two diagrams for $e^+ + e^- \rightarrow \mu^+ + \mu^-$:

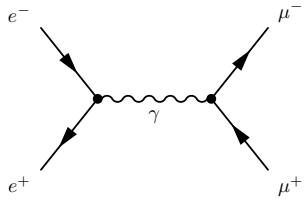

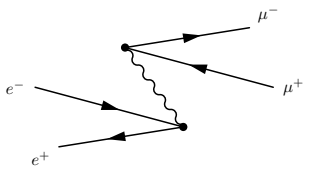

In the left diagram it appears that the incoming particles annihilated to form a virtual photon, which then split to produce the outgoing particles. On the right diagram it appears that the muons and the photon appeared out of the vacuum together, and that the photon subsequently collided with the electron and positron, leaving nothing. Changing the position of the internal vertices does not affect the Feynman diagram – it still represents the same contribution to the amplitude. The left side and right side just represent different time-orderings, so each is just a different way of writing the same Feynman diagram.

On the other hand, changing the way in which the lines in a diagram are connected

[3] In fact if the particle is charged under under more than one force then the anti-particle has the opposite values of all of those charges. For example an anti-quark, which has electromagnetic, strong and weak charges will have the opposite value of each of those compared to the corresponding quark.

to one another does however result in a new diagram. Consider for example the process $e^+ + e^- \rightarrow \gamma + \gamma$

In the two diagrams above the outgoing photons have been swapped. There is no way to move around the vertices in the second diagram so that it is the same as the first. The two diagrams therefore provide separate contributions to $\mathcal{M}_{fi}$, and must be added.

5.2.4 Relativistic propagators

For each internal line – that is each **virtual particle** – we associate a **propagator factor**. The propagator tells us about the contribution to the amplitude from a particle travelling through space and time (integrated over all space and time). For a particle with no spin, the **Feynman propagator** is a factor

$$\boxed{\frac{1}{\mathsf{Q}\cdot\mathsf{Q} - m^2}}$$

where $\mathsf{Q}\cdot\mathsf{Q} = E_{\mathsf{Q}}^2 - \mathbf{q}\cdot\mathbf{q}$ is the four-momentum-squared of the internal virtual particle[4].

These intermediate particles are called **virtual particles**. They do **not** satisfy the usual relativistic energy-momentum constraint $\mathsf{Q}\cdot\mathsf{Q} = m^2$. For an intermediate virtual particle,

$$\boxed{\mathsf{Q}\cdot\mathsf{Q} = E_{\mathsf{Q}}^2 - \mathbf{q}\cdot\mathbf{q} \neq \mathbf{m^2}.}$$

Such particles are said to be **off their mass-shell**.

If this inequality worries you, it might help you if you consider that their energy and momentum cannot be measured without hitting something against them. So you will never "see" off-mass-shell particles, you will only see the effect they have on other objects they interact with.

External particles in Feynman diagrams do always individually satisfy the relativistic energy-momentum constraint $E^2 - p^2 = m^2$, and for these particles we should therefor not include any propagator factor. The external lines are included in the diagram purely to show which kinds of particles are in the initial and final states.

[4] This propagator is the relativistic equivalent of the non-relativistic version of the Lippmann-Schwinger propagator $(E - H + i\epsilon)^{-1}$ that we found in non-relativistic scattering theory. Why are the forms different? Non-relativistic propagators are Greens functions for integration over all space. Relativistic propagators by contrast are Greens functions for integrations over both space and time.

Propagator example

Consider the annihilation-creation process $e^+ + e^- \to \gamma^* \to \mu^+ + \mu^-$ proceeding via a virtual photon γ^*. (The star on the particle name can be added to help remind us that it is off mass shell and virtual). We will ignore the spin of all the particles, so that we can concentrate on the vertex factors and propagators. The Feynman diagram is:

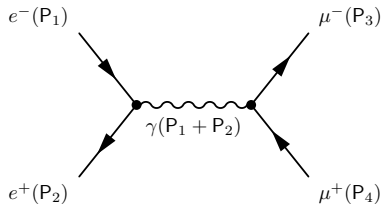

where we have labelled the four-momenta of the external legs. The diagram shows two vertices, and requires one propagator for the internal photon line. We can calculate the photon's energy-momentum four-vector Q_γ from that of the electron P_1 and the positron P_2. Four momentum is conserved **at each vertex** so the photon four-vector is $\mathsf{Q}_\gamma = \mathsf{P}_1 + \mathsf{P}_2$. Calculating the momentum components in the zero momentum frame:

$$\mathsf{P}_1 = (E, \mathbf{p}), \quad \mathsf{P}_2 = (E, -\mathbf{p}). \tag{5.2}$$

Conserving energy and momentum at the first vertex, the energy-momentum vector of the internal photon is

$$\mathsf{Q}_\gamma = (2E, \mathbf{0}).$$

So this *virtual* photon has more energy than momentum.

The propagator factor for the photon in this example is then

$$\frac{1}{(2E)^2 - m_\gamma^2} = \frac{1}{4E^2}.$$

The contribution to $\mathcal{M}_{fi}$ from this diagram is obtained my multiplying this propagator by two vectex factors each of size $g_{\rm EM}$. The modulus-squared of the matrix element is then

$$|\mathcal{M}_{fi}|^2 = \left| \frac{g_{\rm EM}^2}{4E_e^2} \right|^2.$$

We can get the differential scattering cross section by inserting this $|\mathcal{M}_{fi}|^2$ into Fermi's Golden Rule with the appropriate density of states

$$\frac{dN}{dp_\mu} = \frac{p_\mu^2 d\Omega}{(2\pi)^3},$$

and divide by an incoming flux factor $2v_e$. The differential cross section is then

$$d\sigma = \frac{1}{2v_e}\ 2\pi\ |\mathcal{M}_{fi}|^2\ \frac{p_\mu^2}{(2\pi)^3} \frac{dp_\mu}{d(E_0)}\ d\Omega.$$

A little care is necessary in evaluating the density of states. Overall momentum conservation means that only one of the two outgoing particles is free to contribute

to the density of states. The muon energy in the ZMF, for $E_\mu \gg m_\mu$ is $E_\mu = \frac{1}{2}E_0$, so

$$\frac{dp_\mu}{dE_0} = \frac{1}{2}\frac{dp_\mu}{dE_\mu},$$

where p_μ and E_μ are the momentum and energy of one of the outgoing muons. Since those muons are external legs they are on-shell so that

$$p_\mu^2 + m_\mu^2 = E_\mu^2.$$

Taking a derivative $p_\mu\, dp_\mu = E_\mu\, dE_\mu$. Inserting this into the F.G.R. we get

$$\frac{dp_\mu}{dE_0} = \frac{1}{2}\frac{dp_\mu}{dE_\mu} = \frac{1}{2}\frac{E_\mu}{p_\mu} = \frac{1}{2}\frac{1}{v_\mu} \approx \frac{1}{2}.$$

We then integrate over all possible outgoing angles to gain a factor of 4π and note that $g^2/4\pi = \alpha$, and that $\frac{p_\mu}{E_\mu} = v_\mu$. Gathering all the parts together, and taking the limit $v \to c$ we find we have a total cross-section for $e^+ + e^- \to \mu^+ + \mu^-$ of [5]

$$\sigma = \pi\frac{\alpha^2}{s}$$

where $s = (2E)^2$ is the square of the center-of-mass energy.

A quick check of dimensions is in order. The dimensions of s are $[E]^2$, while those of σ should be $[L]^2 = [E]^{-2}$. The fine structure constant α is dimensionless, so the equation is dimensionally consistent.

Other propagator examples

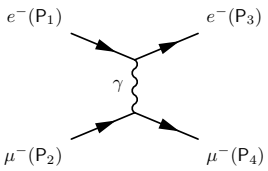

A Feynman diagram for electron–muon elastic scattering, via photon (γ) exchange.

In the previous example the virtual photon's four-momentum vector $(E, \mathbf{0})$ was time-like.

In the electron–muon scattering case $e^- + \mu^- \to e^- + \mu^-$ the virtual photon (γ^*) is exchanged between the electron and the muon. The virtual photon carries momentum and not energy, so the propagator is space-like.

To see this, transform to in the zero-momentum frame. In the ZMF the electron is kicked out with the same energy as it came in with, so it has received no energy from the photon, and conserving energy at the vertex $E_\gamma = 0$. The direction of the electron momentum vector *has* changed so it *has* received momentum from the photon, $\mathbf{p}_\gamma \neq 0$. Therefore $E_\gamma^2 - |\mathbf{p}|_\gamma^2 < 0$ and the propagator is space-like.

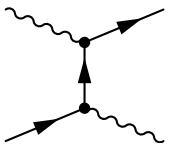

Feynman diagram for Compton scattering, with a virtual internal electron

An internal line requires a propagator regardless of the type of particle. An example of a process in which an electron is the virtual particle is the Compton process in which an electron scatters a photon

$$e^- + \gamma \to e^- + \gamma.$$

[5] Neglecting spin and relativistic normalization and flux factor issues – see 'caveats'.

5.2.5 Trees and loops

In principle to calculate $|\mathcal{M}_{fi}|$ we are supposed to draw and calculate all of the infinite number of possible Feynman diagrams. Then we have to add up all those complex numbers to get the total amplitude $\mathcal{M}_{fi}$.

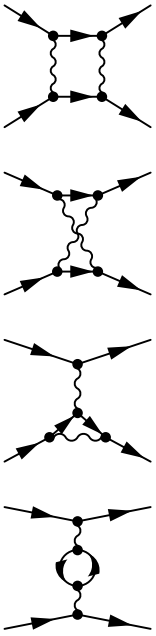

Some of the more complicated loop diagrams for electron–muon scattering.

However in practice we can get away with just summing the simplest diagram(s). To see why, we first note that the electromagnetic fine structure constant is small ($\alpha_{\mathsf{EM}} \ll 1$)

The simplest "tree level" scattering diagram has two vertices so contains two factors of g_{EM}. The diagrams with the loops contain four vertices and hence four factors of g_{EM}. Since $g_{\mathrm{EM}}^2/4\pi = \alpha_{\mathsf{EM}} \ll 1$, we can see that the more complicated diagrams with with more vertices will (all other things being equal) contribute much less to the amplitude than the simplest ones since they contain higher powers of α_{EM}. This process of truncating the sum of diagrams is a form of perturbation theory.

In general tree diagrams are those without closed loops. Loop diagrams – those with internal closed loops – tend to have larger powers of the coupling constant. A good approximation to $\mathcal{M}_{fi}$ can usually be obtained from the sum of the amplitudes for the 'leading order' diagrams – those with the smallest power of α_{EM} that make a non-zero contribution to $\mathcal{M}_{fi}$.

The other forces also have coupling constants, which have different strengths. The **strong force** is so-called because it has a fine structure constant close to 1 which is about a hundred times larger than α_{EM}. In fact the **weak force** actually has a larger coupling constant $\approx 1/29$ than the electromagnetic force $\approx 1/137$. The reason why this force appears weak is because the force is transmitted by very heavy particles (the W and Z bosons) so it is very short-range.

5.3 Key concepts

- Feynman (momentum-space) diagrams help us calculate relativistic, Lorentz-invariant scattering amplitudes.
- Vertices are associated with dimensionless **coupling constants** g with vertex factors that depend on the charge $\mathcal{Q}g$
- Internal lines are integrated over **all time and space** so include all internal time orderings.
- Intermediate/virtual/off-mass-shell particles have $\boxed{\mathsf{Q}^2 \neq m^2}$ and have propagators $\boxed{\dfrac{1}{\mathsf{Q}^2 - m^2}}$.
- For fermions, arrows show the sense of particle flow. Anti-particles have arrows pointing the "wrong way".

Caveats

- Sometimes you will see books define a propagator with a plus sign on the bottom line: $1/(q^2 + m^2)$. One of two things is going on. Either (a) q^2 is their notation for a four-vector squared, but they have defined the metric $(-,+,+,+)$ in the opposite sense to us so that $q^2 = -m^2$ is their condition for being on-mass-shell *or* (b) q^2 is acually intended to mean the three-momentum squared. A bit of context may be necessary, but regardless of the convention used the propagator should diverge in the case when the virtual particle approaches its mass-shell.
- We have not attempted to consider what the effects of spins would be. This is done in the fourth year after the introduction of the Dirac equation – the relativistic wave equation for spin-half particles. The full treatment is done in e.g. Griffiths Chs. 6 & 7.
- We have played fast and loose with phase factors (at vertices and overall phase factors). You can see that this will not be a problem so long as only one diagram is contributing to $\mathcal{M}_{fi}$, but clearly relative phases become important when adding diagrams together.
- Extra rules are needed for diagrams containing loops, because the momenta in the loops are not fully constrained. In fact one must integrate over all possible momenta for such diagrams. We will not need to consider such diagrams in this course.
- The normalization of the incoming and ougtoing states needs to be considered more carefully. The statement "*I normalize to one particle per unit volume*" is **not** Lorentz invariant. The volume of any box at rest will compress by a factor of $1/\gamma$ due to length contraction along the boost axis when we Lorentz transform it. For relativistic problems we want to normalize to a Lorentz invariant number of particles per unit volume. To achieve this we conventionally normalize to $1/(2E)$ particles per unit volume. Since $1/(2E)$ also scales like $1/\gamma$ it transforms in the same manner as V. Therefore the statement "*I normalize to* $1/(2E)$ *particles per unit volume*" **is** Lorentz invariant.

Terminology

$\mathcal{M}_{fi}$	Lorentz invariant amplitude for $\|\Psi_i\rangle \to \|\Psi_f\rangle$ transition
Feynman diagram ...	Graphical representation of part of the scattering amplitude
Vertex	Point where lines join together on such a graph
Constant coupling (g)	Dimensionless measure of strength of the force
Vertex factor ($\mathcal{Q}g$) ..	The contribution of the vertex to the diagram
Propagator	Factor of $1/(\mathrm{Q}\cdot\mathrm{Q} - m^2)$ associated with an internal line
Tree level / leading order	Simplest diagrams for any process with the smallest number of g factors. Contain no closed loops.

References and further reading

- *"Introduction to Elementary Particles"* D. Griffiths Chapters 6 and 7 does the full relativistic treatment, including spins, relativistic normalization and relativistic flux factor.
- *"Femptophysics"*, M.G. Bowler – contains a nice description of the connection between Feynman propagators and non-relativistic propagators.
- *"Quarks and Leptons"*, Halzen and Martin – introduction to the Dirac equation and full Feynman rules for QED including spin.
- *"QED - The Strange Theory of Light and Matter"*, Richard Feynman. Popular book with almost no maths. Even a PPE student could understand it – if you explained it slowly to him. In fact it has a lot to recommend it, not least that you can buy it for about five points.

Chapter 6

The Standard Model

The Standard Model of particle physics provides the most accurate description of nature at the subatomic level. It is based on the quantum theory of fields and has been tested with exquisite precision. In the quantum field theory there is one field for each type of particle – matter particles and force particles.

6.1 Matter particles

The fundamental matter particles in the Standard Model are the **quarks** and the **leptons**. All are spin-half point-like fermions.

We introduced the six quarks in §3 their distinguishing characteristic is that they are charged ('coloured') under the strong force and as a result they are always found to be confined within hadrons.

The second class of matter particles is the **leptons**. These are also spin-$\frac{1}{2}$ fermions but unlike the quarks they do not have any strong interactions, because they carry no colour charge. Like the quarks, there are three families of leptons. The lightest generation (or family) contains the electron e^- and its partner neutrino ν_e.

The second generation consists of the muon μ^- and its partner neutrino ν_μ. The muon is very similar to the electron with the same ($\mathcal{Q} = -1$) electric charge, but is about 200 times heavier. The larger mass of the muon means that it accelerates less than the electron in electric fields, therefore it emits less electromagnetic radiation than the electron when passing through material. Muons are therefore highly penetrating. High energy muons created in the upper atmosphere are able to pass through the atmosphere and can be observed on the earth's surface. The muon lifetime is $2.2\,\mu s$ after which it decays as follows

$$\mu^- \rightarrow e^- + \bar{\nu}_e + \nu_\mu.$$

The third generation contains the tau τ^- and its neutrino ν_τ. The tau also has $\mathcal{Q} = -1$, and is heavier again: about 3,500 times heavier than the electron. The

	Quarks		**Leptons**	
Generation	$\mathcal{Q} = -\frac{1}{3}$	$\mathcal{Q} = +\frac{2}{3}$	$\mathcal{Q} = -1$	$\mathcal{Q} = 0$
First	down (d) $\sim$ 5 MeV	up (u) $\sim$ 2.5 MeV	electron (e) 0.511 MeV	e neutrino (ν_e) < 1 eV
Second	strange (s) ~ 101 MeV	charm (c) 1270 MeV	muon (μ) 105.7 MeV	μ neutrino (ν_μ) < 1 eV
Third	bottom (b) 4200 MeV	top (t) 172 GeV	tau (τ) 1777 MeV	τ neutrino (ν_τ) < 1 eV

Table 6.1: The quark and lepton families, their masses and their charges $\mathcal{Q}$. All are spin-$\frac{1}{2}$ fermions. The corresponding anti-particles have the same masses as the particles, but the opposite charges. The fermionic particles have positive parity while their anti-particles have negative parity.

tau lepton decays very rapidly in 2.9×10^{-13} s. It can decay to either an electron or a muon (plus associated neutrinos)

$$\begin{aligned} \tau^- &\rightarrow e^- + \bar{\nu}_e + \nu_\tau \\ \tau^- &\rightarrow \mu^- + \bar{\nu}_\mu + \nu_\tau \end{aligned}$$

These are not the only options. Because the τ has a mass larger than many hadrons, it also decays into hadrons, through reactions such as

$$\begin{aligned} \tau^- &\rightarrow \pi^- + \nu_\tau \\ \tau^- &\rightarrow \pi^- + \pi^0 + \nu_\tau \\ \tau^- &\rightarrow \pi^- + \pi^+ + \pi^- + \nu_\tau \\ \tau^- &\rightarrow K^- + \nu_\tau. \end{aligned}$$

A summary of the some of the most important properties of the six quarks and six leptons can be found in Table 6.1.

6.1.1 Lepton flavour number

It is useful to define quantum numbers that count the number of leptons. Associated with each lepton is an anti-lepton. We can define **lepton flavour numbers** to be the number of leptons of each generation less the number of corresponding anti-leptons in that generation:

$$\begin{aligned} L_e &= N(e^-) + N(\nu_e) - N(e^+) - N(\bar{\nu}_e) \\ L_\mu &= N(\mu^-) + N(\nu_\mu) - N(\mu^+) - N(\bar{\nu}_\mu) \\ L_\tau &= N(\tau^-) + N(\nu_\tau) - N(\tau^+) - N(\bar{\nu}_\tau) \end{aligned}$$

We can also define a **total lepton number** $L_\ell = L_e + L_\mu + L_\tau$. Total lepton number is conserved in all known reactions. The individual lepton flavour numbers are also

Force	Quantum	Symbol	Mass	Spin	α	Range
Electromagnetic	Photon	γ	0	1	$\frac{1}{137}$	∞
Strong	Gluon ($\times 8$)	g	0	1	~ 1	$\sim 10^{-15}$ m
Weak	$W^{\pm}$		80.4 GeV	1	$\frac{1}{29}$	$\sim 10^{-18}$ m
	Z^0		91.2 GeV	1		
Gravity	Graviton?	G	0	2?		∞

Table 6.2: The force-carrying particles γ, g, $W^{\pm}$ and Z^0 of the Standard Model. The spin is in units of $\hbar$. The symbol α indicates the corresponding dimensionless 'fine structure constant'.

conserved in most reactions. The exception is in the phenomenon of neutrino oscillation, which we shall meet later (§6.5).

6.2 Force particles

There are four fundamental forces which act on the matter particles (Table 6.2). They are: electromagnetism, the weak nuclear force, the strong nuclear force and gravity.

The gravitational force is a special case. It is very familiar, but at the level of individual subatomic particles is so much weaker than the other forces that it has a negligible effect. This makes it difficult to study, and so the microscopic mechanism behind gravitation is yet to be fully understood. We will not discuss it further in this course.

Each of the other three forces is known to be carried by an intermediate particle or particles. The mediating particles are excitations of the associated fields and are **spin-1 bosons**.

The quantum of the electromagnetic force is the **photon**, which is a massless boson with no electrical charge. It is through virtual photons that electromagnetic forces are transmitted between charges. The scattering process by virtual photons is described in §5. The quantum theory of electromagnetism is known as **quantum electrodymanics** or QED.

The electromagnetic interaction is felt by all charged particles. The vertex factor for a particle of with charge quantum number $\mathcal{Q}$ is $\mathcal{Q}g_{\rm EM}$ where $\frac{g_{\rm EM}^2}{4\pi} = \alpha_{\rm EM}$. For example, the u-quark has charge $\mathcal{Q} = \frac{2}{3}$, so the coupling strength in the $uu\gamma$ vertex

is only two thirds as large as that in the $ee\gamma$ vertex, and of the opposite sign.

The electromagnetic interaction does not change quark flavour, nor lepton flavour. Flavour-changing vertices such as:

$$\mu^- + \gamma \not\rightarrow e^- \qquad \text{[violates lepton flavour - forbidden}$$
$$u + \gamma \not\rightarrow c \qquad \text{[violates quark flavour - forbidden}$$

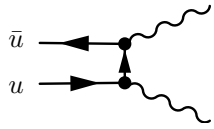

Feynman diagram for neutral pion decay

are forbidden in electromagnetism.

Decays which do not require changes in flavour quantum numbers may proceed via the electromagnetic interaction, for example the decay of the neutral pion to two photons

$$\pi^0 \longrightarrow \gamma + \gamma.$$

Another example is the decay of the Σ^0 baryon to the Λ^0 baryon, both of which having quark content uds,

$$\Sigma^0 \longrightarrow \Lambda^0 + \gamma.$$

6.3 The strong force and the gluon

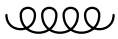

Gluon line.

The quantum theory of the strong force is known as **quantum chromodynamics** or QCD. The strong force is mediated by spin-1, massless particles known as **gluons**. The gluons couple to colour charge, rather like the photons couple to electromagnetic charge. Since the leptons have no colour charge, they do not interact with gluons, and hence do not interact via the strong force.

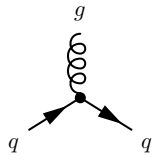

A quark-gluon vertex

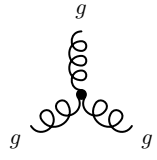

Three-gluon vertex

Quarks carry colour, r, g and b. Anti-quarks carry anti-colour $\bar{r}$, $\bar{g}$ and $\bar{b}$. Each gluon carries both colour and anti-colour. We might then think that there should be $3 \times 3 = 9$ gluons. However one of those nine combinations

$$\frac{1}{\sqrt{3}}(|r\bar{r}\rangle + |g\bar{g}\rangle + |b\bar{b}\rangle)$$

is colourless, and so there are $3^2 - 1 = 8$ orthogonal gluon states. Total colour charge is conserved at each vertex, with any change in the colour of the quark being introduced or carried away by the gluon.

The strong interaction has a larger coupling constant than the electromagnetic force

$$\alpha_S \sim 1 \qquad \text{whereas} \qquad \alpha_{\rm EM} \approx \frac{1}{137},$$

A precise theory

Non-examinable

Quantum electrodynamics has been tested to amazing accuracy. The most precise measurement is of the gyromagnetic ratio g_e of the electron. We define g by the equation

$$\boldsymbol{\mu} = -\frac{g}{2}\frac{e}{m_e}\mathbf{s}$$

where $\boldsymbol{\mu}$ is the electron's magnetic moment, e is the magnitude of its charge, and $\mathbf{s}$ is its spin. The Dirac theory of electromagnetism predicts that

$$g_e^{\mathrm{dirac}} = 2.$$

The Dirac theory prediction is the value obtained by considering the direct coupling of photons to the charge. If one includes the one-loop correction, the prediction can be refined to

$$g_e^{\mathrm{one-loop}}/2 = 1 + \frac{1}{2}\frac{\alpha_{\mathrm{EM}}}{\pi} \approx 1.0011$$

The experimental and theoretical measurements have been improving in precision almost in parallel, competing for higher precision. The current best experimental measurement [10] has been made with the extraordinary accuracy of better than one part per trillion:

$$g^{\mathrm{experiment}}/2 = 1.001\,159\,652\,180\,7\,(3),$$

where the number in brackets shows the uncertainty in the last digit.
To achieve this level of accuracy in the theory, one must calculate a very large number of Feynman diagrams (there are 891 four-loop diagrams and 12672 five-loop diagrams). The five-loop theoretical calculation [4] was completed in 2012, giving

$$g^{\mathrm{theory}}/2 = 1.001\,159\,652\,181\,8\,(8),$$

in agreement with the experimental measurement.

Why eight gluons?

Non-examinable

There are three colours of quarks, which we have labelled r, g and b. We can place them in a basis such that:

$$|r\rangle = \begin{pmatrix} 1 \\ 0 \\ 0 \end{pmatrix} \qquad |g\rangle = \begin{pmatrix} 0 \\ 1 \\ 0 \end{pmatrix} \qquad |b\rangle = \begin{pmatrix} 0 \\ 0 \\ 1 \end{pmatrix}$$

Colour forms a 3-dimensional Hilbert space, and so for colour transformations, induced by gluons, we want the set of linear operators on that space. This can be represented by the group of 3×3 unitary matrices with unit determinant, which is called $SU(3)$.

A group $SU(N)$ has $N^2 - 1$ degrees of freedom (the -1 coming from the requirement of unit determinant). There are therefore $2^2 - 1 = 3$ Pauli matrices acting on the two-dimensional Hilbert space for a spin-half particle. There are $3^2 - 1 = 8$ generators of $SU(3)$ for the three-dimensional complex space of colour. The eight matrices $\{T_1, T_2, \ldots T_8\}$ are the generators and are traceless, Hermitian matrices. They can be represented by $T_a = i\frac{1}{2}\lambda_a$, where the λ_a are the Gell-Mann matrices

$$\lambda_1 = \begin{pmatrix} 0 & 1 & 0 \\ 1 & 0 & 0 \\ 0 & 0 & 0 \end{pmatrix} \qquad \lambda_2 = \begin{pmatrix} 0 & -i & 0 \\ +i & 0 & 0 \\ 0 & 0 & 0 \end{pmatrix} \qquad \lambda_3 = \begin{pmatrix} 1 & 0 & 0 \\ 0 & -1 & 0 \\ 0 & 0 & 0 \end{pmatrix}$$

$$\lambda_4 = \begin{pmatrix} 0 & 0 & 1 \\ 0 & 0 & 0 \\ 1 & 0 & 0 \end{pmatrix} \qquad \lambda_5 = \begin{pmatrix} 0 & 0 & -i \\ 0 & 0 & 0 \\ i & 0 & 0 \end{pmatrix} \qquad \lambda_6 = \begin{pmatrix} 0 & 0 & 0 \\ 0 & 0 & 1 \\ 0 & 1 & 0 \end{pmatrix}$$

$$\lambda_7 = \begin{pmatrix} 0 & 0 & 0 \\ 0 & 0 & -i \\ 0 & +i & 0 \end{pmatrix} \qquad \lambda_8 = \begin{pmatrix} 1 & 0 & 0 \\ 0 & 1 & 0 \\ 0 & 0 & -2 \end{pmatrix}$$

the three-dimensional analogues of the Pauli matrices. A transformation in colour space can then be represented by the unitary transformation

$$|\Psi\rangle \longrightarrow \exp\left(\vec{\lambda} \cdot \vec{\alpha}\right) |\Psi\rangle$$

for some eight-dimensional vector $\vec{\alpha}$.

meaning that if both forces are present, the strong force tends to dominate. The largeness of the strong coupling constant g_S also means that if a reaction can occur both through the strong force and the electromagnetic force, the strong force reaction can be expected to dominate.

However the strong force is more than just a stronger version of the electromagnetic interaction. Gluons (unlike photons) can act as sources for their own field. This means that there is a gluon self-interaction force, involving a three-gluon interaction vertex. This makes a dramatic difference to the way the strong force works.

The self-interactions of gluons help us better understand quark confinement. Consider pulling a meson apart by slowly separating the quark from the antiquark. There is an attractive strong force between the quark and the antiquark, carried by a field of virtual gluons. The self-interaction of the gluons pulls this field into a narrow tube or string of colour-field, which connects the quark with the anti-quark. The cross section of the string, and hence the energy per unit length of the string is approximately constant. When the quark and anti-quark are separated, the string is stretched and the potential energy increases linearly with separation. This phenomenon leads to a term in the strong potential $V(r)$ proportional to r, which then dominates at large separation (see §3.6, equation (3.4)).

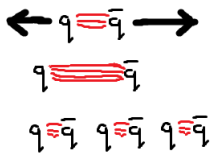

Meson production caused by rapidly separating quarks. A similar mechanism forms baryon-antibaryon pairs.

When sufficient energy has built up in the string it becomes energetically favourable for the string to break by dragging multiple quark-antiquark pairs out of the vacuum. The quarks and anti-quarks rapidly gather together into colour-neutral combinations – mesons or barons. It is those hadrons that are experimentally observed if a quark and an antiquark are forcibly separated. The relativistic 'headlight effect' squeezes the emitted hadrons into a narrow cone or 'jet' of hadrons.

Consider the high energy collision process

$$e^+ + e^- \rightarrow q + \bar{q}.$$

At high energy this process produces a rapidly separating quark-antiquark pair. Each quark leads to a jet of hadrons. The experimental verification of this can be seen in Figure 6.1. The jets indicate the directions, momenta and energies of the out-going quark and anti-quark.

Gluons are coloured particles so, like quarks, they cannot exist in isolation. Gluons cannot be seen directly, but their presence can be inferred. The gluon was discovered in reactions of the sort

$$e^+ + e^- \rightarrow q + \bar{q} + g$$

where the outgoing high-momentum gluon is emitted at large angle from both the quark and the anti-quark. Since each of the three outgoing particles is coloured, each must pull quarks and anti-quarks out of the vacuum to form neutral hadrons. The result is an event containing three jets of hadrons, each following the direction of one of the three out-going coloured particles (Figure 6.2).

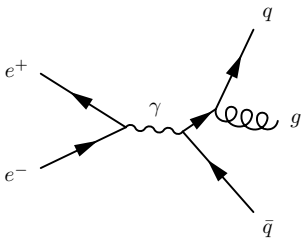

Feynman diagram with gluon emission leading to a three-jet event.

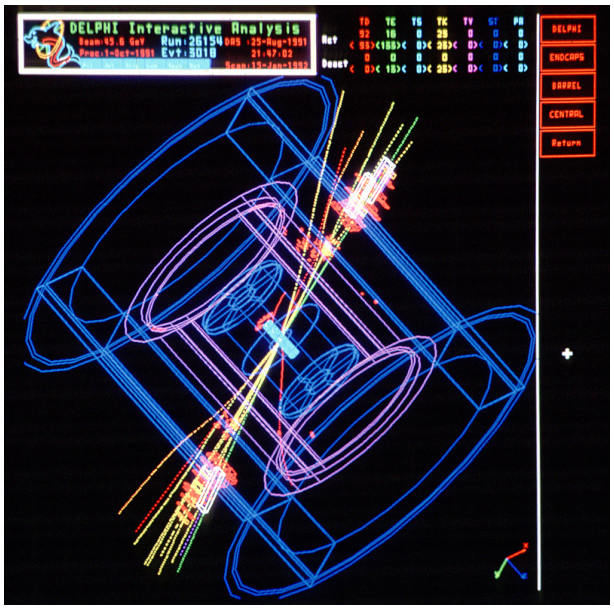

Figure 6.1: A two-jet event in the Delphi detector at a electron-positron centre-of-mass energy close to 100 GeV. © CERN 1992.

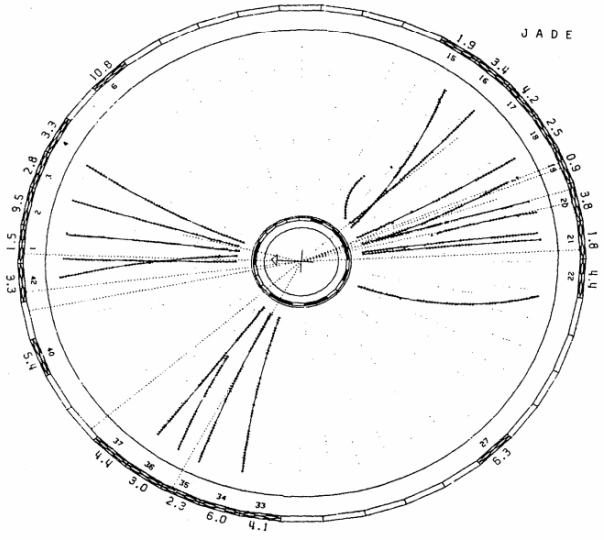

Figure 6.2: A three-jet event in the JADE detector. The process $e^+ + e^- \rightarrow q + \bar{q} + g$ leads to three jets, one from each of the three coloured particles.

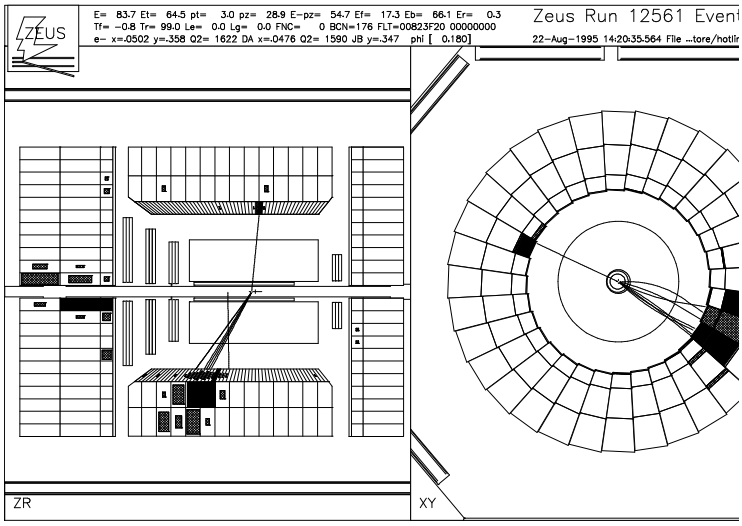

Figure 6.3: Longitudinal (left) and transverse (right) event display showing the debris from a deep inelastic scattering event, as measured in the Zeus detector. The electron has entered the detector from the left hand side on the transverse view, and the proton from the right hand side. The scattered electron forms an isolated track, terminating in an energy deposit in the calorimeter. A jet of hadrons recoils against the scattered electron.

6.3.1 Deep inelastic scattering

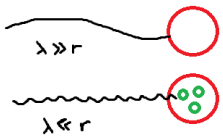

A high momentum probe can resolve the substructure of the proton.

Though it seems to be impossible to isolate an individual quark, it is still possible to perform scattering experiments at the quark level. Consider a high-momentum electron scattering from a proton. A high-momentum electron can resolve distances of order $\frac{\hbar}{p}$. If the momentum is larger than about $1\,\text{GeV}$ (so that its de Broglie wavelength λ is much smaller than the radius of the proton) then it will not scatter coherently from the proton as a whole. Instead it will resolve the proton's internal structure — and at sufficiently high momentum will act as if it has been scattered from one of the constituent quarks.

The scattering of a probe from a quark inside a hadron is known as deep inelastic scattering.[1]

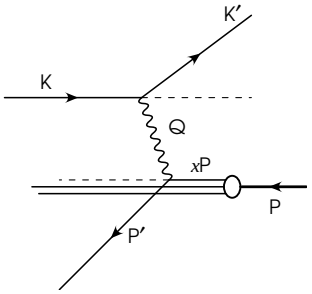

Scattering of an electron (momentum K→K′) from quark (momentum xP) within a proton (momentum P).

The force is transmitted by a virtual photon of momentum Q = K − K′. Note that unusually here the incoming proton is on the right side and the outgoing fragments of that proton are on the left side of the diagram.

At high energies, the energy of the out-going quark will be much larger than typical hadron masses. As the quark is pulled away from the other quarks, some the energy is transferred into the string of gluon field lines that connect the quark and the anti-quark. Eventually the energy is high enough to pull quark-antiquark pairs out of the vacuum. What we observe is a jet of hadrons pointing in the direction of the original outgoing quark. The unscattered 'spectator' quarks in the proton also form a coloured state, and so must also form into hadrons.

Scattering experiments of this sort were performed at the HERA electron-proton collider, near Hamburg. Protons were accelerated to energy of $E_p = 920\,\text{GeV}$, and electrons to energies of $E_e = 27.5\,\text{GeV}$. A quark is scattered out of the proton by

[1] Deep because we are probing deep inside the hadron.

the incident electron. In Figure 6.3 we can see a display of such a scattering event. The scattered electron produces a single track terminating in an energy deposit in the calorimeter. Recoiling against that electron is a jet of hadrons pointing in the direction of the scattered quark. A further jet of hadrons can be seen in the transverse section close to the beam line, formed from the proton di-quark remnant.

Though the individual quark cannot be observed, the jet of hadrons tell us about its direction and momentum, and the electron behaves as if it were scattering from a point-like spin-half particle.

6.3.2 Further evidence for quarks and colour: R

Further evidence for the existence of both quarks and colour can be found in when quark-antiquark pairs are created in electron-positron scattering. Consider the ratio

$$R \equiv \frac{\sigma(e^+ + e^- \to \text{hadrons})}{\sigma(e^+ + e^- \to \mu^+\mu^-)}.$$

Each process involves the collision of an electron and its anti-particle, a transition through a short-lived virtual photon.

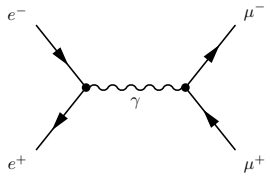

Feynman diagram for electron-positron annihilation, via a virtual photon to a muon-antimuon pair.

The denominator comes from

$$e^+ + e^- \to \gamma^* \to \mu^+\mu^-$$

At the quark level the numerator comes from

$$e^+ + e^- \to \gamma^* \to q + \bar{q}$$

where various different quark flavours may contribute, depending on the centre-of-mass energy available.

The coupling of the photon to the quark i is proportional to the quark charge $\mathcal{Q}_i$. The Feynman diagram for the amplitude for production of the quark-antiquark pair is therefore proportional to $\mathcal{Q}_i$. The rate will therefore be proportional to the mod-squared of the amplitude, and so

$$\sigma_i \propto \Gamma_i \propto \mathcal{Q}_i^2$$

The corresponding amplitude for the creation of the muon-antimuon pair will look the same, but with $\mathcal{Q}(\mu) = 1$

The density-of-states factor for the muon and the quarks are also very similar, provided that $E \gg m$, so that $E \approx p$ for each out-going particle. The main difference in the density of states is that there are three different colours of quarks for any spin and momentum state, so the total density of states for any quark flavour is a factor of three larger than for the corresponding muon. We therefore expect that the value of the ratio will be

$$R = \frac{3 \times \sum_i \mathcal{Q}_i^2}{1 \times 1^2}$$

where the sum is over the $q\bar{q}$ states available at the given centre-of-mass energy, that is those with $m_q < E_{\text{cm}}/2$. Measurements confirm that as the threshold energy for production of new $c\bar{c}$ and $b\bar{b}$ states is passed, the value of R increases as expected. The value of R is also consistent with the three different colours of quarks.

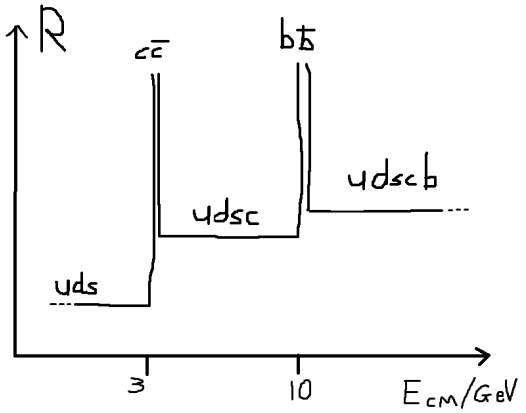

Figure 6.4: Sketch of the ratio of cross sections $R \equiv \frac{\sigma(e^+ + e^- \to \text{hadrons})}{\sigma(e^+ + e^- \to \mu^+ \mu^-)}$.

6.4 The weak interaction: W and Z particles

The weak interaction is mediated by three particles, the charged $W^\pm$ bosons and the neutral Z^0 boson. The W^+ and W^- are antiparticles of one another, while the Z^0, like the photon, is its own antiparticle.

The W and Z particles are spin-1 bosons. The weak force is very short range as a result of their large masses.

$$\boxed{m_W = 80.3\,\text{GeV}} \qquad \boxed{m_Z = 91.2\,\text{GeV}}$$

which from their approximate range $\hbar c/mc^2$ is about 2×10^{-3} fm, which is about 1000 times smaller than the size of the proton.

The weak force is responsible for all flavour-changing reactions. The only particles capable of changing quark flavour are the $W^\pm$ bosons. For example the beta decay of the neutron

$$n \to p + e^- + \bar{\nu}_e$$

requires us to change a d quark into a u quark. This can occur with the emission of a highly virtual W^- which subsequently produces an electron and a neutrino. For this reaction to proceed it is clear that the W boson must be able to interact both with the quarks and with the leptons.

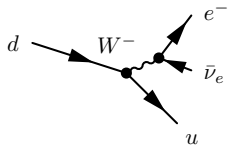

β decay

The emission or absorption of a $W^\pm$ particle changes an up-type quark (u, c or t) into a down-type quark (d, s, or b) or vice versa. For example, the decay of a K^+ meson

$$K^+ \to \pi^0 + \pi^+$$

at the quark level is mediated by a virtual W boson

$$u + \bar{s} \to u + \bar{u} + \left(W^+ \to u + \bar{d}\right).$$

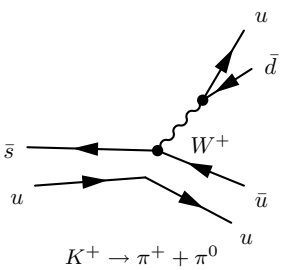

$K^+ \to \pi^+ + \pi^0$

The coupling of the W boson to leptons is **universal**. The vertex factor for each is takes the same value of g_W. This means that the W^- is equally likely to decay to

any of the three lepton species:

$$\begin{aligned} W^- &\rightarrow e^- + \bar{\nu}_e \\ W^- &\rightarrow \mu^- + \bar{\nu}_\mu \\ W^- &\rightarrow \tau^- + \bar{\nu}_\tau. \end{aligned}$$

The coupling constants are equal, and the density of states factors are very similar since each of the decay products is highly relativistic, so the rates for each lepton flavour are identical.

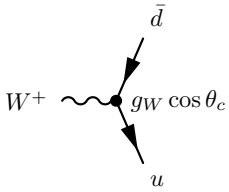

A vertex involving a W and two quarks must include an upper $\mathcal{Q} = +\frac{2}{3}$ quark and a lower $\mathcal{Q} = -\frac{1}{3}$ quark. The vertices which include two quarks from the same generation dominate, while those involving transitions between generations are suppressed. The preference of the W boson for 'keeping it in the family' is one of the reasons why the concept of generations (or families) is useful.

In the first and second generations the couplings for vertices within the same generation — i.e. the vertices for the (W, u, d) vertex or for the (W, c, s) vertex take the value

$$g_W \times \cos\theta_C,$$

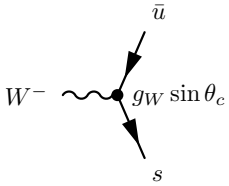

where the θ_C, the **Cabibbo angle**, is about 13°.

The inter-generational couplings between the first and second generations – i.e. the vertex factors for the (W, u, s) vertex and the (W, c, d) vertex — are suppressed by the sine of the Cabibbo angle,

$$g_W \times \sin\theta_C.$$

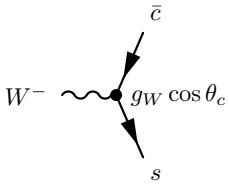

The effect of this same-family favouritism can be seen, for example, when a hadron containing a charm quark decays, when it is likely to produce other hadrons containing strange quarks, since the (W, c, s) vertex is not Cabibbo suppressed.

An explanation for the relative sizes of the couplings can be found if we consider the down-type quarks to have weak interaction eigenstates, $|d'\rangle$ and $|s'\rangle$, each of which is a superposition of the two mass eigenstates $|d\rangle$ and $|s\rangle$. In the interaction basis the couplings of the W are diagonal, so the (W, u, d') and the (W, c, s') couplings each take the same value g_W, whereas the couplings for (W, u, s') and (W, c, d') are each zero.

The flavour eigenstates $\{|d'\rangle, |s'\rangle\}$ in the primed basis must differ from the mass eigenstates $\{|d\rangle, |s\rangle\}$ in the un-primed basis. This can be achieved by rotating the states by a matrix

$$\begin{pmatrix} |d'\rangle \\ |s'\rangle \end{pmatrix} = V_{\rm c} \begin{pmatrix} |d\rangle \\ |s\rangle \end{pmatrix}$$

where the 2×2 Cabibbo rotation matrix is given by

$$V_c = \begin{pmatrix} \cos\theta_c & -\sin\theta_c \\ \sin\theta_c & \cos\theta_c \end{pmatrix}.$$

Three-generation flavour mixing

In the diagram below the solid lines show the unsuppressed transitions, while the dashed and dotted lines show progressively more suppressed transitions for decays between quarks of all three generations.

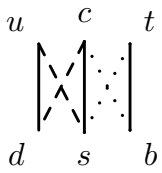

The three-generational extension of the Cabibbo matrix is the 3×3 unitary 'CKM' matrix,

$$V_{\rm CKM} \sim \begin{pmatrix} \square & \square & \cdot \\ \square & \square & \cdot \\ \cdot & \cdot & \square \end{pmatrix}.$$

where the larger boxes indicate larger couplings, and the dots show small couplings. The upper-left 2×2 block of the CKM matrix contains the mixing between the first two generations, which is also represented by the simpler 2×2 Cabibbo matrix.

The third generation is almost completely decoupled from the first two. Couplings involving either t or b any any of the quarks from the first two generations are very small. Top quarks almost always produce b quarks in when they decay. Hadrons containing b quarks have CKM suppressed decays and can travel macroscopic distances before they decay.

6.4.1 The Z^0 particle

The third weak boson is the Z^0. Like the $W^\pm$ bosons it is about 100 times heavier than the proton. Unlike the $W^\pm$ bosons it is electrically neutral.

The Z^0 also interacts with all of the fundamental fermions. Indeed since the neutrinos have no electrical or colour charge, interactions involving the weak force are the *only* way in which they may interact. The first evidence for the Z^0 boson was the discovery of scattering of neutrinos via the 'neutral current' exchange of a Z^0 boson.

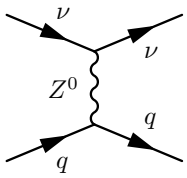

Neutral current neutrino scattering

The Z^0 does *not* change quark or lepton flavour, so there is for example no (u, c, Z^0) vertex. This is an example of the rule that there are 'no flavour-changing neutral currents' in the Standard Model. The branching ratios of the Z^0 to the different charged leptons are all consistent with one another, demonstrating that the couplings to each generation of leptons are equal.

ℓ	$\mathcal{B}\left(Z^0 \to \ell^+ + \ell^-\right)$
e	$(3.363 \pm 0.004)\%$
μ	$(3.367 \pm 0.007)\%$
τ	$(3.370 \pm 0.008)\%$

The branching ratios of Z^0 boson to different charged leptons are all consistent with one another. [12].

6.4.2 Production and decay of the $W^\pm$ and Z^0 particles

The $W^\pm$ and Z^0 particles were first directly observed in 1983 in proton-antiproton collisions at the CERN Sp$\bar{\text{p}}$S proton-antiproton collider. The $p\bar{p}$ centre-of-mass energy of 540 GeV was sufficiently high that, even though the incoming (anti-)quarks carried only a fraction of the (anti-)proton momenta, collisions with $q - \bar{q}$ centre-of-mass energy close to the ~ 100 GeV mass of the W or Z were likely.

In each case the intermediate vector bosons are created when a quark from the proton annihilates with an anti-quark from the anti-proton. To produce a Z^0 the quarks must be of the same flavour — either $u + \bar{u}$ or $d + \bar{d}$. To produce a W^+ or a W^-, the combinations $u + \bar{d}$ and $d + \bar{u}$ respectively are required.

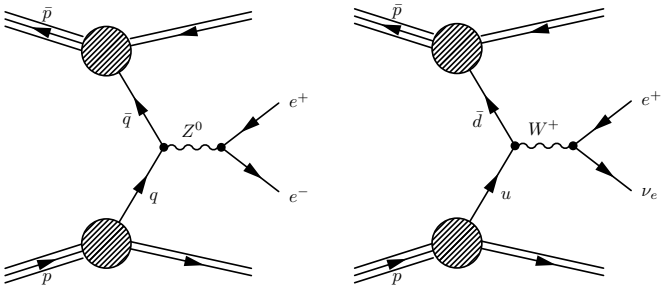

The diagrams above show the production of the Z^0 (left) and the W^+ boson (right) in proton-proton collisions, followed by their leptonic decays.

If the quark carries momentum fraction x_1 of the proton, and the anti-quark carries momentum fraction x_2 of the anti-proton, then to produce a Z^0 close to its mass

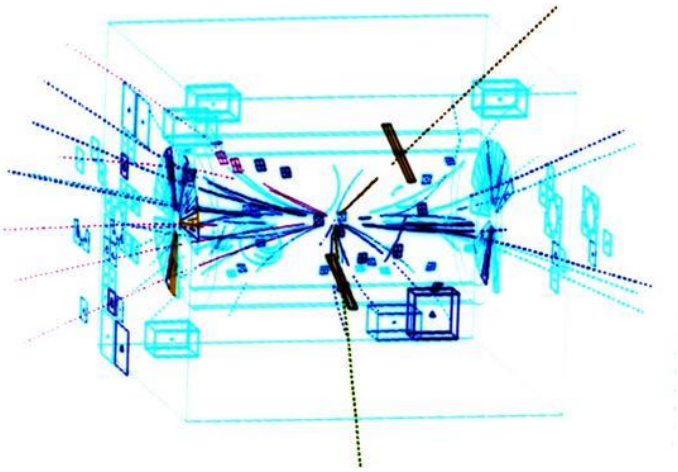

$q + \bar{q} \rightarrow Z^0 \rightarrow e^+ + e^-$

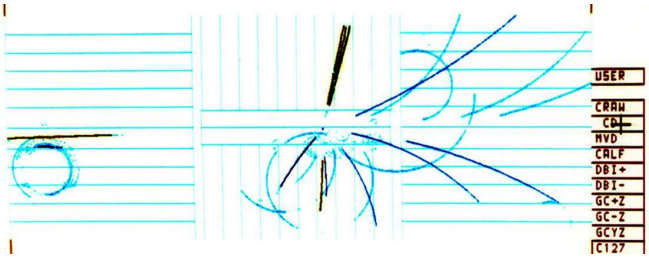

$q + \bar{q}' \rightarrow W \rightarrow \tau + \nu$

Figure 6.5: Event displays from the UA1 experiment for Z^0 production (top) and W production (bottom). In the top figure, the electrons follow in the direction of the black dotted lines. They leave straight, high-momentum tracks in the inner tracking detector and then are absorbed in the calorimeter, as indicated by the dark cuboids. In the bottom figure, the tau lepton from the W decay has itself decayed to three charged hadrons, visible as high-momentum straight tracks close to one another in the upper part of the plot. Other hadrons are also emitted from the proton remnants. These are more tightly curved tracks in the magnetic field.

shell, where the cross section is largest, we require that

$$\begin{aligned} m_Z^2 &= (\mathsf{P}_q + \mathsf{P}_{\bar{q}})^2 \\ &= \mathsf{P}_q^2 + \mathsf{P}_{\bar{q}}^2 + 2\,\mathsf{P}_q \cdot \mathsf{P}_{\bar{q}} \\ &\approx 0 + 0 + 2x_1x_2\mathsf{P}_p \cdot \mathsf{P}_{\bar{p}} \\ &= x_1x_2 \times E_{CM}(p\bar{p}) \end{aligned}$$

Where $E_{CM}(p\bar{p})$ is the centre-of-mass energy of the proton antiproton system.

The W and Z particles were discovered in the leptonic decay modes. There are large backgrounds to the hadronic decay modes from elastic $q\bar{q}$ scattering through the strong interaction. Event displays of collisions producing Z and W bosons can be found in Figure 6.5.

The $W^{\pm}$ bosons then each decay to the fermions. For the W^+ these are

$$W^+ \to u + \bar{d}'$$
$$W^+ \to c + \bar{s}'$$
$$W^+ \to e^+ + \nu_e$$
$$W^+ \to \mu^+ + \nu_\mu$$
$$W^+ \to \tau^+ + \nu_\tau$$

The other possible quark-antiquark state, $t+\bar{b}$, is inaccessible for W bosons close to their mass shells, since the top quark is much heavier than the W boson. We have ignored the mixing in the quark sector, in which approximation the coupling of the W to each of the fermions is the same. The couplings to the fermions are universal in the flavour basis, but are mixed by CKM matrix factors in the mass–energy basis. Decays to the quark states are enhanced by a colour factor of 3, since the $q\bar{q}$ pair can be in any of the colour states $r\bar{r}$, $b\bar{b}$ or $g\bar{g}$.

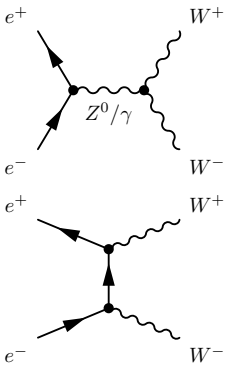

W production via a highly virtual γ or Z propagator (top) or via neutrino exchange (bottom).

Many of the most precise measurements of the W and Z bosons have been determined from in electron-positron collisions

$$e^- + e^+ \longrightarrow W^- + W^+$$

Three different leading order Feynman diagrams contribute to this process (a) via a photon γ (b) via a Z^0 or (c) via ν_e exchange.

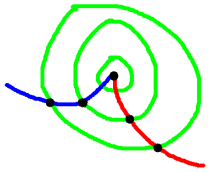

Tracks bending in the magnetic field.

Particle detectors

General purpose particle detectors at colliders generally have a series of different layers surrounding the interaction point.

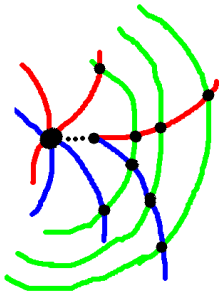

Secondary vertex reconstruction.

The inner part of the detector is used to track the trajectory of charged particles and measure their momenta as they bend in an externally applied magnetic field. The direction of curvature of the track indicates the sign of the charge, and the radius of curvature R permits calculation of the component of the momentum $p_\perp$ perpendicular to the field

$$p_\perp = \mathcal{Q}BR.$$

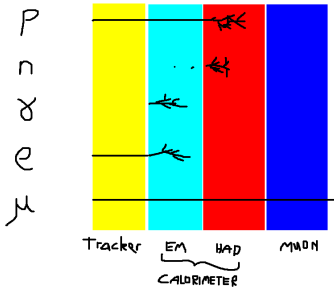

Different particles leave different signatures in the detector.

Closest to the interaction point are usually high precision semiconductor pixel detectors, or microstrip detectors. By measuring tracks to precisions of order $10\,\mu$m, it's possible to reconstruct the position of the decay of particles with lifetimes as short ~ 100 ps. Charged particles traversing the semiconductor layers generate electron-hole pairs, allowing a current to flow.

Beyond the tracker are layers of **calorimeter** which are designed to stop the particles and convert their energies into electrical signal. Electromagnetic calorimeters rely on cascades caused by sequential Bremsstrahlung and pair creation in the electromagnetic field of an atomic nucleus:

$$e^{\pm} + \text{nucleus} \to e^{\pm} + \gamma + \text{nucleus}$$
$$\gamma + \text{nucleus} \to e^- + e^+ + \text{nucleus}$$

Electromagnetic calorimeters are effective at detecting (anti-)electrons and photons.

Hadronic calorimeters lie beyond the electromagnetic calorimeters, and are used to measure the energies of the long-lived baryons and mesons. The hadrons interact with the atomic nuclei via the strong interaction, producing inelastic scattering reactions such as

$$\begin{aligned} n + \text{nucleus} &\rightarrow n + \pi^0 + \text{nucleus} \\ p + \text{nucleus} &\rightarrow n + \pi^+ + \text{nucleus} \\ \pi^- + \text{nucleus} &\rightarrow \pi^- + \pi^+ + \pi^- + \text{nucleus} \\ \pi^+ + \text{nucleus} &\rightarrow \pi^+ + \pi^0 + \text{nucleus.} \end{aligned}$$

Rather like in the electromagnetic case, cascades of such interactions create large numbers of charged pions — the lightest strongly interacting particles — and photons from the subsequent decay $\pi^0 \rightarrow \gamma + \gamma$.

The final layer in the detector is usually a **muon tracker**. Muons are highly penetrating, and are the only particles to pass through the calorimeters. Most large muon detectors work by measuring the ionization caused in a gas by the passage of the muon. By bathing the muon detector in a magnetic field, the measurement of the muons' momenta can be improved.

The invisible width of the Z^0 boson

A beautiful experiment allows us to count the number of neutrino families to which the Z^0 decays, even though the neutrinos themselves are not directly observed.

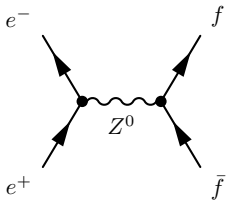

Production and decay of a Z^0 boson.

Consider the production of Z^0 bosons via the resonant process

$$e^+ + e^- \rightarrow Z^0 \rightarrow f + \bar{f}$$

where f represents one of the Standard Model fermions, which could be a quark, a charged lepton or a neutrino. The total width of the Z^0 boson will be given by the sum of the partial widths,

$$\Gamma = \Gamma_{\text{Had}} + \Gamma_{ee} + \Gamma_{\mu\mu} + \Gamma_{\tau\tau} + \Gamma_{\text{Invis}}. \tag{6.1}$$

The decays to each of the five kinematically available quarks ($u\bar{u}$, $d\bar{d}$, $s\bar{s}$, $c\bar{c}$, $b\bar{b}$) all lead to hadronic final states. The partial width Γ_{Had} represents decays into any of these final states. The invisible width – the rate of decay to neutrinos – is given by the simple product of the partial width to a particular neutrino species $\Gamma_{\nu\nu}$ and the number of such species N_ν,

$$\Gamma_{\text{Invis}} = N_\nu \times \Gamma_{\nu\nu},$$

since the Z^0 couples equally to each of the generations within the Standard Model.

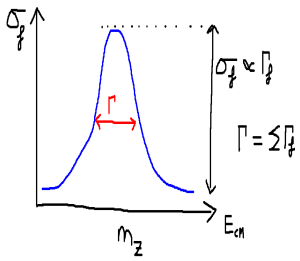

Cross section for $e^+ + e^- \rightarrow f + \bar{f}$ as a function of centre-of-mass energy.

The width of the Z^0 boson peak was precisely measured at the LEP $e^+ + e^-$ collider at CERN. The full width at half max of the Breit Wigner, Γ, was measured from the dependence of σ_{Had} on electron-positron centre-of-mass energy. The partial widths

to each of the observable final states can each be calculated from their production cross sections at the Z^0 peak.

Knowing of all of the other widths in (6.1), $\Gamma_{\mathrm{Invisib}}$ can be calculated. The partial width $\Gamma_{\nu\nu}$ is calculable from the related process of neutral-current scattering of neutrinos. Treating N_ν as an unknown, the following value was obtained:

$$N_\nu = 2.984 \pm 0.008,$$

consistent with the three generational model, and excluding the existence of another similar generation of particles.

6.4.3 Parity violation in the weak interaction

The strong and the electromagnetic interaction both respect parity. That is the part of the Hamiltonian that involves those interactions commutes with the parity operator, $\mathbb{P}$.

The parity operator generates the transformation of inversion of coordinates

$$\mathbb{P} : \mathbf{x} \mapsto -\mathbf{x}.$$

Under the parity operation, polar vectors such as those for position $\mathbf{x}$, velocity $\mathbf{v}$, momentum $\mathbf{p}$, and electric field $\mathbf{E}$ pick up a minus sign. Axial vectors such as angular momentum $\mathbf{J}$, and magnetic field $\mathbf{B}$ remain unchanged. An example of an axial vector is the orbital angular momentum L which transforms as follows:

$$\mathbf{L} \overset{\mathbb{P}}{\mapsto} L' = \mathbf{x}' \times \mathbf{p}' = -\mathbf{x} \times -\mathbf{p} = \mathbf{x} \times \mathbf{p} = \mathbf{L},$$

that is, like J and B, it is unmodified.

The electromagnetic laws of Maxwell and Lorentz remain valid after the parity operation. For example under a parity transformation, the Lorentz force law $\mathbf{F} = q(\mathbf{E} + \mathbf{v} \times \mathbf{B})$ transforms to

$$\begin{aligned} \mathbb{P}(\mathbf{F}) &= \mathbb{P}(q(\mathbf{E} + \mathbf{v} \times \mathbf{B})) \\ -\mathbf{F} &= q(-\mathbf{E} + -\mathbf{v} \times +\mathbf{B}) \\ \mathbf{F} &= q(\mathbf{E} + \mathbf{v} \times +\mathbf{B}) \end{aligned}$$

which remains a valid statement of the same law.

This may seem obvious, but becomes much less so when it is realized that unlike the electromagnetic and the strong forces, both of which are insensitive to the parity operation, the weak interaction is peculiar in that the law that describes it does not remain valid after a parity operation.

The discovery of parity violation

A test for parity violation in the weak interaction was suggested in 1956 [11]. The proposed experiment involved the beta decay

$$^{60}\mathrm{Co} \rightarrow {}^{60}\mathrm{Ni} + e^- + \bar{\nu}_e.$$

The cobalt nucleus, which has $J^P = 5^+$, decays to the $J^P = 4^+$ nickel nucleus.

The cobalt is cooled to 0.01 K and immersed in a strong magnetic field $\mathbf{B}$ so that the nuclear spins are preferentially aligned along the magnetic field, due to a term in the Hamiltonian $-\boldsymbol{\mu} \cdot \mathbf{B}$. The directions of the outgoing beta electrons are then observed.

Consider the behaviour of the momentum vector $\mathbf{p}$ of the observed electrons and the magnetic moment direction $\boldsymbol{\mu}$ of the nuclei under the parity operation:

$$\begin{aligned} \mathbf{p} &\xrightarrow{\mathbb{P}} -\mathbf{p} \\ \boldsymbol{\mu} &\xrightarrow{\mathbb{P}} +\boldsymbol{\mu} \end{aligned}$$

After a parity operation the momentum vector is inverted, but the nuclear spin points in the same direction. Therefore if parity is to be conserved, there must be as many electrons emitted in the $+\mathbf{B}$ direction as in the $-\mathbf{B}$ direction.

What was observed [16] was that the emission of beta particles was *not* symmetric with respect to the $\mathbf{B}$-field direction. When measured, there were more beta electrons found in the direction opposite to that of the nuclear spin. The implication is that parity is not conserved in this interaction. The weak force behaves differently after the parity operation.

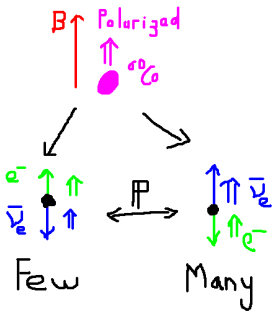

Angular momentum in the $^{60}\mathrm{Co}$ decay.

Parity is not conserved in weak interactions

The laws of physics are therefore not the same after reflecting a system in a mirror.

Parity and neutrino helicity

$$h = \frac{\mathbf{S} \cdot \mathbf{p}}{|\mathbf{p}|}$$

Another striking example of the violation of parity is found in the helicity of the neutrinos. Helicity h is the projection of the spin onto the direction of motion of a particle. Neutrinos are produced only with $h = -\frac{1}{2}$, and anti-neutrinos only with $h = +\frac{1}{2}$. No $h = +\frac{1}{2}$ neutrino has ever been observed. Since under the parity operation, helicity is reversed

	h	
ν	$-\frac{1}{2}$	$\xleftarrow{}$
$\bar{\nu}$	$+\frac{1}{2}$	$\xrightarrow{}$

$$h \xrightarrow{\mathbb{P}} -h,$$

we can infer that the laws which control the neutrino production cannot conserve parity, since if they did we should find as many $h = +\frac{1}{2}$ as $h = -\frac{1}{2}$ neutrinos.

The implication of parity violation is that nature has an inherent 'handedness', seen only in the weak decay. Left-handed particles feel the weak force more strongly than right-handed ones. The opposite is true for antiparticles: the weak force interacts with right-handed antiparticles rather than left-handed ones.

6.5 Neutrino Oscillations

There are three different types of neutrino, which we have labelled

$$\{\nu_e,\ \nu_\mu,\ \nu_\tau\}$$

according to the flavour of charged lepton they interact with via the W boson interaction.

But flavour is not necessarily 'good' quantum number — by which we mean a quantum number which is conserved. If lepton flavour is not strictly conserved then a neutrino that is born as an electron-type neutrino might not still be an electron-type neutrino later on. More precisely, if the flavour eigenstates are not eigenstates of the Hamiltonian, then flavour will not be conserved, and the amplitude to find the neutrino in a particular flavour eigenstate will be a time-dependent quantity.

Let us label the energy eigenstates according to their mass

$$\{\nu_1,\ \nu_2,\ \nu_3\}.$$

A neutrino is created as an electron-type neutrino if it is produced in association with an antielectron $W^+ \rightarrow \nu_e + e^+$. The amplitude $a(t)$ for it still to be an electron-type neutrino at some later time t is

$$a(t) = \langle \nu_e(t) | \nu_e(0) \rangle.$$

If flavour is conserved, then $|a(t)|^2 = 1$ for all t. However if the Hamiltonian does not conserve flavour then $|a|^2$ will be a time dependent quantity, and in general will oscillate with time.

Let us consider the simplified two-neutrino system. We label the flavour eigenstates $|\nu_e\rangle$ and $|\nu_\mu\rangle$ as mixtures of the the energy (i.e. mass) eigenstates $|\nu_1\rangle$ and $|\nu_2\rangle$

$$\begin{aligned} |\nu_e\rangle &= |\nu_1\rangle \cos\theta + |\nu_2\rangle \sin\theta \\ |\nu_\mu\rangle &= -|\nu_1\rangle \sin\theta + |\nu_2\rangle \cos\theta. \end{aligned}$$

where θ is the mixing angle.

Let the neutrino start off as an electron-type neutrino at its initial position $\mathbf{x} = 0$ when $t = 0$. At later times the neutrino's state $|\Psi\rangle$ is given by

$$|\Psi(L,T)\rangle = |\nu_1\rangle \cos\theta\, e^{-i\phi_1} + |\nu_2\rangle \sin\theta\, e^{-i\phi_2}$$

where

$$\phi_i = E_i T - |\mathbf{p}_i| L.$$

where, without loss of generality, we have reduced to single spatial dimension for the propagating wave. The amplitude for the initial (electron) neutrino to then be found as a muon neutrino can be found by bra-ing through with $\langle \nu_\mu |$,

$$\langle \nu_\mu | \Psi(x,t) \rangle = \sin\theta \cos\theta \left(e^{-i\phi_2} - e^{-i\phi_1} \right).$$

The flavour-change probability $P(\nu_e \to \nu_\mu)$ is then

$$|\langle \nu_\mu | \Psi(L,T) \rangle|^2 = \sin^2 2\theta \, \sin^2 \left(\frac{\phi_1 - \phi_2}{2} \right)$$

If the masses of the two neutrinos are the same, then the phases ϕ_1 and ϕ_2 will remain in synch and no flavour change results. However if $m_1 \neq m_2$ then we have a phase change

$$\Delta\phi_{12} \equiv \phi_1 - \phi_2 = (E_1 - E_2)T - (|\mathbf{p}_1| - |\mathbf{p}_2|)\, L$$

To work out the phase difference in full we ought to use a wave-packet analysis, but we can quickly arrive at the correct answer by assuming[2] $|\mathbf{p}_1| = |\mathbf{p}_2|$, and expanding for $m \ll E$, to find

$$\begin{aligned} \Delta\phi_{12} &\approx |p| \left(\sqrt{1 + \frac{m_1^2}{|p|^2}} - \sqrt{1 + \frac{m_2^2}{|p|^2}} \right) L \\ &\approx \frac{m_1^2 - m_2^2}{2E} L. \end{aligned}$$

The probability $P(\nu_e \to \nu_\mu)$ is therefore (in SI units)

$$\boxed{P(e \to \mu) = \sin^2 2\theta \, \sin^2 \left(\frac{\Delta m^2 c^3 L}{4\hbar E} \right)} \tag{6.2}$$

where $\Delta m^2 = m_1^2 - m_2^2$. The survival probability $P(\nu_e \to \nu_e)$ is, for the two-state system, simply $1 - P(\nu_e \to \nu_\mu)$. In more convenient units the argument of the oscillation phase can be written

$$\frac{\Delta m^2 c^3 L}{4\hbar E} = 1.3 \frac{\Delta m^2}{\mathsf{eV}^2} \frac{L}{\mathsf{km}} \frac{\mathsf{GeV}}{E},$$

making it clear that for differences in mass-squared $\Delta m^2 \ll \mathsf{eV}^2$ the distance oscillations will happen over a length of many kilometers.

The masses of the neutrinos are very small, and so extremely difficult to measure directly. Cosmological constraints indicate that the sum of the three neutrino masses must be less than about 0.6 eV. We can find out about the (differences in squares of) masses of the three different neutrinos ν_1, ν_2 and ν_3 by examining the oscillations between the the three different flavours. Experiments over many kilometres are needed to search for such oscillations, otherwise the oscillation probability will be negligible. The long distances over which they are oscillating come from a combination of the near-degeneracy of the masses, and the neutrinos' large Lorentz gamma factors (of order 10^{12}), meaning that they are subject to a huge time dilation.

[2] If this makes you a little uncomfortable, it should. This is the 'textbook' method, but not terribly convincing, since it's hard to convince yourself that the state is in a momentum eigenstate. A little more confidence can be gained by noting that the expression for the phase difference could also have been written

$$\Delta\phi_{12} = (E_1 - E_2) \left(T - \frac{E_1 + E_2}{|\mathbf{p}_1| + |\mathbf{p}_2|} L \right) + \frac{m_1^2 - m_{,2}^2}{|\mathbf{p}_1| + |\mathbf{p}_2|} L.$$

Therefore had we chosen to demand that $E_1 = E_2$ or even $\beta_1 = \beta_2$ the first term would have vanished and we would have arrived at the same answer as under the equal-momentum assumption.

6.5.1 Solar neutrinos

The earliest indication of neutrino oscillations was found in **solar neutrinos**. The sun emits only electron-type neutrinos, through processes such as

$$p + p \rightarrow {}^{2}_{1}\mathrm{H} + e^{+} + \nu_e$$

After they travel to earth we can capture the higher energy solar neutrinos as ν_e using isotopes like $^{37}\mathrm{Cl}$ in the inverse beta decay reaction

$$\nu_e + {}^{37}\mathrm{Cl} \rightarrow e^{-} + {}^{37}\mathrm{Ar}.$$

This reaction cannot occur for other neutrino flavour states, so any deficit in the expected amount of $^{37}\mathrm{Ar}$ will indicate that electron-type neutrinos have either disappeared or have oscillated into another flavour state.

The experiment was first performed in the Homestake Gold Mine in South Dakota using a 390,000 litre tank of dry-cleaning fluid, C_2Cl_4 [7]. To perform the experiment, the team had to isolate about one atom of $^{37}\mathrm{Ar}$ produced per day in all that cleaning fluid, while working in a mine 1.5 km underground. The rate predicted by consideration of the solar nuclear reactions was 7.6 SNU, where one SNU (solar neutrino unit) is 10^{-36} captures per target atom per second. The observed rate was 2.56 SNU. Only about a third of the expected number of neutrinos was observed, indicating that the ν_e had oscillated into an equal mixture of ν_e, ν_μ and ν_τ by the time they reached earth.

Confirmation of the oscillation hypothesis was found from the Sudbury Neutrino Observatory in Ontario, Canada. SNO could detect three different reactions

$$\begin{aligned} \nu_e + D &\rightarrow p + p + e^{-} && (CC) \\ \nu_x + D &\rightarrow p + n + \nu_x && (NC) \\ \nu_x + e^{-} &\rightarrow \nu_x + e^{-} && (ES) \end{aligned}$$

where ν_x is any neutrino species, and D is a duterium nucleus ${}^{2}_{1}\mathrm{H}$. The charged current (CC) reaction is only sensitive electron-type neutrinos, while the neutral current (NC) and elastic scattering (ES) reactions each detect all three neutrino flavours. Comparison of the rates [13] shows that CC reactions are reduced to a third of what would be expected in the absence of neutrino oscillations. Both NC and ES reactions occur at the rate one would expect with or without reactions, showing that the total number of neutrinos is unchanged. The initially electron-type neutrinos are therefore oscillating into an approximately equal mixture of ν_e, ν_μ and ν_τ.

6.5.2 Atmospheric neutrinos

Neutrinos are also produced in the upper atmosphere when high-energy cosmic rays strike the upper atmosphere producing pions. The charged pions decay to muons, which decay to electrons, a sequence of reactions which emits neutrinos of both electron-type and muon-type flavours:

$$\begin{aligned} \pi^{+} &\rightarrow \mu^{+} + \nu_\mu \\ \mu^{+} &\rightarrow e^{+} + \bar{\nu}_\mu + \nu_e \end{aligned}$$

A corresponding reaction occurs for the negative pions.

Most of these neutrinos will pass through the earth unhindered. Occasionally we can see one if it happens to hit our target. A neutrino experiment sensitive to direction will see some neutrinos coming down from the atmosphere, which will have travelled only a few km. Those neutrinos which have passed through the earth, and travel up through the detector will have travelled up to about 13,000 km before we observe them. By recording the direction and flavour of the arriving neutrinos, an experiment can test the survival probability of the neutrino flavour (6.2) as a function of distance (or rather as a function of L/E).

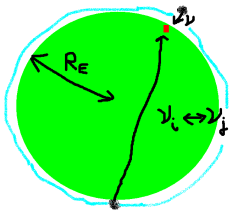

Upward-coming neutrinos have travelled further than have those coming directly down from the atmosphere.

The Super-Kamiokande experiment in Japan measured electron and muon type neutrinos of $\sim$ GeV energies using a 50 kton water Čerenkov detector. The experiment did not have sensitivity to tau-type neutrinos, since the neutrino energies were not high enough to produce τ leptons in charged current interactions. A deficit of muon neutrinos was found in the up-coming neutrinos which had travelled longer distances. The electron-type neutrinos were as would be expected in the absence of oscillations. These results indicate that flavour oscillations of the sort

$$\nu_\mu \rightleftharpoons \nu_\tau$$

were leading to loss of muon-type neutrinos. In the atmospheric experiment, the baseline L is too short for $\nu_e \rightleftharpoons \nu_\tau$ or $\nu_e \rightleftharpoons \nu_\mu$ oscillations.

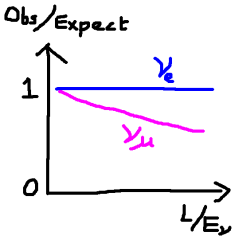

Super-Kamiokande found fewer upward coming muon neutrinos than expected.

6.6 The Higgs field

[non-examinable]

One particle, the spinless Higgs particle, plays a particularly special role in the Standard Model. It has unique properties in that it interacts with the other particles with couplings proportional to their masses.

To understand why the Higgs boson is necessary, consider the masses of the force-carrying particles. In quantum field theory, gauge bosons, the force-carrying particles, naturally arise as *massless* spin-1 excitations of the field carrying the force. This is fine for the photon and the gluons, which are indeed spin-1 bosons without mass. However the W and Z particles, though having spin 1 as expected, have large masses $\approx 100\,\text{GeV}$, so cannot so easily be explained as the massless excitations of the weak field. A mechanism is needed to provide the W and Z bosons with mass.

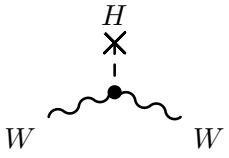

The Higgs field is non-zero in the vacuum (indicated by the cross). The vacuum interactions of the Higgs field with the W boson, of the sort shown in the diagram, give the W bosons its mass.

In the Higgs theory, the whole of space – the vacuum itself – is filled with a non-zero expectation value of the Higgs field. The particles which interact with this scalar field have modified properties. Those particles which interact with the field acquire masses according to their strength of interaction with the field. The W and Z particles, which would otherwise be massless, acquire their masses by interacting with the Higgs field in the vacuum. The photon is massless because it does not interact with the (electrically neutral) Higgs field.

The fundamental fermions – the quarks and leptons – also obtain their mass by interacting with this all-pervasive Higgs field. The top is the heaviest of the quarks

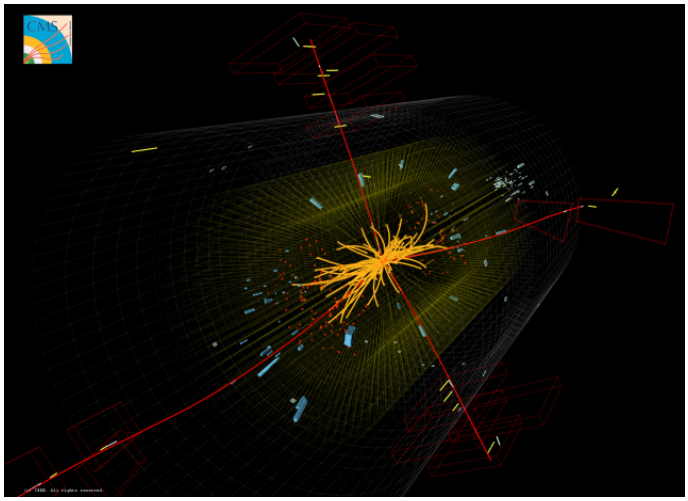

Figure 6.6: Display of a candidate Higgs boson event with the CMS detector. The red lines show muon tracks. The invariant mass of the four muons is equal to the mass of the Higgs boson.

exactly because it couples most strongly to the Higgs field. The electron is much lighter because its coupling to the Higgs field is much weaker.

How does the vacuum get filled with Higgs field? Consider a 'Mexican hat' potential,

$$V(\varphi) = \mu^2 |\varphi|^2 + \lambda |\varphi|^4 ,$$

associated with a field φ, where $\mu^2 < 0$ and $\lambda > 0$. This potential has a local maximum at the origin (where $\varphi = 0$), and a minimum elsewhere where the fields are non-zero. The vacuum will settle into one of the states around the circle where V is minimum, meaning that φ takes a non-zero value in the vacuum. Thus the vacuum is filled with the field.[3]

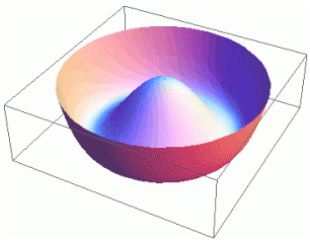

The potential associated with the Higgs field has a 'Mexican hat' shape. The vertical axis shows the potential $V(\varphi)$, as a function of the real and imaginary parts of the Higgs field φ. The potential has a local maximum at $\varphi = 0$, and a degenerate minimum at which $\varphi \neq 0$.

The excitation – or quantum – of the Higgs field is the Higgs boson. The Higgs boson is unique amongst the fundamental particles, in being a scalar – it has no intrinsic spin. It is responsible for a new Higgs interaction. This is a new type of force in nature, different from the electromagnetic, weak, strong and gravitational forces.

The couplings of the Higgs boson are fixed by the interactions of the Higgs field. The Standard Model particles must couple to the Higgs boson H with couplings proportional to their masses if they are to acquire their mass from the Higgs field. This means that the Higgs boson must couple strongly to heavy particles, light the top quark, and very weakly to light particles like the electron.

The discovery of the Higgs boson, was announced by the two large experiments at the Large Hadron Collider (LHC) in July 2012. Its mass was found to be close to

[3] In fact because a *particular* vacuum state is chosen by nature we break the gauge symmetry. This type of symmetry breaking happened in the very early universe, before the formation of hadrons. This is similar to what happens when directional symmetry is broken when a crystal freezes, selecting a particular direction.

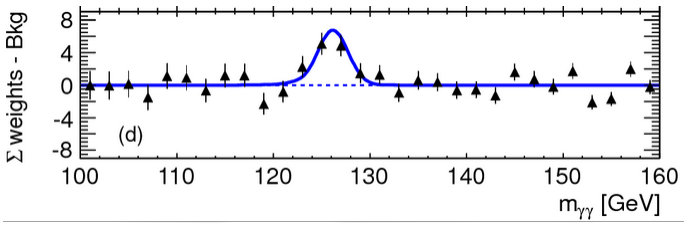

Figure 6.7: The discovery of the Higgs boson in the di-photon channel. The x-axis shows the di-photon invariant mass. The y-axis show the number of weighted events observed, after subtracting backgrounds. A peak can be observed at $m_{\mathrm{H}} \approx 125\,\mathrm{GeV}$. The width of the peak is dominated by experimental resolution.

125 GeV and its properties consistent with being those expected from the Standard Model theory.[4]

6.6.1 Finding a Higgs boson

The Large Hadron Collider, where the Higgs boson was discovered, accelerates protons. Protons can be accelerated to the high energies required to make the Heavy Higgs boson. However protons are less than ideal for making Higgs particles, because the proton's constituent quarks – the up and down quarks – are the lightest of the quarks, and so couple only very weakly to Higgs boson. At the LHC the Higgs boson is dominantly made from gluon-gluon interactions. This seems counter-intuitive, since the gluon is massless, and so there is no direct coupling between the Higgs and the gluon at all. Instead the H must be made via an intermediate state - a triangular loop diagram,. The largest contribution comes from the top quark triangle diagram. The top quark can exist briefly in this virtual state, and has the advantage of a very large coupling to the Higgs boson.

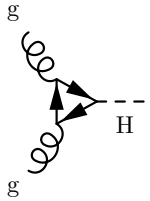

Production of a Higgs boson from a pair of gluons, via a top quark loop.

The Higgs boson has been observed decaying in a variety of different ways, including

$$H \rightarrow W \ + \ W^* \rightarrow (e^+ + \nu_e) \ + \ (\mu^- + \bar{\nu}_\mu)$$
$$H \rightarrow Z \ + \ Z* \rightarrow (e^+ + e^-) \ + \ (\mu^+ + \mu^-)$$
$$H \rightarrow \gamma + \gamma$$
$$H \rightarrow \tau^- \ + \ \tau^+$$

The stars on the W and Z indicate that one or other of the W or Z particles is well off its mass shell. Both cannot be on-shell (or near-shell) since the Higgs boson mass $m_H \approx 125\,\mathrm{GeV}$ is less than either $2m_W$ or $2m_Z$. The Higgs boson has no spin, and is represented as dashed line (reserved for scalars) on a Feynman diagram. The photon γ is massless, the Higgs boson does not couple to it directly. Instead that decay must proceed via a loop diagram, typically involving a W boson or a t quark.

The ATLAS and CMS experiments each observe a clear (Figure 6.7) a characteristic Breit-Wigner peak in the histogram of the diphoton invariant mass $m_{\gamma\gamma}$ for events

[4] For a good series of articles explaining the discovery, try the special edition of 'Science' magazine published in December 2012: ATLAS paper and CMS paper.

containing pairs of photons. This, together with similar evidence in decays to τ leptons, and W and Z bosons led to confirmation of the Higgs boson's existence.

Experiments are currently on-going to determine the couplings of the Higgs boson to all of the Standard Model fermions and bosons, and to measure the shape of the Higgs potential.

6.7 Beyond the Standard Model

[Non-examinable]

The Standard Model provides an extremely successful description of the fundamental constituents of nature as we observe them. However, it is known to have a limited range of validity, and it fails to address some of the most important questions about the matter and forces in our universe.

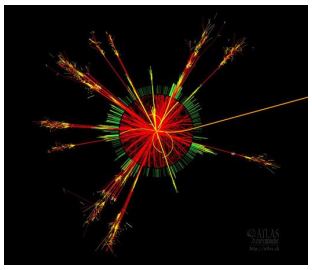

A simulation of a microscopic TeV-energy black hole evaporating through Hawking radiation at the LHC.

6.7.1 Gravity

Gravity is notably absent from the Standard Model. While a description of gravity exists at the classical level in the form of General Relativity, this provides no microscopic explanation for gravity. We don't yet know what is transmitting the force at the quantum level. The difficulty in finding out is because gravity is so weak, despite it being the most familiar of the fundamental forces. Gravity can be incorporated within wider theories, such as string theories, however such theories do not yet make predictions that can be tested by experiment.

It has been suggested that a spin-2 *graviton* is responsible for the gravitational force. Such a particle might be detectable at extremely high energies, close to the Planck energy which in natural units is

$$E_{\text{Planck}} = \frac{1}{\sqrt{G_{\text{Newton}}}} \approx 10^{28}\,\text{eV}.$$

This energy scale is well beyond the reach of current colliders.

Some theories with extra dimensions of space suggest that gravity could become exponentially strong at TeV energies. In such theories gravitons (and/or microscopic black holes) could be observed at existing high-energy colliders, such as the LHC. Every time a collider reaches higher energies one of the first things one does is to perform a search for the effects of quantum gravity.

Figure 6.8: Dark matter detectors require low radioactive backgrounds, and are operated deep underground to shield them from cosmic rays. Some make use of copper from sunken Roman ships, which has particularly low induced radioactivity because it has been shielded from cosmic rays by the sea for centuries.

6.7.2 A theory of flavour

6.7.3 Matter / antimatter asymmetry

6.7.4 Unification of the forces?

6.7.5 The dark side of the universe

The Standard Model only accounts for the 5% of the matter-energy content of the universe. The astronomical and cosmologically evidence clearly favours a preponderance of Dark Matter (24% of the matter/energy content) and Dark Energy 71%.

The evidence for dark matter comes from a variety of sources, from the rotation curves of galaxies, to the formation of galaxies, to the acoustic oscillations in the early universe, to the evolution of the universe as a whole. So far we have no microscopic description for the source of the Dark Matter particles. We can infer some properties, for example we know that such particles cannot have electromagnetic interactions, otherwise they would not be 'dark'. They can't have strong interactions or they would already been observed as they bounce off our detectors. It's possible that they may interact only via the Weak or Higgs forces.

There are three major ways of looking for dark matter, all of which are competing to find it first. One method is to search for such particles being produced in colliders. The dark matter particles would not be observed directly, but would betray their presence through apparent non-conservation of energy or momentum, rather similar to the way neutrinos were first found.

An alternative search strategy is to look for the effects of naturally-occuring dark matter particles, as they bump into a very precise detector. The energy transmitted to the detector is observed as light, or as an electrical signal. Such detectors have to be radiologically pure, otherwise the energy signal from the dark matter particle would be lost in a background from nuclear interactions. They are also placed deep

underground, in order to shield them from cosmic rays.

A third method is to search for Dark Matter particles annhilating against one another in space. Such annihilations could produce high energy Standard Model particles which we could be able to observe.

If dark matter does have Weak or Higgs interactions, it could be discovered soon via any of these methods.

Dark Energy

Dark Energy is believed to form the remaining 71% of the matter/energy contents of the universe. It takes the form of an energy density of empty space, and makes itself felt via the acceleration it causes in the expansion of the universe.

No good particle physics explaination yet exists for the Dark Energy. A non-zero energy of space is expected from quantum field theory, but unfortunately the calculated value is a factor of about 10^{120} too large. This has been called the worst prediction in physics. A value as large as that calculated would not allow structure to form in the universe. This has led some to speculate that there are many universes with different energy densities, and that we find ourselves, necessarily, in one which is 'antropically selected' to favour the formation of structure, stars and intellegent life.

6.7.6 The hierarchy problem

6.7.7 Strings and things

Key concepts

- The fundamental matter particles are **spin-$\frac{1}{2}$ fermions**
- There are three families of **quarks**, and three corresponding families of **leptons**
- The forces and interactions between the quarks and leptons are mediated by **spin-1 bosons**
- The **electromagnetic force** is mediated by the neutral, massless photon γ
- The **strong force** is mediated by the eight massless gluons g which are themselves coloured, and so interact with one another.
- In deep inelastic scattering, a projectile scatters off the constituent quarks
- Free quarks are **not observed**, instead, when a quark is knocked hard, we find **jets** of colourless mesons and baryons.
- The **weak force** is mediated by the $W^{\pm}$ and Z^0 particles, which have large masses, and so only interact over $\sim 10^{-18}$ m

- The weak force violates conservation of parity
- The $W^{\pm}$ bosons are the only particles that can change quark flavour
- Neutrinos are observed to change flavour (oscillate) when travelling over long distances

Further reading

- B. Martin, *Nuclear and Particle Physics: An Introduction*
- W. S. C. Williams, *Nuclear and Particle Physics*
- K.S. Krane *Introductory Nuclear Physics*

6.A Conservation laws

Operator	Strong	EM	Weak
Charge, $\mathcal{Q}$	✓	✓	✓
Baryon number	✓	✓	✓
Lepton number	✓	✓	✓
Parity, $\mathbb{P}$	✓	✓	×
Charge conjugation $\mathbb{C}$	✓	✓	×
$\mathbb{CP}$	✓	✓	almost
Strangeness	✓	✓	×
Charm	✓	✓	×
Bottomness	✓	✓	×
Isospin	✓	×	×

Table 6.3: Some important operators and their invariance properties for different interactions. A tick ✓ indicates that the interaction conserves that quantity. A cross × indicates that it does not conserve that quantity. The combined operation $\mathbb{CP}$ is almost conserved in the weak interaction.

Chapter 7

Applications

> "Anyone who expects a source of power from the transformation of these atoms is talking moonshine."
>
> *Ernest Rutherford, 1933*

Rutherford was wrong. The energy changes during nuclear reactions are of order 10^6 times larger than those during chemical reactions. They are responsible for the energy emitted by stars, including our own sun, the geothermal heat that keeps the centre of the earth. Nuclear fuels represent the overwhelming majority of the available energy resources on earth.

We have previously seen that the binding energy per nucleon B/A is typically 8 MeV. The different contributions to the binding energy, as represented in the Semi-Empirical Mass Formula, lead to a maximum B/A close to the common isotope $^{56}\mathrm{Fe}$ which has $B/A = 8.79$ MeV.

Isotope	$^{2}\mathrm{H}$	$^{4}\mathrm{He}$	$^{6}\mathrm{Li}$	$^{16}\mathrm{O}$	$^{44}\mathrm{Ca}$	$^{56}\mathrm{Fe}$	$^{107}\mathrm{Ag}$	$^{238}\mathrm{U}$
B/A [MeV]	1.112	7.074	5.332	7.976	8.658	8.790	8.554	7.570

Table 7.1: Examples of binding energy per nucleon.

7.1 Fission

7.1.1 Energy and barriers

From the Table 7.1 we see that it would be energetically favourable for nuclei in the region of $A \sim 100$ to split into two lighter nuclei, each with larger values of B/A. It is then reasonable to ask why it is that nuclei with values of $A \sim 100$ do not split into two parts, given that it is energetically possible. The reaction would be exothermic, and so must be suppressed by some mechanism.

Consider the splitting of a large sphere into two smaller, equally sized, spheres. The intermediate steps must involve the first sphere elongating, then becoming ellipsoid, pinching in the middle, and finally separating. During the elongation and separation, the charges move further apart, decreasing the size of the Coulomb term. However the surface area, and hence the surface energy must increase.

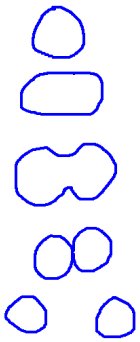

Fission of a nucleus into two smaller nuclei

At the point where the daughter nuclei have only just separated, the electrostatic energy from their proximity will be of order the Coulomb potential of

$$E_{\text{barrier}} = \frac{\alpha\,(Z/2)^2}{2r_0(A/2)^{1/3}} \tag{7.1}$$

where $Z/2$ and $A/2$ are the atomic number and mass number respectively of the daughter nuclei, and a symmetric split has been assumed. For $Z = 40$ and $A = 100$ the energy barrier is of height 65 MeV, which is large enough to prevent fission.

For larger values of A, the barrier (7.1) continues to increase relative to the final state of two well-separated daughters. However the heavier parent nucleus also has less binding energy, and so moves closer to the top of the Coulomb barrier. For A as large as about 200, the barrier becomes sufficiently small (relative to the initial parent's energy) that it becomes possible to tunnel through that barrier. Fission proceeds, at a rate determined by the tunnelling probability. Since the barrier is small, it may also be possible to push the nucleus over the barrier, if a relatively small amount of energy can be added, for example from a projectile.

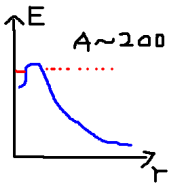

The potential barrier is small for $A \sim 200$.

If one considers values of A as large as 300, there is no barrier at all from the parent's side, and so the nucleus will immediately fall apart. Such nuclei are not observed in nature.

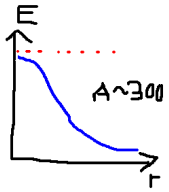

The potential barrier disappears for $A \sim 300$.

Let us consider how energy might be added to induce fission for two example $A \sim 200$ nuclei. For the uranium isotop $^{238}_{92}\mathrm{U}$ the energy barrier is of order 6 MeV. We can induce fission in this nucleus by bombarding it with sufficiently high-energy neutrons:

$$^{238}\mathrm{U} + n(E > 6\,\text{MeV}) \longrightarrow \text{fission products.}$$

Low-energy neutrons impacting on $^{238}\mathrm{U}$ have a relatively high capture cross section through the (n,γ) process

$$^{238}\mathrm{U} + n \rightarrow {}^{239}\mathrm{U}^* \rightarrow {}^{239}\mathrm{U} + \gamma \tag{7.2}$$

leading to neutron capture without fission.

Fission is easier to induce in the other naturally occuring isotope of uranium $^{235}\mathrm{U}$. The arrival of even very low-energy (thermal) neutrons on $^{235}\mathrm{U}$ leads to fission with 84% probability. The radiative neutron capture reaction (n,γ) occurs with only 16% probability.

To understand why a very low-energy neutron can cause fission in $^{235}\mathrm{U}$, but that a much higher energy neutron is required to push $^{238}\mathrm{U}$ over the energy barrier, we need to consider the change in the Z and N numbers as the two isotopes gain a neutron.

Fissionable nuclei

Nuclei that are fissionable with slow-moving neutrons include: $^{235}_{92}\mathrm{U}$ and $^{239}_{94}\mathrm{Pu}$. Plutonium-239 does not occur naturally, since it has only a 24 kyr half life. It is produced as a by-product in nuclear reactors, when $^{239}\mathrm{U}$, created via reaction (7.2), followed by successive β decays

$$\begin{aligned} ^{239}_{92}\mathrm{U} &\longrightarrow {}^{239}_{93}\mathrm{Np} + e^- + \bar{\nu}_e \\ ^{239}_{93}\mathrm{Np} &\longrightarrow {}^{239}_{94}\mathrm{Pu} + e^- + \bar{\nu}_e. \end{aligned}$$

Reactors designed specifically to produce and burn fissionable $^{239}\mathrm{Pu}$ fuel during their operation are called **breeder** reactors.

Isotope	Z	N	Type
$^{235}\mathrm{U}$	92	143	Even-Odd
$^{238}\mathrm{U}$	92	146	Even-Even

On addition of a neutron, $^{235}\mathrm{U}$ moves from being even-odd to being being even-even, thus releasing pairing energy δ. By contrast $^{238}\mathrm{U}$ on absorbing a neutron moves from even-even to even-odd, for which one must pay the price of an additional δ of pairing energy. It is the release of the pairing energy δ that taps $^{235}\mathrm{U}$ over the energy barrier, no matter how low-energy the incident neutron may be.

7.1.2 Cross sections for fission reactions

The important reactions for fissionable reactors are elastic scattering of neutrons (n, n) radiative absorption of neutrons (n, γ) and neutron-induced fission (n, f). The radiative absorption cross section is important because it removes neutrons which would otherwise be able to induce fission. For fission to proceed we will need to know the cross sections for each of these processes, and their energy dependences.

The elastic (n, n) scattering cross section is found to be approximately independent of the speed of the neutron – other than where resonant scattering occurs. By contrast, for the (n, γ) radiative capture reaction, the cross section falls rapidly with the speed v_{in} of the incoming neutron,

$$\boxed{\sigma_{\mathrm{capture}} \propto \frac{1}{v_{\mathrm{in}}}.}$$

The same fall-off with v_{in} is seen for the fission reaction

$$\boxed{\sigma_{\mathrm{fission}} \propto \frac{1}{v_{\mathrm{in}}}.} \tag{7.3}$$

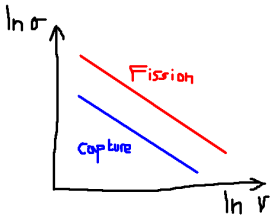

Graph of $\ln\sigma$ against $\ln v$

7.1.3 Chain reactions

When $^{235}\mathrm{U}$ fissions, it releases about 200 MeV of energy. The products are two fission fragments, and several neutrons. The reason for the emission of neutrons is

Neutron scattering, capture and fission cross sections.
We can understand the functional dependence of the cross sections σ_{elastic}, σ_{capture} σ_{fission} on neutron speed as follows. The rate is governed by the Fermi golden rule (2.15). The matrix element is M_{fi} and the density of states will be proportional to

$$p_f^2 \frac{dp_f}{dE}.$$

Now, cross section is rate divided by incoming neutron flux, and flux is proportional to v_{in}. Hence the cross section has the following dependence on v_{in} and p_{f}:

$$\sigma \propto \frac{1}{v_{\text{in}}} |M_{fi}|^2 \; p_f^2 \frac{dp_f}{dE}, \tag{7.4}$$

We can simplify the equation by noting that the energy-momentum relation $E^2 = p^2 + m^2$ implies that[a]

$$\frac{dp}{dE} = \frac{E}{p} = \frac{1}{v}$$

For elastic (n, n) reactions, the incoming and outgoing speeds are the same ($v_f = v_{\text{f}}$) in the centre-of-mass frame, hence for a low energy neutron with $p = mv$ the energy dependence simplifies to

$$\sigma_{\text{elastic}} \propto \frac{1}{v_{\text{in}}} |M|^2 \frac{m_n^2 v_f^2}{v_f} = |M|^2 m_n^2$$

Hence we expect the elastic cross section to be approximately **constant**, except perhaps where resonant scattering causes sharp peaks.

For the very exothermic (n, γ) and (n, f) reactions, the starting point (7.4) is the same, but the density of states factor is now completely dominated by the energy released to the decay products – the photon for the radiative case, or the fission products. The density of final states is now almost completely independent of the incoming neutron speed. Aside from any energy dependence of the matrix element, the capture and fission cross sections will be proportional to the reciprocal of the flux, i.e.

$$\sigma_{\text{exothermic}} \propto 1/v_{\text{in}}.$$

[a] The same v dependence is found using the non-relativistic formula $E = p^2/(2m)$.

as follows. Heavy nuclei, such as the parent, are more neutron-rich than lighter ones (recall the curve in the valley of stability in §2.2.1). Hence the fission products, if they had the same ratio of protons-to-neutrons as their parent, would be too neutron for their value of A. This leads to the direct emission of on average 2.5 neutrons per fission.

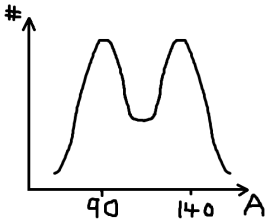

The fission tends to be asymmetric, resulting in fragments peaked around $A \sim 90$ and $A \sim 140$.

These fission fragments are also **neutron rich** and hence they must **beta-decay** towards the valley of stability.

If the ejected neutrons can be induced to cause further (n, f) reactions, then a **chain reaction** can occur in which neutrons produced in one generation of decays initiate the next.

For a power station, the chain reaction must proceed in a controlled manner. The rate of fissions, and hence the number density of neutrons at fissionable energies, must be controlled. Possible fates of neutrons within a reactor are:

- Neutrons can decay with an average lifetime of $\tau_n = 885$ s
- Lost from the reactor core
- Radiatively captured on the fuel
- Induce further fissions

We might try to improve reaction rates by using pure uranium-235. In pure $^{235}\mathrm{U}$, the mean-free path travelled by a neutron before it will induce fission is

$$\lambda_{\text{fission}} = \frac{1}{n_{235}\sigma_{\text{fission}}} \approx 10 \text{ cm}$$

where n_{235} is the number density of $^{235}\mathrm{U}$ nuclei. We would need to make our pure-235 reactor at least this large. Neutrons will be emitted from fissions with $\sim$ MeV energies and so will be travelling at $v = \sqrt{2m_n E_n} \approx 0.1c$. Since these speeds are much faster than the speed of sound in the material, the emitted neutrons will induce fission in further nuclei the before the material structure is disrupted by the release of energy. A chain reaction started in a critical mass of pure $^{235}\mathrm{U}$ will therefore exponentially increase in number of neutrons emitted and energy released. This fast release of a large amount of energy in a short time will not provide the controlled release of energy desired for a power station.

7.1.4 Fission reactor principles

Naturally-occurring uranium is approximately only 0.07% $^{235}\mathrm{U}$ with the rest made up from $^{238}\mathrm{U}$.

The majority isotope $^{238}\mathrm{U}$ has a series of sharp resonances in (n, γ) reactions in the approximate energy range $10\,\text{eV}$ to 10 keV. These resonances absorb neutrons and make it difficult to sustain a chain reaction. To keep a reaction going one must increase the probability for fission relative to absorption by: (a) increasing the fraction of uranium-235 in the fuel or (b) increasing σ_{fission} compared to σ_{capture}, or both.

Increasing the fraction of uranium-235 is known as **enrichment**. It can only be achieved using the difference in the physical properties caused by the mass differences of the isotopes — the chemical properties of the two isotopes are identical. Enrichment can be achieved by e.g. mass spectrometers for small amounts of material, or by exploiting differential gaseous UF_6 diffusion rates, or with centrifuges.

It is possible to further reduce the radiative capture on 238U by rapidly cooling the $\sim$MeV energy neutrons. Cooling of neutrons is known as **moderation**. Cooling neutrons to thermal temperatures ($< 0.1\,\text{eV}$) reduces their energies below the energy at which the resonances in 238U lead to radiative neutron capture. Cooling also increases the fission cross-section since, as shown in (7.3), the fission cross section $\sigma_{\text{fission}} \propto 1/v_n$. To avoid captures, and to increase efficiency, we wish to cool the neutrons in a space away from the fuel. This requirement leads to a heterogeneous

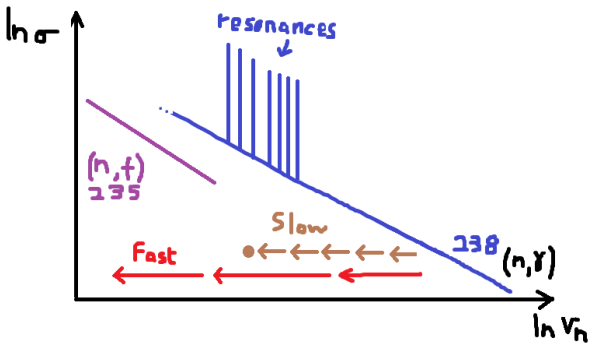

Figure 7.1: If a neutron can be cooled rapidly, there is a decreased probability for it to be lost to radiative capture.

reactor design, in which lumps (usually rods) of fuel are embedded in a matrix of moderating material[1].

The moderating material must have low neutron capture cross section and, for efficient cooling, should contain nuclei with small A. Typical moderating materials are graphite $^{12}\mathrm{C}$ or heavy water D_2O, where $D = {}^{2}_{1}\mathrm{H}$ is the deuteron. Rapid cooling — in a small number of collision steps — reduces the probability of a neutron having energy close to the $^{238}\mathrm{U}(n,\gamma)$ resonant peaks (Figure 7.1).

In a chain reaction the number of neutrons at any time will be given by

$$n = n_0 e^{(k-1)t/T}$$

where k is the average number of neutrons produced per fission less the number lost through decays, radiative captures, or loss from the core. T is the characteristic time for one generation of fissions. Since the neutron transit time between reactions is of order nanoseconds, even if $k = 1.001$ such a chain reaction can lead to exponential growth with a short doubling time. In order for the reaction to be controlled one must maintain k very close to unity.

Loss of neutrons to the surrounding material can be reduced by increasing the size of the reactor, and/or by surrounding it with a neutron reflector – a material with a large elastic scattering cross section. The reactor core is usually held within a steel pressure vessel, which is itself within a concrete shield. The steel reflects neutrons, and absorbs γ radiation. The concrete absorbs residual γ radiation and provides physical protection.

Energy is extracted from the reactor by circulating a fluid inside the core. Air, water or liquid sodium coolants have all been used. The thermal energy is transferred through a heat exchanger, used to boiling water, and to generate electricity using steam turbines.

The fission fragments are neutron rich, and so waste products include isotopes unstable to beta decay. Products with half-lives less than a day decay rapidly and

[1] There is also a more subtle reason why lumps of fuel are better. Since the de Broglie wavelength of the thermal neutron is larger $\lambda_{\text{thermal}} > \lambda_{\text{capture}}$, more of the fuel lump is 'seen' by the thermal neutron than by the higher energy, shorter wavelength, ~ 100 eV ready-to-capture neutron.

Moderators and energy loss

Consider an elastic collision between a moving body of mass m with another, initially stationary, body of mass M. In the zero momentum frame (ZMF), let the speed of the first mass be u and that of the second be $U = um/M$, and let the scattering angle in the ZMF be θ. In the lab the speed of m before the collision is

$$v_{\text{in}} = U + u,$$

whereas after the collision it is given by v_{out} where

$$\begin{aligned} v_{\text{out}}^2 &= v_{\text{out}\parallel}^2 + v_{\text{out}\perp}^2 \\ &= (U + u\cos\theta)^2 + (u\sin\theta)^2 \\ &= U^2 + u^2 + 2Uu\cos\theta \end{aligned}$$

The fraction of energy lost by m by in the lab frame is $v_{\text{out}}^2/v_{\text{in}}^2$. To find the average energy loss, we need to average over the scattering angle θ. For isotropic scattering

$$\langle\cos\theta\rangle = -\int_{-1}^{+1} \cos\theta\, d(\cos\theta) = 0$$

so the average fraction of energy lost by m is

$$\left\langle \frac{E_{\text{out}}}{E_{\text{in}}} \right\rangle = \frac{U^2 + u^2}{(U+u)^2} = \frac{m^2 + M^2}{(M+m)^2}$$

A moderator material will be maximally efficient when M is equal to m, meaning that we want materials with small A. At maximum efficiency, with $A = 1$, half of the initial neutron energy will be lost on average. An initial 1 MeV neutron will then cool to 0.1 eV after about $\log_2(\,\text{MeV}/0.1\,\text{eV}) \approx 23$ collisions.

do not present a problem. At the other extreme, products with half-lives larger than about 10^6 years have such small decay rates that they too are safe. In between lie the more awkward waste products. Small quantities of ^{90}Sr ($T_{1/2} = 29\,\text{yr}$), ^{137}Cs ($30\,\text{yr}$) and ^{99}Tc ($200\,\text{kyr}$) must be dealt with. There are proposals to use proton beams to transmute these into other safe isotopes, but for the moment such isotopes are typically encased in glass (vitrified) and held in secure storage.

7.2 Fusion

Since the most stable elements are found in the middle of the table of nuclides, energy can also be released by fusing together nuclei with very small A. The fusion process is responsible for the power of the stars, including the sun. Fusion is also a necessary step in the formation of the chemical elements. It also offers the potential of providing clean and abundant power for the future.

An example of a reaction which would liberate a large amount of energy is

$$4H \rightarrow {}^4_2\text{He} + 2e^+ + 2\nu_e \quad [Q = 28\,\text{MeV}]. \tag{7.5}$$

The isotope ^4He is particularly tightly bound[2], so this reaction is very energetically favourable. Despite being energetically favourable it is inhibited by the requirement

[2] ^4He is a doubly magic nucleus, with the special property that all four nucleons occupy essentially the same spatial wave function.

Reactor control

Control on timescales of order seconds is possible by inserting and withdrawing control rods with high neutron-capture cross section. Nuclides with large capture cross sections include the boron isotope $^{10}\mathrm{B}$ and the cadmium isotope $^{113}\mathrm{Cd}$.

How is it possible to control reactors by moving rods over timescales of seconds when the typical time between fission reaction generations is of order nanoseconds? Fortunately about 1% of neutrons emitted after fission come not from fission fragments themselves, but from their daughters after beta decay.

$$^{\mathrm{A}}_{\mathrm{Z}}\mathrm{X} \xrightarrow{\beta^-} {}_{\mathrm{Z}+1}{}^{\mathrm{A}}\mathrm{Y} \longrightarrow {}^{\mathrm{A}-1}_{\mathrm{Z}+1}\mathrm{Y} + n.$$

These neutron emissions are **delayed** by time taken for the the beta decays, which have typical time constants of 0.1 s – 1 s. The reactor is then operated at such that it is subcritical ($k < 1$) with fast neutrons alone. The reactor is then critical only because of the delayed neutrons, and the effective time constant for control increases to of order seconds.

that four protons need to come together overcoming Coulomb repulsion. In addition two factors of the Fermi coupling constant G_F enter the matrix element, one for each of the proton to neutron transitions.

	Nuclide		$T_{1/2}$
D	Deuterium	$^2_1\mathrm{H}$	stable
T	Tritium	$^3_1\mathrm{H}$	12.3 yr

What fuel to use in man-made fusion reactions?

Prototype fusion reactors achieve best fusion rates using a duterium-tritium fuel mixture.

The barrier height for $D + D$ and $D + T$ fusion would appear to be the same as for H+H using our naive calculation. In fact the barrier is reduced since the nucleons within these composite nuclei have some freedom to arrange themselves to reduce the height of the Coulomb barrier.

The rate for $D + T$ is further enhanced by a resonant reaction involving an intermediate excited state of $^5\mathrm{He}$:

$$^3_1\mathrm{T} + {}^2_1\mathrm{D} \longrightarrow {}^5\mathrm{He}^* \longrightarrow {}^4\mathrm{He} + n \quad [+17.6\ \mathrm{MeV}]$$

The D+T reaction is used because it combines a large resonant cross section and a large Q value.

The simpler reaction

$$p + p \to D + e^+ + \nu_e,$$

has the advantage of not requiring the coincidence of four particles, but it is also inhibited by Coulomb repulsion. The Coulomb barrier is of size

$$E_b \approx \alpha_{\mathrm{EM}} \frac{\hbar c}{2\,\mathrm{fm}} = \frac{1}{137} \frac{(197\,\mathrm{MeV\,fm})}{2\,\mathrm{fm}} \approx 0.7\ \mathrm{MeV}.$$

Fusion will therefore only proceed uninhibited by this barrier at temperatures where each proton has energy of order $E_b/2$. We can use the Boltzman constant k_B to convert this to a temperature, which is of order $E_b/(2k_B) \approx 4 \times 10^9\,\mathrm{K}$. Uninhibited fusion therefore requires extremely high temperatures.

$$p(v) \propto \exp\left(-\frac{mv^2}{2k_B T}\right)$$

The Maxwell-Boltzmann velocity distribution.

Fusion can proceed at lower temperatures — indeed the temperature in the centre of the sun is a relatively 'mild' $1.6 \times 10^7\,\mathrm{K}$. Two factors enable fusion to happen at temperatures significantly lower than $10^9\,\mathrm{K}$. The first is that fusion may occur

via quantum tunnelling through the Coulomb barrier. The calculation is analogous to that performed during the consideration of α decay (§2.3.1). The second factor that assists fusion at lower temperatures is the high-energy tail of the Maxwell-Boltzmann velocity distribution.

In man-made fusion reactors, a duterium-tritium plasma is held within a toriodal volume using magnetic confinement. In these **Tokamaks**, the plasma is heated to temperature of 1.5×10^8 K. The best reaction rates and largest energy release is found at the lowest temperatures by using the reaction

$$ {}^3_1\mathrm{T} + {}^2_1\mathrm{D} \longrightarrow {}^4\mathrm{He} + n. \tag{7.6} $$

Duterium fuel can be efficiently extracted from sea water. Tritium is unstable, with a half-life of about 12 years, so must be artificially produced. The main waste product is inert helium gas. The 14 MeV neutrons from the fusion reaction can be used to produce extra tritium. We can place a 'blanket' of lithium in the wall of the reactor vessel. Tritium is then generated within the blanket through the reactions

$$ n + {}^6_3\mathrm{Li} \rightarrow {}^3_1\mathrm{T} + {}^4_2\mathrm{He} $$

and

$$ n + {}^7_3\mathrm{Li} \rightarrow {}^3_1\mathrm{T} + {}^4_2\mathrm{He} + n. $$

The ${}^6_3\mathrm{Li}$ reaction is exothermic, so contributes to the energy that can be extracted from the reactor. The ${}^7_3\mathrm{Li}$ reaction is endothermic, but has the advantage of recycling the neutron. We require more than one triton to be produced per neutron to maintain a continuous supply of tritium, since the fusion reaction (7.6) consumes a triton for each neutron it produces. The ${}^7_3\mathrm{Li}$ reaction meets this need, and allows a sufficient supply of tritium fuel to be maintained.

7.3 Solar reactions and nucleosynethesis

Nuclear reactions in stars are important not only because they generate light and heat, but also because they are the only method by which nuclei heavier that lithium can exist. All of the carbon, oxogen, nitrogen in our bodies is the result of nucleus building within stars, in a series of processes called **nucleosynthesis**.

The sun predominantly burns hydrogen to form helium. We have argued that the direct combination (7.5) of four protons to form ${}^4\mathrm{He}$ is very improbable, but the reaction can occur via a series of steps as follows.

First two protons fuse to form a deuteron:

$$ p + p \rightarrow {}^2\mathrm{D} + e^+ + \nu_e. \tag{7.7} $$

This first pp fusion reaction involves the transmutation of a proton into a neutron, and so must proceed via the four-fermion vertex of the Fermi beta-decay theory (§2.3.2). It involves both tunnelling through a Coulomb barrier, and a Fermi matrix element containing a factor of G_F, so occurs at a fairly small rate — it is the rate limiting step. Next is radiative capture of a proton on a deuteron:

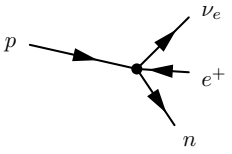

Hydrostatic equilibrium and stellar temperatures

We can find the temperature and pressure inside a star of mass M and radius R as follows. Consider an element of a stellar shell, at radius r, of thickness δr and of area A. The gravitational force F_G on that element is of size

$$F_G = \frac{Gm\rho}{r^2} A\,\delta r,$$

where $m(r)$ is the mass contained with the sphere of radius r and $\rho(r)$ is the local density. For hydrostatic equilibrium the gravitational attraction must be balanced by a repulsive force caused the pressure gradient of size

$$F_P = A\Delta P = A\frac{dP}{dr}\delta r.$$

By equating these two forces we can find a bound on the pressure at the centre of the star as follows. First we recognise that

$$\frac{dm}{dr} = 4\pi r^2 \rho(r)$$

allowing us to re-express the equilibrium condition as

$$\frac{dP}{dm} = \frac{Gm}{4\pi r^4}.$$

The integral over the whole star

$$P(M) - P(0) = -\int_{m=0}^{M} \frac{Gm\,dm}{4\pi r^4}$$

cannot be exactly evaluated without knowing how the density varies with radius, but nevertheless it must be larger than

$$-\int_{m=0}^{M} \frac{Gm\,dm}{4\pi R^4} = \frac{GM^2}{8\pi R^4}.$$

where R is the radius of the star.

The calculation places a lower bound on the pressure at the centre of the sun of 4.4×10^{13} Pa, which is equivalent to 450 million atmospheres. We may then use the ideal gas law $PV = nk_BT$ to calculate a lower bound on the temperature of the centre of the sun. The lower limit we obtain will be found to be somewhat lower than the value (of about $T_c = 1.6 \times 10^7$ K) that we would have obtained from a more exact numerical calculation.

$$D + p \rightarrow {}^3\mathrm{He} + \gamma. \tag{7.8}$$

Finally, two of these ${}^3\mathrm{He}$ nuclei may fuse, generating an alpha particle and recycling two protons:

$${}^3\mathrm{He} + {}^3\mathrm{He} \rightarrow {}^4\mathrm{He} + 2p. \tag{7.9}$$

The net effect of the three reactions (7.7)-(7.9) is that of reaction (7.5) above. The combined set of reactions (7.7)-(7.9) is known as the **pp-I chain**.

7.3.1 The pp-II and pp-III chains

Several other competing reactions also occur which have the net effect of turning Hydrogen into Helium. At temperatures above that at which the pp-I chain occurs, two helium isotopes (produced as described in §7.3 above) may fuse to form Beryllium-7,

$${}^3_2\mathrm{He} + {}^4_2\mathrm{He} \rightarrow {}^7_4\mathrm{Be} + \gamma.$$

At this point the reaction can take one of two branches.

In the **pp-II branch** the subsequent series of reactions is electron capture

$${}^7_4\mathrm{Be} + e^- \rightarrow {}^7_3\mathrm{Li} + \nu,$$

followed by the lithium-7 absorbs a further proton

$${}^7_3\mathrm{Li} + p \rightarrow 2\ {}^4_2\mathrm{He}$$

generating two further Helium-4 nuclei.

In the **pp-III chain** a different series of reactions leads to the same end result. First the Beryllium-7 absorbs a proton

$${}^7_4\mathrm{Be} + p \rightarrow {}^8_5\mathrm{B} + \gamma.$$

The resulting ${}^8_5\mathrm{B}$ is unstable to β^+ decay

$${}^8_5\mathrm{B} \rightarrow {}^8_4\mathrm{Be} + e^+ + \nu_e$$

generating ${}^8_4\mathrm{Be}$. Because of the particularly large binding energy of the Helium nucleus, Beryllium-8 spontaneously splits in two

$${}^8_4\mathrm{Be} \rightarrow 2\,{}^4_2\mathrm{He}$$

generating two Helium nuclei.

In each of these two chains — pp-II and pp-III — the net reaction is

$${}^3_2\mathrm{He} + {}^4_2\mathrm{He} + {}^1_1\mathrm{p} \rightarrow {}^4_2\mathrm{He} + {}^4_2\mathrm{He} + e^+ + \nu_e.$$

7.3.2 The CNO cycles

Protons are also burned to helium through carbon-nitrogen-oxygen catalysis. These reactions are catalysed by ${}^{12}\mathrm{C}$, which must therefore be formed within stars.

Producing carbon – Helium burning

There are roadblocks in forming elements heavier than Helium caused by the absence of any stable isotopes with mass numbers 5 or 8. Because Helium is particularly tightly bound, the candidate isotopes with $A = 5$ and $A = 8$ decay in the following manners:

$$\begin{aligned} {}^{5}_{3}\mathrm{Li} &\longrightarrow {}^{4}_{2}\mathrm{He} + p \\ {}^{5}_{2}\mathrm{He} &\longrightarrow {}^{4}_{2}\mathrm{He} + n \\ {}^{8}_{4}\mathrm{Be} &\longrightarrow 2\ {}^{4}_{2}\mathrm{He} \end{aligned}$$

Fortunately, in thermal equilibrium there will exist a small but non-zero population of ${}^{8}_{4}\mathrm{Be}$ through the equilibrium process

$${}^{8}_{4}\mathrm{Be} \rightleftharpoons 2\ {}^{4}_{2}\mathrm{He}$$

A further ${}^{4}_{2}\mathrm{He}$ nucleus can react with the equilibrium population of ${}^{8}_{4}\mathrm{Be}$ to generate ${}^{12}\mathrm{C}$. We are fortunate that there is an excited state of ${}^{12}\mathrm{C}^{*}$ at just the right energy to cause resonant production via

$${}^{8}_{4}\mathrm{Be} + {}^{4}_{2}\mathrm{He} \rightarrow {}^{12}\mathrm{C}^{*} \longrightarrow {}^{12}\mathrm{C} + \gamma$$

There are two important catalysis cycles. The first (**CNO-I**) is:

$$\begin{aligned} {}^{12}_{6}\mathrm{C} + p &\rightarrow {}^{13}_{7}\mathrm{N} + \gamma \\ {}^{13}_{7}\mathrm{N} &\rightarrow {}^{13}_{6}\mathrm{C} + e^{+} + \nu_e \\ {}^{13}_{6}\mathrm{C} + p &\rightarrow {}^{14}_{7}\mathrm{N} + \gamma \\ {}^{14}_{7}\mathrm{N} + p &\rightarrow {}^{15}_{8}\mathrm{O} + \gamma \\ {}^{15}_{8}\mathrm{O} &\rightarrow {}^{15}_{7}\mathrm{N} + e^{+} + \nu_e \\ {}^{15}_{7}\mathrm{N} + p &\rightarrow {}^{12}_{6}\mathrm{C} + {}^{4}_{2}\mathrm{He} \end{aligned}$$

which recycles the ${}^{12}\mathrm{C}$, and has the same net effect of converting four protons to ${}^{4}_{2}\mathrm{He}$ plus two positrons and two neutrinos – i.e. the same reaction as shown in (7.5).

The second cycle of the CNO set of reactions shares several of the reactions of the first:

$$\begin{aligned} {}^{14}_{7}\mathrm{N} + p &\rightarrow {}^{15}_{8}\mathrm{O} + \gamma \\ {}^{15}_{8}\mathrm{O} &\rightarrow {}^{15}_{7}\mathrm{N} + e^{+} + \nu_e \end{aligned}$$

but has a different way of recycling the ${}^{14}_{7}\mathrm{N}$, via somewhat heavier elements.

$$\begin{aligned} {}^{15}_{7}\mathrm{N} + p &\rightarrow {}^{16}_{8}\mathrm{O} + \gamma \\ {}^{16}_{8}\mathrm{O} + p &\rightarrow {}^{17}_{9}\mathrm{F} + \gamma \\ {}^{17}_{9}\mathrm{F} &\rightarrow {}^{17}_{8}\mathrm{O} + e^{+} + \nu_e \\ {}^{17}_{8}\mathrm{O} + p &\rightarrow {}^{14}_{7}\mathrm{N} + {}^{4}_{2}\mathrm{He} \end{aligned}$$

The net effect is that of conversion of four protons to ${}^{4}_{2}\mathrm{He}$ plus two positrons and two neutrinos – i.e. the same reaction as shown in (7.5).

These reactions are most important in stars more massive than the sun, in which higher temperatures can be reached, and for which the large Coulomb barrier for these larger-Z reactants is relatively less important.

7.3.3 Solar neutrinos

In the reactions above β^+ decays and electron capture reactions lead to the emission of electron-type neutrinos. In a three-body decay process, such as β^+ decay, the final energy is shared out between the electron and the neutrino, and so a continuum spectrum of neutrino energies is produced (up to some maximum close to Q). For a two-body decay process, such as electron capture, there energy and momentum conservation constrain the size of the neutrino energy to a single value, equal to the Q value of the reaction minus the recoil energy of the daughter nucleus.

There is a continuum distribution of low-energy neutrinos from the initial proton fusion reaction

$$2\,p \rightarrow {}^{2}_{1}\mathrm{D} + e^{+} + \nu_e.$$

This competes with the 'pep' reaction

$$p + e^{-} + p \rightarrow {}^{2}_{1}\mathrm{D} + \nu_e.$$

which has a smaller cross-section, but which has a two-body final state, so produces a source of mono-energetic neutrinos.

We can see that there are also mono-energetic ν_e emissions from the pp-II chain from the electron capture process

$${}^{7}_{4}\mathrm{Be} + e^{-} \rightarrow {}^{7}_{3}\mathrm{Li} + \nu.$$

There is continuum of neutrino energies from the pp-III chain from the β^+ decay process

$${}^{8}_{5}\mathrm{B} \rightarrow {}^{8}_{4}\mathrm{Be} + e^{+} + \nu_e.$$

In all cases the type of neutrino produced is an electron-flavour neutrino ν_e.

One can calculate the flux of neutrinos expected from these reactions at different energies. Detecting the solar neutrinos on earth requires sensitive detectors. We must also be careful to reduce the backgrounds from cosmic rays, radioactivity, and other noise sources. Solar neutrino experiments provided the early evidence for neutrino oscillations (§6.5.1).

7.3.4 Heavier elements

During the lifetime of a sun-like star, the temperature and the fuel change. When the hydrogen fuel is exhausted, the core starts to collapse under its own gravity, and it heats until the temperature is high eneough for helium to be effective as a fuel. When the helium is expended the temperature rises again and the next fuel comes into use, and so on.

Beyond ${}^{12}_{6}\mathrm{C}$ further α particle addition can generate ${}^{16}_{8}\mathrm{O}$ and ${}^{20}_{10}\mathrm{Ne}$. Fusion of two ${}^{12}_{6}\mathrm{C}$ isotopes can lead to production of ${}^{24}_{12}\mathrm{Mg}$.

The Coulomb barrier prevents fusion of large nuclei. However in the late stages of heavy stars, elements up to ${}^{56}\mathrm{Fe}$ can be produced through a process in which neutrons are radiatively captured (n, γ). The neutrons themselves are bled off from other reactions such as ${}^{13}\mathrm{C}(\alpha, n){}^{16}\mathrm{O}$.

Supernovae and the heaviest elements

Stars larger than about nine solar masses finish their lives with a bang. Their inner core collapses several times as it sequentially consumes different fuels, leading to a onion-layered structure with Hydrogen burning in the outer layers, with inner layers using He, C, Ne, O, and finally Si as fuels. Successive fuels require higher temperatures to overcome the Coulomb barrier, but liberate smaller energies, so burn increasingly rapidly. When all the silicon in the core burns to nickel and iron a cataclysmic implosion takes place over several seconds. The shock wave from this implosion detaches the outer layers of the star, and briefly provides the only natural conditions under which elements heavier than iron are produced.

The mechanism starts with photo-disintegration of Fe by high-energy gamma rays producing large fluxes of free neutrons. These neutrons bombard heavy nuclei, and are accreted with successive beta decays bringing the resulting heavy nucleus back to the valley of stability. Elements as heavy as ${}^{238}\mathrm{U}$ can be produced in this way.

Supernovae are expected to lose a large fraction of their energy through neutrinos, which pass through the outer layers relatively unimpeded. A total of 19 neutrinos from SN1987A were observed by two detectors within a 13 s interval.

Key concepts

- Neutron-induced fission of ${}^{235}\mathrm{U}$ can be controlled in self-sustaining **chain reactions**
- Cooling of the neutrons with a **moderator** to thermal temperatures allows a chain reaction since

$$\sigma_{\text{fission}} \propto \frac{1}{v_n}$$

  and because such cooling reduces the loss of neutrons via resonant radiative capture ${}^{238}\mathrm{U}(n, \gamma)$.
- Fission of light elements is possible at high temperature through high-energy tail of the **Maxwell-Boltzmann** distribution and **tunnelling** through the Coulomb barrier.
- Nucleosynthesis in stars occurs via reactions including the **pp-I**, **pp-II** and **pp-III** chains, and the **CNO bi-cycle**.
- Heavier elements are created via sequential burning of larger-Z fuels as lower-Z fuels are expended.

Further reading

- W. N. Cottingham and D. A. Greenwood, *An Introduction to Nuclear Physics*
- B. Martin, *Nuclear and Particle Physics: An Introduction*
- W. S. C. Williams, *Nuclear and Particle Physics*
- K.S. Krane *Introductory Nuclear Physics*
- M.G. Bowler *Nuclear Physics*
- N.A. Jelley *Fundamentals of Nuclear Physics*
- Ed. S. Esposito and O. Pisanti, *Neutron Physics for Nuclear Reactors: Unpublished Writings by Enrico Fermi*
- D.D. Clayton, *Principles of Stellar Evolution and Nucleosynthesis* (1968).

Chapter 8

Accelerators and detectors

8.1 Basics

To understand the properties of an object we need to see how it interacts with other objects. The typical experiment in nuclear or particle physics involves firing a projectile (e.g. proton, neutron, electron, ...) at a target. The projectile and target undergo an interaction (possibly creating a long-lived excited intermediate state which then decays). The particles at the end may not be the same ones you started with, but nevertheless we wish to detect them.

In some cases we don't have to do the 'firing' ourselves. For example many of the excited states of interest in nuclear physics – the unstable nuclei – were created long ago by high-energy collisions within stars. We just have to wait for them to decay.

The topic of how to make, accelerate, detect and identify particles is an enormous one. If you can answer the in-line questions marked marked with arrows ($\Rightarrow$) you are doing well.

8.2 Accelerators

Scattering experiments are easiest to interpret if the initial state is a beam of particles with a known momentum $\mathbf{p}$. To make such a beam particles must either be accelerated to large $\mathbf{p}$, or must come from the decay of a parent which itself had large $\mathbf{p}$.

To accelerate the beam of particles, they will need to have interactions with an external field. The only forces which are active over macroscopic length scales are the electromagnetic and gravitational forces. The gravitational forces on subatomic particles are very much smaller than the electromagnetic ones, so we conclude that we should use electromagnetic fields to change $\mathbf{p}$. The particles to be accelerated will then have to be charged. We can achieve this by (for example) pulling electrons

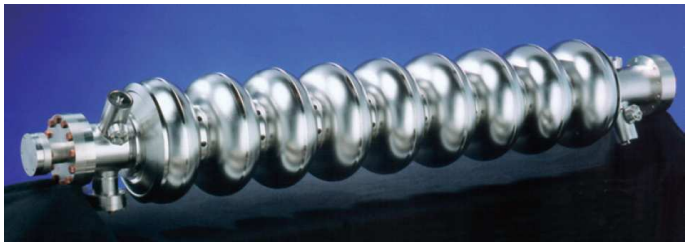

Figure 8.1: A superconducting niobium cavity designed for a high-energy e^+e^- linear collider. The cavities operate at radio frequencies and can support fields up to $50\,\mathrm{MV\,m^{-1}}$.

off a hot cathode (e^- beam) or using such an electron beam to strip electrons from atoms to create positively-charged ions (e.g. protons beam from kicking the electrons off Hydrogen).

$$\frac{d\mathbf{p}}{dt} = Q[\mathbb{E} + \mathbf{v} \times \mathbf{B}]$$

The Lorentz force law. Q is the particle's charge, $\mathbf{p}$ its momentum, $\mathbf{v}$ its velocity, and $\mathbb{E}$ and $\mathbf{B}$ the electric and magnetic fields, respectively.

Since the magnetic field changes only the direction of $\mathbf{p}$, we have to use electrical fields to increase the energy of the particles. How big an $\mathbb{E}$ field can be achieved? From knowledge of atomic energy levels, we expect that the electric strength is of order $0.1\,\mathrm{V}/10^{-10}\,\mathrm{m} \sim 10^8\,\mathrm{V\,m^{-1}}$. Fields stronger than this will pull electrons from the metal surface, so cannot be sustained. To get energies of order MeV can therefore be done in a small scale,[1] whereas to get TeV-scale energies from linear acceleration would require constant acceleration over distances of order $10^{12}\,\mathrm{V}/(10^8\,\mathrm{V\,m^{-1}}) \sim 10^4\,\mathrm{m}$.

Linear accelerators

The problem we encounter with a constant electric field is that to achieve high energies we need an enormous potential difference. Large potential differences tend to break down because of electrical discharge (sparking) to nearby objects.

We can get around this by realizing that only that only the local $\mathbb{E}$ field needs to be aligned along $\mathbf{v}$, and only while the particle is in that particular part of space.

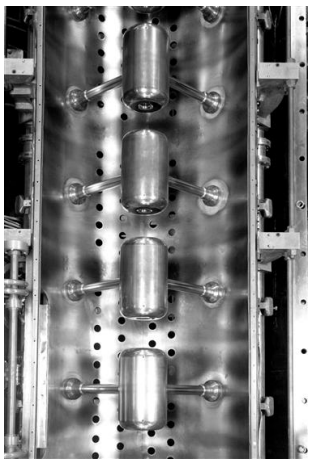

The linear accelerator injector to the CERN proton synchrotron. ©CERN

We can use time-varying electric fields to achieve large energy without large static potential differences. In the margin you can see a picture of a **linear accelerator** or **linac**. In this device we have a series of cylindrical electrodes with holes through the middle of each which allow the beam to pass through. Electrodes are attached alternately to either pole of an alternating potential. The particles are accelerated in bunches. As each bunch travels along we reverse the potential while the bunch is inside electrode (where this is no field). We can then ensure that when the bunch is in the gap between the electrodes the field is always in the correct direction to keep the particle accelerating.

The oscillating potential on the electrodes may be created by connecting wires directly from the electrodes to an oscillator. For radio frequency AC oscillations we instead bathe the whole system in an electromagnetic standing wave, at the right

[1] An exception will be discussed in lectures.

frequency and phase to provide continuous acceleration.

8.2.1 Bending, and circular accelerators

By bending our particle beams into a circle we can reuse the same accelerating components many times over.

Beams are bent by magnetic fields, $\mathbf{B}$, with a force given by

$$\mathbf{f} = \mathcal{Q}\mathbf{v} \times \mathbf{B}.$$

The acceleration is perpendicular to the velocity, so the Lorentz factor γ is unchanged, and the Lorentz force law reduces to

$$\mathcal{Q}v_\perp B = \gamma_v m a,$$

where a is the lab acceleration, and $v_\perp$ is the velocity perpendicular to the magnetic field. The particle's motion will describe a circle (or a helix if we start it off with non-zero momentum component $p_\parallel$ in the direction parallel to **B**). The acceleration in the lab frame must satisfy

$$a = \frac{v_\perp^2}{R},$$

where R is the radius of the circle. Combining this with the Lorentz force gives

$$\mathcal{Q}v_\perp B = \frac{\gamma m v_\perp^2}{R}.$$

For $\mathbf{p}_\parallel = 0$ the particle describes a circle of radius

$$R = \frac{p_\perp}{\mathcal{Q}B},$$

where $\mathbf{p}_\perp = \gamma_v m \mathbf{v}_\perp$ are the momentum components perpendicular to $\mathbf{B}$.

If we have a particle with charge $|e|$ and we express $p_\perp$ in GeV, B in Tesla and R in meters then we have the simple scaling law that

$$\boxed{p_\perp = 0.3BR} \qquad \text{[GeV, Tesla, meters]}.$$

The maximum energy achievable for proton beams (currently $E = 3.5$ TeV for protons at the LHC, CERN, Geneva) is limited by the product BR. Large scale superconducting magnets can reach fields of order of a few Tesla, so for a TeV-momentum beam we'll need $R \sim$ km.[2]

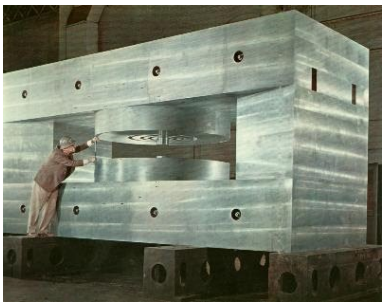

To make a high-momentum beam you might want one big magnet...

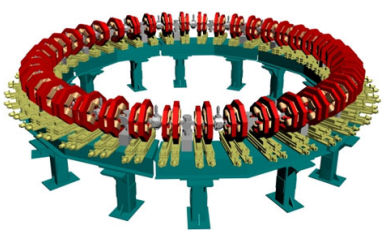

...or perhaps lots of small ones.

The other effect one needs to worry about in circular accelerators is **synchrotron radiation**. This is the electromagnetic radiation emitted when relativistic charges accelerate, which they must do to describe a circle. The synchrotron energy loss is proportional to γ^4. Electrons have a much smaller mass than e.g. protons and hence a larger γ for the same energy or momentum. Electron beam energies are

[2] Astronomical sources can have large magnetic fields over longer distances, and accelerate particles to even higher energies. Cosmic rays impinging on the earth's atmosphere from space have been observed with energies above 10^{20} eV! [14]

are usually limited by synchrotron losses [3]. Electrons in circular colliders have have been accelerated to energies of up to about $105\,\text{GeV}$ at LEP (CERN, Geneva).

$\Rightarrow$ Find out what is meant by a **cyclotron** and a **synchrotron**. Explain the difference to a friend.

8.3 Introduction to detectors

We want to study the properties of particles. For us to infer their presence they have to undergo *interactions* with some material that then leads to a detectable signal.

Historically a variety of techniques have been used to detect the presence of particles. Geiger and Marsden worked with α particles. They bashed them off nuclei and then into a **phosphor screen**. When the α hits the screen it partially ionized the atoms there. When those atoms de-excite they can create visible light [8]. (Old cathode ray tube televisions and monitors work on similar principles.) **Cloud chambers** contain a super-saturated gas solutions. The gas is ready to form droplets, but there is an energy barrier caused by surface tension which prevents the formation of small droplets (and hence large ones). Charged particles depositing energy via ionization allow droplets to form along their path, forming a visible track.

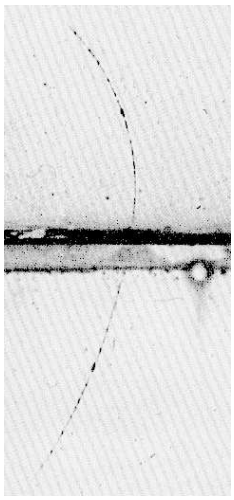

Cloud chamber photograph showing a positively charged particle with the same mass as the electron – an anti-electron or **positron**. This is how anti-matter was discovered. The lead plate in the middle of the picture is used to slow the positron so that the direction of motion (and hence the charge) can be inferred. From [3].

Bubble chambers are not so different. They use a super-heated liquid (e.g. liquid Hydrogen), just ready to boil. When the particle passes through, it generates enough energy for gas bubbles form, creating a trail of bubbles along the track.[4]

Both droplets and bubbles will scatter light, so can be photographed, producing snazzy pictures that show the particle trajectories.

Most modern particle detectors are rather different. They are almost all designed to produce **electrical** signals, rather than photographic ones. They need some method of liberating charge — charge which is subsequently amplified and digitized. By feeding the signals into a computer, very large numbers of interactions can be analyzed. Computer analysis is easier on the eyes than scanning thousands of photos.

8.4 Particle interactions with matter

If we are going to detect a particle then it had better **interact** with something.

The interactions of particles depend on their properties – particularly their masses, charges, and couplings to other particles. We don't need to know about them all,

[3] These losses are a pain if you want to get the beam to high energy. But they have their uses. The intense x-rays emitted are just what you want if you are a materials scientists, crystallographer or biologist.

[4] One of the few instances of a great physics idea being inspired by someone staring at a pint of beer.

but let's consider some examples.

8.4.1 Photon interactions

When a photon strikes some material object the result depends on the energy of that photon.

The dominant interactions of photons in some example materials are shown in Figure 8.2 for a range of photon energies. At low energy the photon is usually coherently absorbed by the atom, leading to the ejection of the electron in a process known as **photoelectric absorption**. In the figure you can see the large cross-section, with sharp spikes when the photon has enough energy to knock electrons out of more tightly-bound shells.

Compton Scattering At higher energy the photon acts as if scattering elastically from stationary 'free' electrons. This is known as **Compton scattering**:

$$\gamma + e^- \rightarrow \gamma + e^-.$$

Let's investigate the kinematics. Let the photon four-momentum be P and the electron four-momentum be Q. We'll use the same symbols but with primes after the scatter. Then energy-momentum conservation is given by

$$\mathsf{P} + \mathsf{Q} = \mathsf{P}' + \mathsf{Q}'.$$

To eliminate the components of Q′, recognize that we get rid of the energy and momentum components of the electron by taking

$$\mathsf{Q}'^2 = (\mathsf{P} + \mathsf{Q} - \mathsf{P}')^2 \ . \tag{8.1}$$

The electron can be assumed to be at rest. Without loss of generality the four-vectors can be expressed as

$$\mathsf{P} = \begin{pmatrix} E \\ E \\ 0 \\ 0 \end{pmatrix} \qquad \mathsf{Q} = \begin{pmatrix} m_e \\ 0 \\ 0 \\ 0 \end{pmatrix} \qquad \mathsf{P}' = \begin{pmatrix} E' \\ E'\cos\theta \\ E'\sin\theta \\ 0 \end{pmatrix}.$$

Expanding (8.1) we find that

$$EE'(1-\cos\theta) = m_e(E - E').$$

which can be rewritten

$$E' = \frac{m_e E}{E(1-\cos\theta) + m_e}.$$

But what do we observe? If the photon is scattered through sufficiently small angles that all of its energy *and all of the energy of the scattered electron* end up being absorbed in the detector then one gets a *peak* corresponding to E.

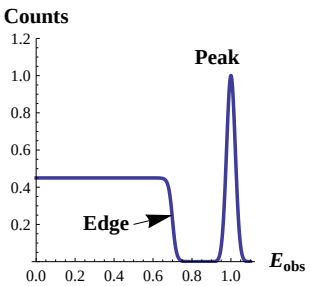

Rate as a function of fraction of the observed photon energy.

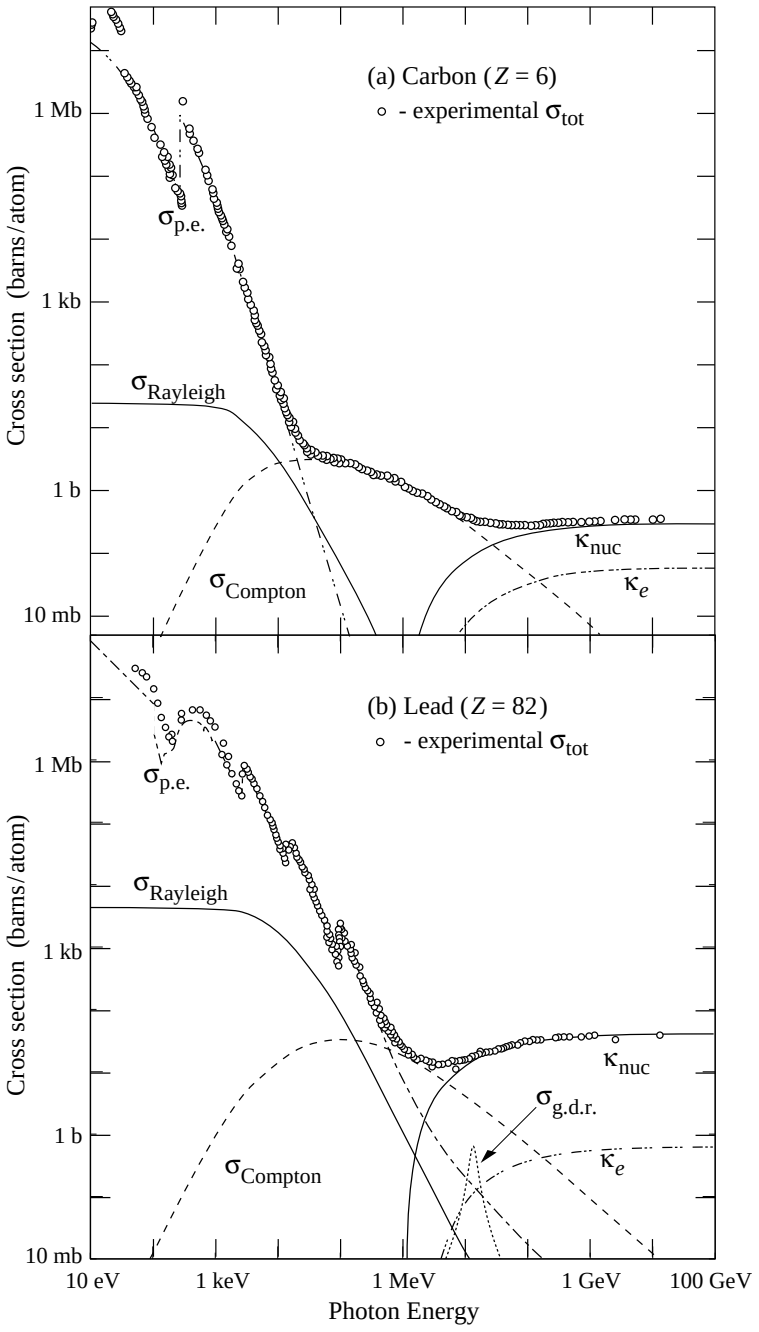

Figure 8.2: Photon total cross sections as a function of energy in carbon and lead, showing the contributions of different processes. Most important are:
(p.e.) Atomic photoelectric effect (electron ejection, photon absorption)
(Compton) Compton scattering from an electron: $\gamma + e^- \rightarrow \gamma + e^-$
(nuc) $\gamma \rightarrow e^+e^-$ pair production in the nuclear electric field.
From [12].

What if the photon scatters through a sufficiently large angle that it is not subsequently absorbed by the material? Then some of the energy will not be observed, and the visible signal will be smaller. The energy lost depends on the angle through which the photon is scattered.

Assuming the photon is lost, the *minimum* energy is lost when E' is smallest, which is when the photon back-scatters such that $\cos\theta$ is close to -1. When an ensemble of scattering events are observed (e.g. when detecting many individual gamma rays one-by-one from an isotopic decay) the distribution of *observed* energies shows a sharp drop corresponding to scattered photon energy

$$E' = \frac{m_e E}{2E + m_e}.$$

The sharp drop at visible energy $E - E'$ is known as the **Compton edge**.

Pair creation At still higher energies, photons with $E > 2m_e$ can create e^+e^- pairs from interactions in the vicinity of an atomic nucleus,

$$\gamma + \text{nucleus} \rightarrow e^+ + e^- + \text{nucleus}.$$

The nucleus absorbs some of the momentum from the photon. The energy of the incoming photon clearly has to be greater than twice the rest-mass-energy of the electron for the reaction to proceed.
$\Rightarrow$ Why can the above reaction *not* happen in a vacuum?

8.4.2 Very high-energy electrons and photons

Very high energy electrons in the presence of a charged nucleus will accelerate (electrons more so than e.g. protons). Accelerated charges emit electromagnetic radiation – photons:

$$e^\pm + \text{nucleus} \rightarrow e^\pm + \gamma + \text{nucleus}.$$

The process above is known as **Bremsstrahlung** (from the German 'braking radiation'.)

As described above in §8.4.1, the photons produced — if they have enough energy — can lead to **pair-creation** of further electrons and positrons in the nuclear electric field

$$\gamma + \text{nucleus} \rightarrow e^+ + e^- + \text{nucleus}.$$

Those electrons and positrons can themselves undergo further Bremsstrahlung. More electrons, positrons and photons are created through repeated cycles of Bremsstrahlung and pair-creation until the energy of the photons is too small to generate electron-positron pairs.

The net effect is to creates a *cascade* or shower of electrons, photons, and positrons. As these come to rest they create a lot of subsequent ionization. The average amount of ionization will be proportional to the energy of the incoming electron or photon. A particle sensitive to this ionization — for example a crystal which

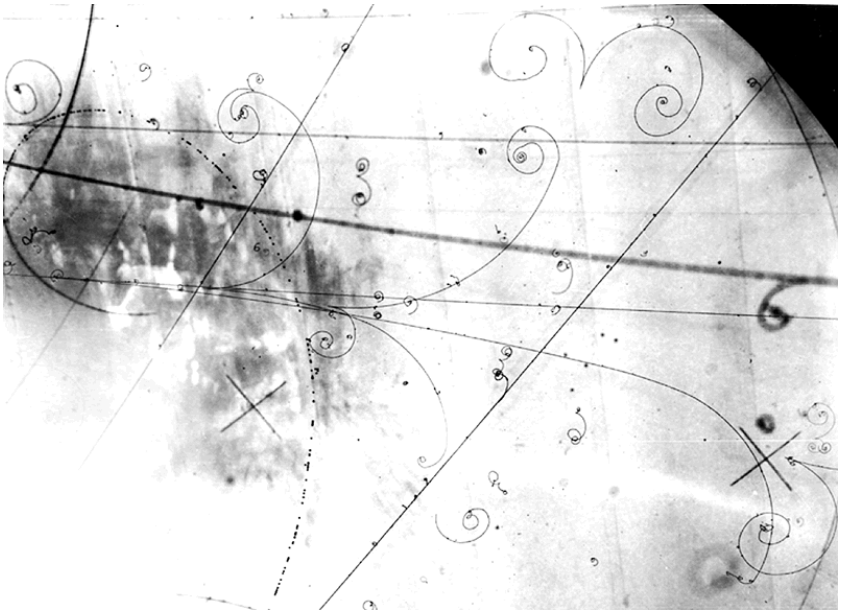

Figure 8.3: Bubble chamber photograph showing the creation of electron-positron pairs $\gamma \rightarrow e^+ + e^-$, and photon creation from Bremsstrahlung.

produces light proportional to the energy deposited in it — then acts as an **electromagnetic calorimeter**.[5]

8.4.3 Very high-energy, strongly interacting particles

Particles which couple to the *strong nuclear force* – such as neutrons, protons, kaons and pions can undergo strong-force reactions with atomic nuclei. For very high-energy projectiles these mostly result in the creation of new strongly-interacting particles, e.g.

$$\begin{aligned} n + \text{nucleus} &\rightarrow n + \pi^0 + \text{nucleus} \\ p + \text{nucleus} &\rightarrow n + \pi^+ + \text{nucleus} \\ \pi^- + \text{nucleus} &\rightarrow n + \pi^- + \pi^+ + \pi^- + \text{nucleus} \\ \pi^+ + \text{nucleus} &\rightarrow \pi^+ + \pi^0 + \text{nucleus.} \end{aligned}$$

Rather like in the electromagnetic case, cascades of such interactions create large numbers of charged pions — the lightest strongly interacting particles — and photons from the subsequent decay $\pi^0 \rightarrow \gamma\gamma$. This is known as a 'hadronic shower', and devices which exploit it to determine the energy of the original strongly-interacting particle are imaginatively referred to as **hadronic calorimeters**.

[5] Calorimeter = device for measuring energy.

8.4.4 Detecting neutrons

High energy neutrons will create hadronic showers (described above). If the neutron energy is less than or even close to $m_\pi \approx 140$ MeV they won't be able to play that game.

Low energy neutrons can be detected by inducing them to undergo nuclear reactions which lead to ionizing particles. For example neutrons impinging on a gas of BF_3 can undergo the reaction

$$n + {}^{10}\mathrm{B} \to \alpha + {}^{7}\mathrm{Li}$$

which has a large cross-section. The α particle ionizes the gas which, in the presence of an electric field, leads to a current.

8.4.5 Detecting neutrinos

Neutrinos have extremely small cross sections, so one needs very large fluxes – and preferably very large detectors – to stand a chance of detecting them.

Though the cross-section is very small (see problem set 1), rare collision reactions can be observed. For example when a neutrino strikes a neutron the following reaction can occur

$$\nu + n \to p + e^-. \tag{8.2}$$

The interaction which allows this – the weak nuclear interaction – is the same one that is responsible for nuclear beta decay:

$$n \to p + e^- + \bar{\nu}.$$

Neutrinos can undergo other interactions, for example elastic scattering from electrons

$$\nu + e^- \to \nu + e^-.$$

The moving electron from this reaction, or from the nucleon-changing scattering reaction (8.2), can then be detected. We'll talk more about the interactions of neutrinos after we discuss the only force they couple to – the weak nuclear force.

8.4.6 Measuring properties

Momentum can be measured using the bending radius of the particle in an applied magnetic field, $p_\perp = \mathcal{Q}BR$.

Speed can be measured from:

- **Time of flight** (to of order ps timing resolution).
- Energy deposited through **ionization**. Energy loss $-\frac{dE}{dx}$ depends on v (see the first problem sheet), so if you measure the amount of ionization you will learn about the speed.

- The electromagnetic equivalent to the sonic boom – the **Čerenkov radiation** created when a particle passes through a medium faster than the local speed of light in that medium.

$\Rightarrow$ Look up the meaning of Čerenkov radiation. Convince yourself that this sort of radiation should be emitted at angle $\theta = \cos^{-1}\frac{1}{\beta\eta}$ from the particle's trajectory, where $\beta = v/c$ and η is the refractive index of the medium.

Energy can be measured by total absorption of the particle within some active medium (a **calorimeter**).

Lifetime can be measured with a good clock for reasonably long-lived species. For short-lived species we can infer the lifetime from from the distance travelled before decaying — provided that the lifetime and speed are such that the mean distance travelled $\beta\gamma c t_{\mathrm{decay}}$ is a measurable length. If the particle is very short-lived, we can measure its Breit-Wigner width, Γ, and infer the lifetime $\tau = \hbar/\Gamma$.

Key ideas

- Charged particles can be accelerated according to the Lorenz force law

$$\boxed{\frac{d\mathbf{p}}{dt} = \mathcal{Q}[\mathbb{E} + \mathbf{v} \times \mathbf{B}]}$$

- Linear accelerators are limited by the strength of the electric field achievable.
- Circular accelerators are limited by the strength of the magnetic field for protons, and by synchrotron radiation for electrons.
- The momentum of particles can be measured from their bending in magnetic fields
- A useful formula relating bending radius, momentum, and magnetic field is

$$\boxed{p_\perp = 0.3BR} \qquad \text{[GeV, Tesla, meters].}$$

- For a particle to be detected it has to interact with some sensitive material.
- The energy of particles can be measured by absorbing them in a calorimeter.
- Modern particle detectors are designed to produce electrical signals that can be amplified and digitised.

8.A Details of a linear acceleration

Non-examinable

Constant electric field

Let's calculate how the speed and position of an particle will vary when it is accelerated from rest in a constant electrical field.

For a constant electric field $\mathbb{E} \parallel \mathbf{v}$, and starting at rest we can work in one dimension. Since the parallel component of the field stays the same under the Lorentz transformation

$$\mathbb{E}'_\parallel = \mathbb{E}_\parallel,$$

and since the Lorentz force law reduces to

$$f = \mathbb{E}\mathcal{Q}$$

the proper acceleration (i.e. the acceleration in the frame in which the particle is instantaneously at rest) is

$$a_0 = \frac{\mathbb{E}\mathcal{Q}}{m}. \tag{8.3}$$

If the motion is relativistic it's convenient to work in terms of the rapidity ρ which is defined by

$$\boxed{\tanh\rho = v/c} \tag{8.4}$$

The reason that rapidity is useful is that it is easy to add successive Lorentz transformations if their relative rapidity is known. To show this, we rewrite the usual 1D Lorentz transformation in terms of the rapidity,

$$\Lambda_a = \begin{pmatrix} \gamma_a & -\beta_a\gamma_a \\ -\beta_a\gamma_a & \gamma_a \end{pmatrix} = \begin{pmatrix} \cosh\rho_a & -\sinh\rho_a \\ -\sinh\rho_a & \cosh\rho_a \end{pmatrix}$$

showing only the ct and x components. Here Λ_a is the L.T. corresponding to a boost by rapidity ρ_a or equivalently by a velocity $v_a = c\tanh\rho_a$.

By multiplying a pair of such matrices together with different rapidities we can see that the combined operation of two Lorentz transformations along the same axis is given by

$$\Lambda_b\Lambda_a = \Lambda_{a+b}.$$

This is a neat result. The Lorentz transformation for a combined boost has rapidity given by *the straight sum* of the rapidities of the two individual transforms:

$$\rho_{a+b} = \rho_a + \rho_b. \tag{8.5}$$

Remember that the same can *not* be said for the velocity. The resultant velocity is *not* the direct sum of the two individual velocities (unless $v \ll c$):

$$v_{a+b} = \frac{v_a + v_b}{1 + v_a v_b/c^2} \neq v_a + v_b.$$

By taking derivatives of (8.4) we can see that, close to the instantaneous rest frame (IRF) of the particle,

$$\left.\frac{d\beta}{d\rho}\right|_{\text{IRF}} = 1.$$

This means that we can use the proper acceleration (in the series of instantaneous rest frames) to calculate the rate of change of rapidity with respect to proper time

$$a_0 = \left.\frac{dv}{dt}\right|_{\text{IRF}} = c\left.\frac{d\beta}{d\tau}\right|_{\text{IRF}} = c\frac{d\rho}{d\tau}.$$

The IRF subscript shows quantities calculated very close to the instantaneous rest frame.

In the last expression all of the quantities (c, $d\tau$, $d\rho$) are unchanged by any boost along the x-axis.[6] So the expression $a_0 = c\frac{d\rho}{dt}$ is valid in *any* x-boosted frame, not just the IRF.

[6] This is clear for a_0, c, and $d\tau$ all of which are invariants by definition. To see that $d\rho$ is not changed by the boost let us show that *differences* in rapidity must be unmodified by the L.T. along the x-axis. Consider a general difference of rapidity $(\rho_a - \rho_b)$. If both a and b are boosted by rapidity ρ_c, then from (8.5) the difference becomes $(\rho_a + \rho_c) - (\rho_b + \rho_c) = \rho_a - \rho_b$, i.e. the rapidity difference is unchanged. This is true for *any* difference in rapidities (along the x-axis) so it must be true for $d\rho$.

Since (8.5) implies that rapidities are additive, we can calculate the rapidity at any proper time τ as the sum of lots of little boosts, each of rapidity $d\rho$:

$$\rho = \int d\rho = \int \frac{d\rho}{d\tau}\, d\tau = \frac{a_0\tau}{c} = \frac{\mathbb{E}\mathcal{Q}\tau}{mc} \tag{8.6}$$

(substituting for $a_0 = c\, d\rho/d\tau$ from above).

It's now easy to find a parametric equation for the motion. We just Lorentz transform using the matrix Λ_ρ to boost from the lab frame to the IRF, which we can do for any proper time. For a particle initially at rest at $\mathsf{X}_0 = (0, x_0, 0, 0)$ (with x_0 to be determined later),

$$\mathsf{X} = \Lambda_\rho \mathsf{X}_0.$$

The components of the boosted vector can then be parametrized in terms of the proper time,

$$\begin{aligned} x &= x_0 \cosh(a_0\tau/c) \\ ct &= x_0 \sinh(a_0\tau/c), \end{aligned} \tag{8.7}$$

since $\rho = a_0\tau/c$.

We can also find the speed in terms of the proper time using the definition of the rapidity (8.4)

$$v = c\tanh\rho = c\tanh(a_0\tau/c).$$

We haven't yet worked out the constant x_0. Let's do so. First we find the small velocity at very early times when t is small and (since v is small) $t \approx \tau$. Differentiating (8.7) at early times gives

$$v|_{v\ll c} = \left.\frac{dx}{dt}\right|_{v\ll c} = \left.\frac{dx}{d\tau}\right|_{v\ll c} = \frac{x_0 a_0}{c}\sinh\left(\frac{a_0\tau}{c}\right)_{v\ll c} \approx \frac{x_0 a_0^2}{c^2}\tau.$$

Comparing with this with $v = a_0 t$ we see that our conveniently-chosen coordinates were such that our previously undetermined initial position must have been $x_0 = c^2/a_0$.

To get the energy and momentum we recognize that the components $\mathsf{P} = (E, pc)$ can be obtained from the energy-momentum four-vector of the initially stationary particle $\mathsf{P}_0 = (m, 0)$ by the same overall Lorentz transform as above,

$$\mathsf{P} = \Lambda_\rho \mathsf{P}_0.$$

Therefore the energy at any proper time is given by $E = m\cosh\rho$ and the momentum is $p = m\sinh\rho$ where the rapidity ρ at proper time τ can again be found from (8.6).

Where should the electrodes on a linac be placed? The bunches are accelerating so will travel progressively longer distances during each period of the oscillator. Let's make the approximation that constant acceleration is very similar to lots of little accelerations, and use the results of the previous section. Eliminating the proper time from (8.7) we find the following relationship between lab-frame position and time,

$$x^2 - (ct)^2 = x_0^2 \tag{8.8}$$

If the frequency of the applied AC voltage is f we want to change the field every half cycle, i.e. at times $t_n = n/(2f)$. We should therefore place the nth gap at the position the particles will be at that time, which is

$$x_n = \sqrt{x_0^2 + \left(\frac{nc}{2f}\right)^2}.$$

Let's check this answer for the non-relativistic case. For $v \ll c$ we can Taylor expand

$$x_n = x_0\sqrt{1 + \left(\frac{nc}{2fx_0}\right)^2} \approx x_0 + \frac{1}{2}\frac{n^2c^2}{4x_0f^2}.$$

Since we found above that $x_0 = c^2/a_0$ we have $x_n = \text{const} + \frac{1}{2}a_0\frac{n^2}{4f^2}$ as expected from the non-relativistic formula $x = \text{const} + \frac{1}{2}at^2$.

8.B Charged particle ionization

Non-examinable

Charged particles e.g. protons will kick atomic electrons out of their ground states as they pass through the material. In the first problem set we calculated the rate at which energy is lost, assuming a 'free electron gas', and found that (in natural units)

$$\boxed{-\left\langle \frac{dE}{dx} \right\rangle = \frac{4\pi n_e \alpha^2}{m_e v^2} \int_{z_{\min}}^{z_{\max}} \frac{z\,dz}{1+z^2}}$$

where $z = bm_ev^2/\alpha$, b is the impact parameter, α is the electromagnetic fine structure constant, and n_e is the number density of electrons. in the material. A relativistic variation of this result is known as the **Bethe-Bloch** formula.[7]

The limits of the integration are set by the energies at which the approximation breaks down – which at the low-energy end is where E_e approaches the ionization energy of the material.

8.C Detector technologies

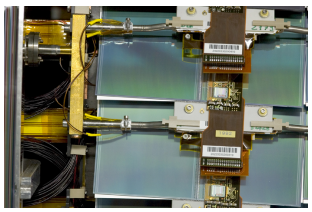

Detail of the ATLAS Semiconductor tracker barrel during its assembly in Oxford. The silicon detector elements are approximately 60 mm wide [2].

Below are a few techniques we can exploit to turn an interaction of a particle with a material into a recordable signal.

8.C.1 Semiconductor detectors

When a charged particle passes through a semiconductor it creates electron–hole pairs – charge carriers – which can be accelerated by an applied electric field to create currents.

[7] See [12] for the full relativistic version.

To work well, the semiconductor must previously have been depleted of charge carriers. This can be achieved by applying a voltage (a so-called *reverse bias*) to a junction between what are known as 'p-type' doped and 'n-type' doped types of silicon.

Low energy photons or electrons striking a semiconductor can deposit all of their energy within the material, resulting in a signal peak that corresponds to the total energy of the particle. The electrical signal is then a measure of the energy of the incoming photon or electron.

Very thin layers of semiconductor (often less than 1 mm thick), suitably instrumented, are used to detect the passage of a charged particle while only very slightly reducing that particle's energy.

8.C.2 Gas and liquid ionization detectors

Charged particles traversing a gas or a noble liquid will create electron–ion pairs. In the presence of an electric field, those ions will create an electrical current which can be amplified (in the gas and/or electronically) and digitized.
$\Rightarrow$ How can we get amplification *in the gas*?

8.C.3 Scintillator detectors

Scintillators are materials which emit visible light when atomic electrons, excited by the passage of an ionizing particle, fall back to their ground states. The visible photons can be then be picked up by photomultiplier tubes, which converts that light to an electrical signal proportional to the energy deposited in the scintillator.
$\Rightarrow$ How does a photomultiplier work?

Further Reading

Many of the books on nuclear and particle physics include chapters on experimental techniques. Examples in some general texts include:

- *"Introductory Nuclear Physics"*, P.E. Hodgeson, E. Gadioli and E. Gadioli Erba, OUP, 2003. Chapters 4 and 5 are good introductions to accelerators and detectors respectively.
- *"Particle Physics"* B.R. Martin and G. Shaw. Chapter 3 gives a brief introduction at about the right level.
- *"Nuclear and Particle Physics"* W.E. Burcham and M. Jobes. Chapter 2 has lots of good stuff in it

More specialized books include...

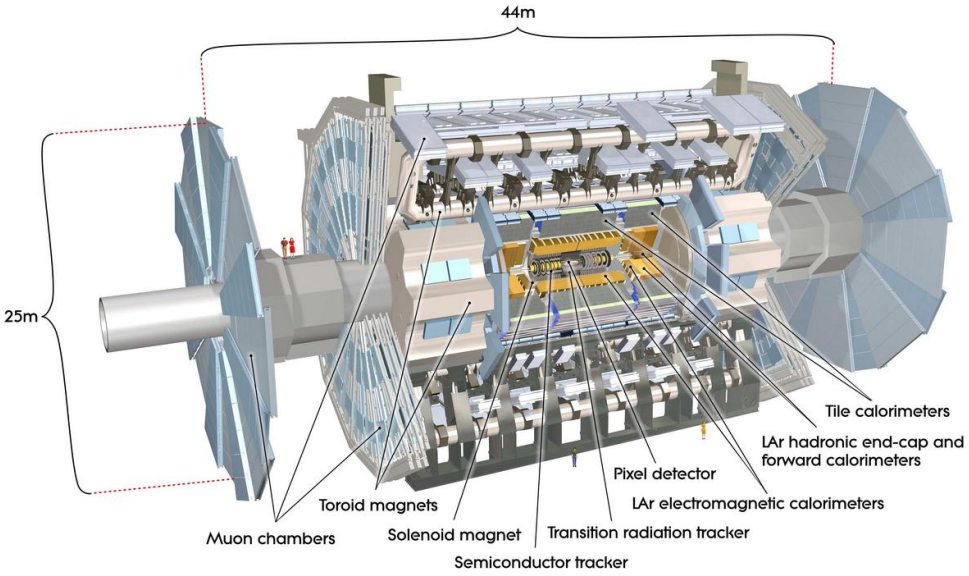

Figure 8.4: Diagram showing the major detector components of the ATLAS detector for the CERN Large Hadron Collider. The detector is built in concentric layers surrounding the beam-beam interaction point. LAr means liquid argon. The 'tile' hadronic calorimeter is made of alternating layers of iron and scintillator. From [1].
$\Rightarrow$ Muons have the same interactions as electrons but are about 200 times heavier. Why are the muon detection chambers on the outer-most layers?

- *An Introduction to Particle Accelerators*, E.J.N. Wilson, OUP (2001)
- *The Physics of Particle Detectors*, Dan Green, CUP (2000)

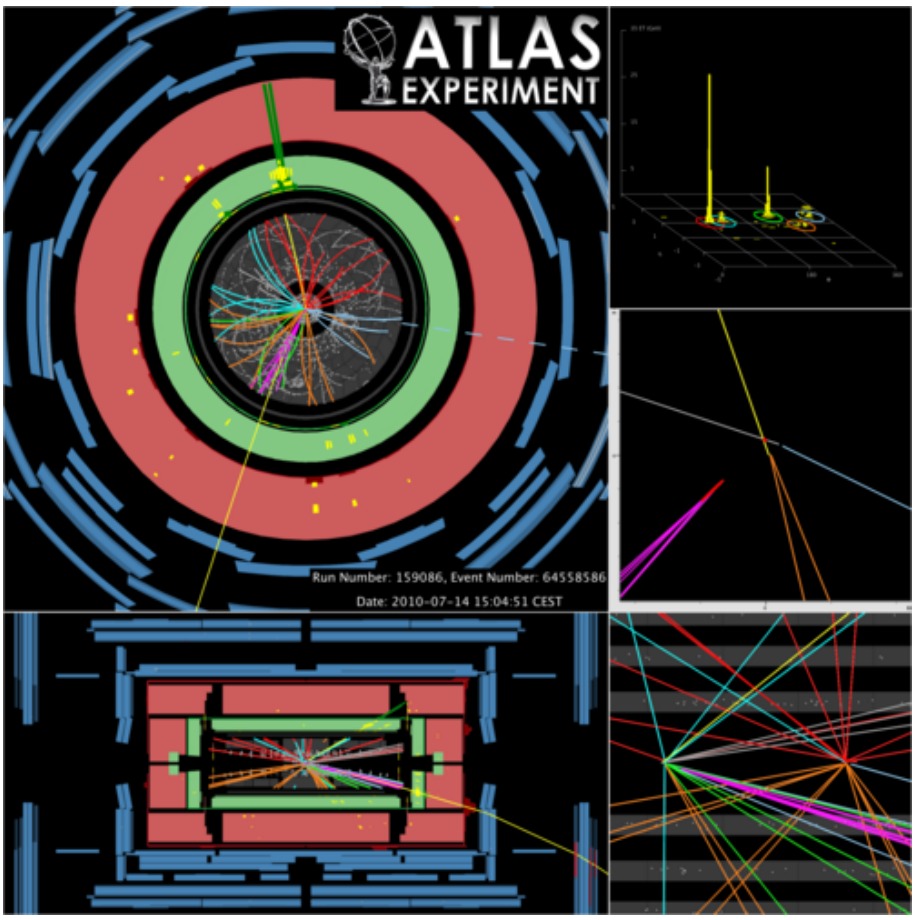

Figure 8.5: Event display of one of the first $E_{\mathrm{cm}} = 7\,\mathrm{TeV}$ proton-proton collisions detected by the ATLAS experiment. Lots of particles and anti-particles have been created in the collision. They stream away from the interaction point and are detected by the various concentric layers of the detector. In the central region the charged particle tracks, which curve in the solenoidal field, are constructed from hits in layers of silicon detectors and gaseous ionization detectors. The lines represent tracks found by pattern-recognition algorithms.

Top left (scale $\sim 10\,\mathrm{m}$) Projection of the detectors perpendicular to the beam.

Bottom left (scale $\sim 10\,\mathrm{m}$) Projection along the line of the beam. The beam pipe would pass horizontally through the middle of this view.

Top right Energy deposited in the calorimeters, as a function of angle relative to the beam direction and azimuthal angle.

Mid right Detail (scale $\sim 0.1\,\mathrm{mm}$) showing tracks pointing towards a **secondary vertex** caused by the decay of a 'long-lived' particle, probably one containing a b-quark.

Bottom right Detail (scale $\sim$ cm) showing that two independent proton-proton collisions have coincided in time.

From `http://atlas.web.cern.ch/`

Chapter 9

Examples

9.1 Problems 1

Three vectors are written in bold e.g. $\mathbf{x}$.
Four vectors are written sans-serif, e.g. P.
The metric is $\mathrm{diag}(1,-1,-1,-1)$ so that with $\mathsf{X}\cdot\mathsf{X} = c^2t^2 - \mathbf{x}\cdot\mathbf{x}$, time-like intervals have positive signs, and propagating particles satisfy $\mathsf{P}\cdot\mathsf{P} = +m^2$.

Core questions

1.1. a) What assumptions underlie the radioactivity law

$$\frac{dN}{dt} = -\Gamma N \ ?$$

b) If some number N_0 of nuclei are present at time $t = 0$ how many are present at some later time t?

c) Calculate the mean life τ of the species.

d) Relate the half-life $t_{\frac{1}{2}}$ to τ.

e) How do things change when the particle moves relativistically?

1.2. A sample consists originally of nucleus A only, but subsequently decays according to

$$A \xrightarrow{\Gamma_A} B \xrightarrow{\Gamma_B} C.$$

Write down differential expressions for $\frac{dA}{dt}$, $\frac{dB}{dt}$ and $\frac{dC}{dt}$. Solve for, and then sketch, the fractions of, $A(t)$, $B(t)$ and $C(t)$. At what time is the decay rate of B maximum?

1.3. Consider Compton scattering $\gamma + e^- \to \gamma + e^-$ of a photon of energy E_γ ($\sim$ MeV) from a stationary electron.

a) Show that the energy of the scattered photon is

$$E'_\gamma = \frac{m_e E_\gamma}{m_e + E_\gamma(1-\cos\theta)},$$

where θ is the angle through which the photon is scattered.

b) If an incoming photon is scattered through an angle $\sim 180^\circ$ at the surface of a material, how much of the original photon's energy would you expect *not* to be deposited in the material?

1.4. Briefly explain the origin of each of the terms in the semi-empirical mass formula (SEMF)

$$M(N,Z) = Zm_p + Nm_n - \alpha A + \beta A^{\frac{2}{3}} + \gamma\frac{(N-Z)^2}{A} + \epsilon\frac{Z^2}{A^{\frac{1}{3}}} + \delta(N,Z)$$

and obtain a value for ϵ.

Show that we can include the gravitational interaction between the nucleons by adding a term to the SEMF of the form

$$-\zeta A^{5/3}$$

and find the value of ζ.

Use this modified SEMF to obtain a lower bound on the mass of a gravitationally-bound 'nucleus' consisting only of neutrons (a neutron star).

1.5. An analysis of a chart showing all stable ($t_{\frac{1}{2}} > 10^9$ years) nuclei shows that there are 177 even-even, 121 even-odd and 8 odd-odd stable nuclei and, for each A, only one, two or three stable isobars. Explain these observations qualitatively using the SEMF. Energetically $^{106}_{48}\mathrm{Cd}$ could decay to $^{106}_{46}\mathrm{Pd}$ with an energy release of greater than 2 MeV. Why does $^{106}_{48}\mathrm{Cd}$ occur naturally?

1.6. The radius r of a nucleus with mass number A is given by $r = r_0 A^{\frac{1}{3}}$ with $r_0 = 1.2\,\mathrm{fm}$. What does this tell us about the nuclear force?

a) Use the Fermi gas model (assuming $N \approx Z$) to show that the energy ϵ_F of the Fermi level is given by

$$\epsilon_F = \frac{\hbar^2}{2mr_0^2}\left(\frac{9\pi}{8}\right)^{\frac{2}{3}}.$$

b) Estimate the total kinetic energy of the nucleons in an $^{16}\mathrm{O}$ nucleus.

c) For a nucleus with neutron number N and proton number Z the asymmetry term in the semi-empirical mass formula is

$$\frac{\gamma(N-Z)^2}{A}.$$

Assuming that $(N-Z) \ll A$ use the Fermi gas model to justify this form and to estimate the value of γ. Comment on the value obtained.

1.7. Alpha-decay rates are determined by the probability of tunnelling through the Coulomb barrier. Draw a diagram of the potential energy $V(r)$ as a function of the distance r between the daughter nucleus and the α particle, and of the wave function $\langle r|\psi\rangle$.

The decay rate can be expressed as $\Gamma = fP$, where f is the frequency of attempts by the alpha particle to escape and $P = \exp(-2G)$ is the probability for the alpha particle to escape on any given attempt.

By using a one-dimensional Hamiltonian

$$H = \frac{p_r^2}{2m} + V,$$

with a 1D momentum operator $p_r = -i\hbar\frac{\partial}{\partial r}$, and by representing the wave function by

$$\langle r|\Psi\rangle = \exp[\eta(r)],$$

with $r = x$ show that

$$G = \frac{\sqrt{2m}}{\hbar}\int_a^b \sqrt{V(r) - Q}\,\mathrm{d}r.$$

Integrate (a substitution $r = r_b\cos^2\theta$ helps) to give

$$G = \frac{\pi}{2}Zz\alpha\sqrt{\frac{2mc^2}{Q}}\mathcal{F}(r_a/r_b)$$

where the dimensionless function

$$\mathcal{F}(r) = \frac{2}{\pi}\left(\cos^{-1}\sqrt{r} - \sqrt{r(1-r)}\right)$$

lies in the range between 0 and 1, and for small Q approaches 1.

[Hint: can you convince yourself that $\eta'' \ll (\eta')^2$?]

1.8. a) What are the basic assumptions of the Fermi theory of beta decay?

b) The Fermi theory predicts that in a beta decay the rate of electrons emitted with momentum between p and $p + dp$ is given by

$$\frac{d\Gamma}{dp_e} = \frac{2\pi}{\hbar}G^2|M_{fi}^{\mathrm{nuc}}|^2\frac{1}{4\pi^4\hbar^6c^3}(E-Q)^2p^2,$$

where E is the energy of the electron, and Q is the energy released in the reaction. Justify the form of this result.

c) Show that for $Q \gg m_ec^2$ the total rate is proportional to Q^5

d) What spin states are allowed for the combined system of the electron + neutrino?

e) ‡ Why are transitions between initial and final nuclei with angular momenta differing by more than $\hbar$ suppressed?

Optional questions

1.9. A high energy photon can create an electron-positron pair within the material. When a positron comes to rest it will annihilate against an electron from the material

$$e^+ + e^- \rightarrow \gamma + \gamma.$$

What will be the energy of these secondary photons?

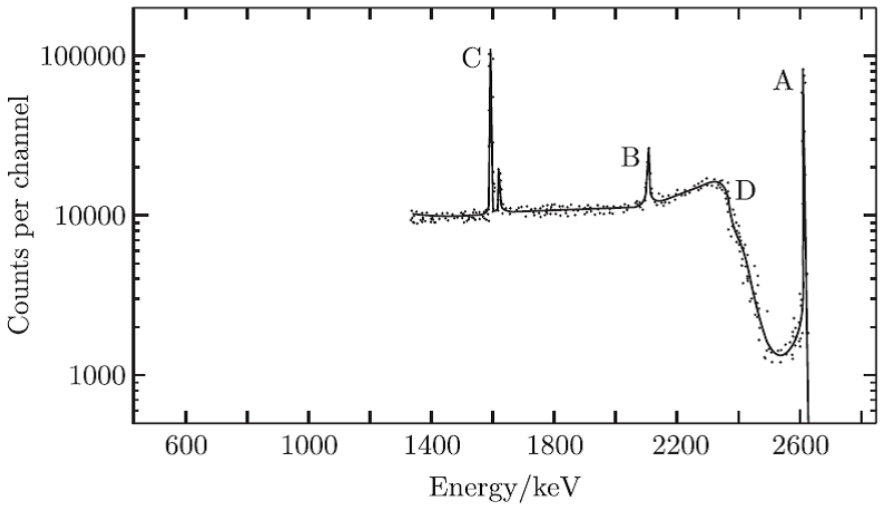

The figure shows the energy spectrum from the gamma decay of $^{24}\mathrm{Na}$ as measured in a small Ge(Li) detector. Suggest the origins of the peaks A, B, C and the edge D. For such a detector describe the stages by which gamma ray energy is converted into a measurable voltage pulse.

1.10. The figure shows the α-decay scheme of $^{244}_{96}\mathrm{Cm}$ and $^{240}_{94}\mathrm{Pu}$.

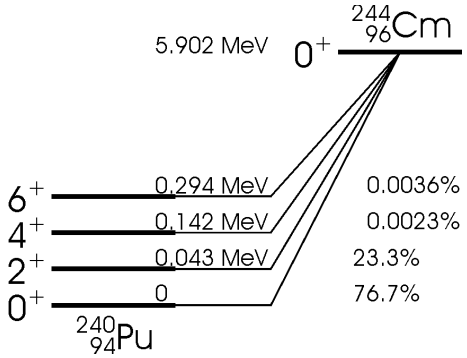

Show — either by (a) using a suitable approximation of $\mathcal{F}$ calculated in a previous question or (b) by redoing the corresponding integral neglecting Q — that we would expect the rates to satisfy and equation of the form

$$\log \Gamma = A - \frac{BZ}{\sqrt{Q}}.$$

The Q value for the ground state to ground state transition is $5.902\,\mathrm{MeV}$ and for this transition $A = 132.8$ and $B = 3.97(\,\mathrm{MeV})^{1/2}$ when Γ is in s^{-1}. The branching ratio for this transition is given in the figure. Calculate the mean life of $^{244}\mathrm{Cm}$.

Estimate the transition rate from the ground state of $^{244}\mathrm{Cm}$ to the 6^+ level of $^{240}\mathrm{Pu}$ using the same A and B and compare to the branching ratio given in the figure.

Suggest a reason for any discrepancy.

[Hint: what form does the Schrödinger equation take for angular momentum quantum number $l \neq 0$?]

1.11. Discuss the evidence for shell structure in the atomic nucleus. Indicate how closed shells for proton and neutron numbers of 2, 8, 20, 28, 50 can be explained. What are the other 'magic numbers'?

Deduce from the shell model the spins and parities of the ground states of the following nuclei, stating any assumptions you make: $^{7}_{3}\mathrm{Li}$, $^{17}_{8}\mathrm{O}$, $^{20}_{10}\mathrm{Ne}$, $^{27}_{13}\mathrm{Al}$, $^{14}_{7}\mathrm{N}$, $^{39}_{19}\mathrm{K}$, $^{41}_{21}\mathrm{Sc}$.

9.2 Problems 2

Core questions

2.1. What is meant by the 'cross section' and the 'differential cross section'?

Consider classical Rutherford scattering of a particle with mass m and initial speed v_0 from a potential

$$V(r) = \frac{\alpha}{r}$$

a) Show from geometry that the change in momentum is given by

$$|\Delta \mathbf{p}| = 2p \sin(\Theta/2).$$

b) Considering the symmetry of the problem, show that

$$bv_0 = r^2 \frac{d\theta}{dt}$$

where b is the impact parameter, $\mathbf{r}$ is the location of the particle from the origin and θ is the angle $\angle(\mathbf{r}, \mathbf{r}^*)$ where $\mathbf{r}^*$ is the point of closest approach.

c) Starting from Newton's second law show that

$$|\Delta \mathbf{p}| = \frac{2\alpha}{v_0 b} \cos\left(\frac{\Theta}{2}\right).$$

d) Show that the scattering angle Θ is given by

$$\tan(\Theta/2) = \frac{\alpha}{2bT} \tag{9.1}$$

where b is the impact parameter (the closest distance of the projectile to the nucleus if it were to be undeflected) and $T = \frac{p^2}{2m}$ is the initial kinetic energy.

e) Calculate the Rutherford scattering cross section σ for scattering of projectiles by angles greater than $\Theta_{\min}$.

f) Show that the differential cross section

$$\frac{d\sigma}{d\Omega} = \frac{1}{16}\left(\frac{\alpha}{T}\right)^2 \frac{1}{\sin^4(\Theta/2)}$$

where T is the kinetic energy of the particle.

Why is it not possible to calculate the total cross section for this reaction?

2.2. The $J^P = \frac{3}{2}^+$ decuplet contains the following baryons:

$$\Delta^- \ \Delta^0 \ \Delta^+ \ \Delta^{++}$$
$$\Sigma^{*-} \ \Sigma^{*0} \ \Sigma^{*+}$$
$$\Xi^{*-} \ \Xi^{*0}$$
$$\Omega^-$$

What is the quark content of each of these baryons?

The constituent quarks have no relative orbital angular momentum. How does the Ω^- baryon state behave under exchange of any pair of quarks? Explain how this is achieved in terms of the space, spin, flavour and colour parts of the state vector.

Account for the absence of sss, ddd and uuu states in the $J^P = \frac{1}{2}^+$ octet.

What is meant by *quark confinement*?

2.3. Write down the valence quark content for each of the different particles in the reactions below and check that the conservation laws of electric charge, flavour, strangeness and baryon number are satisfied throught.

$$\begin{array}{lrcl} (1) & \pi^- + p & \rightarrow & K^0 + \Lambda \\ (2) & K^- + p & \rightarrow & K^0 + \Xi^0 \\ (3) & \Xi^- + p & \rightarrow & \Lambda + \Lambda \\ (4) & K^- + p & \rightarrow & K^+ + K^0 + \Omega^- \end{array}$$

Draw a quark flow diagram for the last reaction.

2.4. Consider the decay of the ρ^0 meson ($J^P = 1^-$) in the following decay modes:

a) $\rho^0 \rightarrow \pi^0 + \gamma$

b) $\rho^0 \rightarrow \pi^+ + \pi^-$

c) $\rho^0 \rightarrow \pi^0 + \pi^0$

For case (b) and (c), draw a diagram to show the quark flow.

Consider the symmetry of the wave-function required for $\pi^0 + \pi^0$ and explain why this decay mode is forbidden.

From consideration of the relative strength of the different fundamental forces, determine which of the other two decay modes will dominate.

2.5. A wave function is modelled as the sum of the incoming plane wave and an outgoing (scattered) spherical wave,

$$\langle \mathbf{x} | \Psi^{(+)} \rangle = A \left[e^{i\mathbf{k}\cdot\mathbf{x}} + \frac{e^{ikr}}{r} f(\mathbf{k}', \mathbf{k}) \right].$$

Calculate the flux associated with the plane wave and the spherical wave separately. Hence show that the cross section into solid angle $d\Omega$ is

$$\frac{d\sigma}{d\Omega} = |f(\mathbf{k}', \mathbf{k})|^2 .$$

justifying any assumptions you make.

[Hint: Remember that the flux is given by $\frac{\hbar}{2mi}(\psi^*\nabla\psi - \psi\nabla\psi^*)$*.]*

2.6. In the Born approximation, the scattering amplitude is given by

$$f^{(1)}(\mathbf{k}', \mathbf{k}) \quad = \quad -\frac{1}{4\pi}(2m)(2\pi)^3\langle\mathbf{k}'|V|\mathbf{k}\rangle$$

Explain the terms in this equation, and state the conditions for which it is valid.

b) The Yukawa potential is given by

$$V(r) = \frac{g^2}{4\pi}\frac{e^{-\mu r}}{r}.$$

Show that for this potential

$$\langle\mathbf{k}'|V|\mathbf{k}\rangle = \frac{g^2}{4\pi}\frac{1}{(2\pi)^3}\int d^3x\, e^{-i\boldsymbol{\Delta}\mathbf{k}\cdot\mathbf{x}}\frac{e^{-\mu r}}{r}$$

where $\Delta\mathbf{k} = \mathbf{k}' - \mathbf{k}$.

c) Hence show that

$$|\langle\mathbf{k}'|V|\mathbf{k}\rangle| = \frac{g^2}{(2\pi)^3}\frac{1}{q^2+\mu^2}$$

where $q = |\Delta\mathbf{k}|$.

d) Show that within the Born approximation

$$\frac{d\sigma}{d\Omega} = \frac{g^4}{(4\pi)^2}\frac{4m^2}{\left[2k^2(1-\cos\Theta)+\mu^2\right]^2} \tag{9.2}$$

where Θ is the scattering angle.

e) Find the total cross section for the case when $\mu \neq 0$.

f) When $\mu \to 0$, $V(r) \propto 1/r$. Compare the differential cross section (9.2) to the classical Rutherford scattering cross section

$$\frac{d\sigma}{d\Omega} = \frac{1}{16}\left(\frac{\alpha}{T}\right)^2\frac{1}{\sin^4(\Theta/2)}.$$

What must be the relationship between g and α for Born approximation to reproduce the classical Rutherford formula for electron–proton scattering?

2.7. Consider the scattering of an electron from a nucleus with extended spherical charge density $N(|\mathbf{x}''|)$ which is normalised such that $\int d^3x'' N(|\mathbf{x}''|) = 1$. The potential at any point is then

$$V(x') = zZ\alpha\int d^3x''\frac{N(|\mathbf{x}''|)}{|\mathbf{x}' - \mathbf{x}''|},$$

where Z and z are the charges of the nucleus and the projectile respectively.

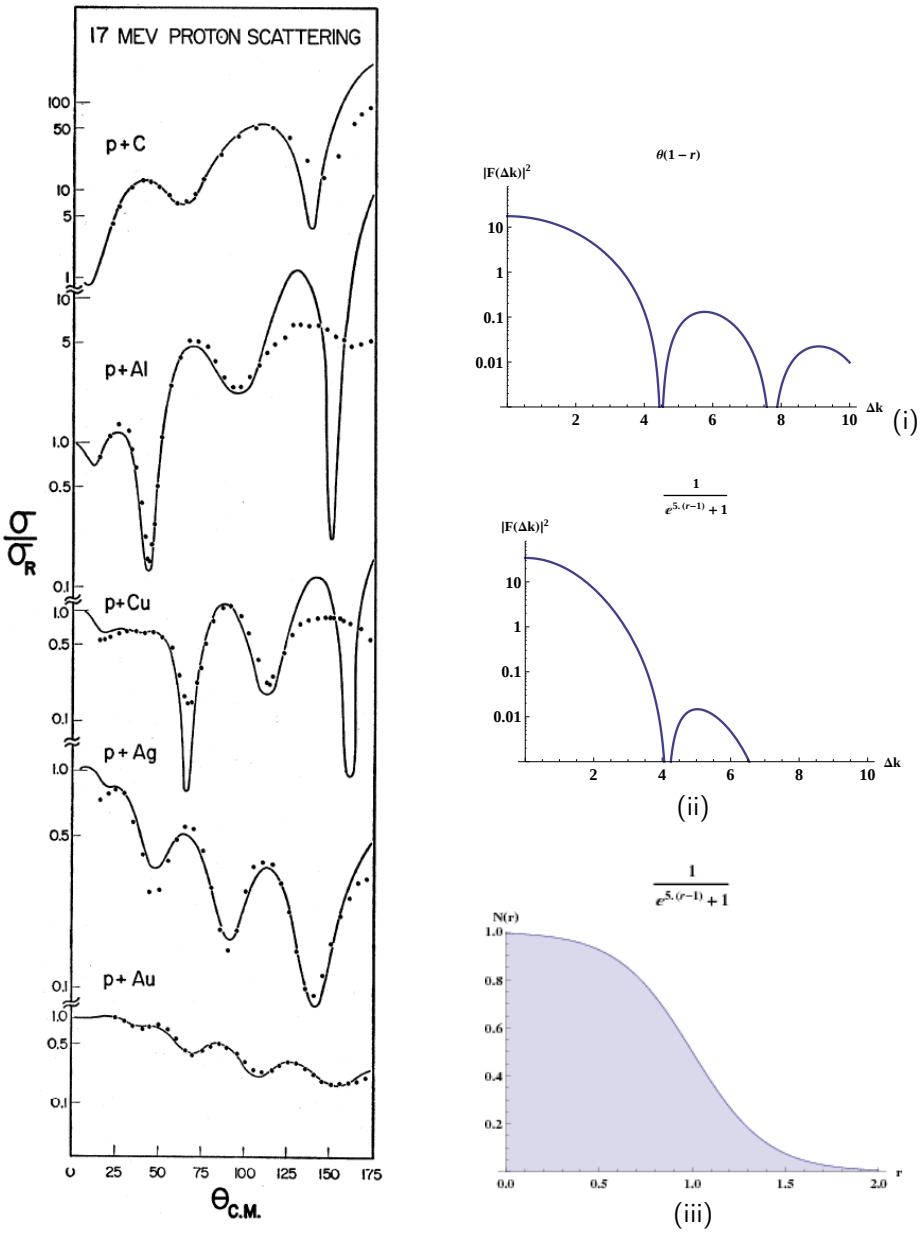

Figure 9.1: **(LHS)** Scattering cross section for K.E. = 17 MeV protons normalized to the Rutherford scattering cross section (from [9]).
(RHS) Examples of nuclear form factors $|F(|\mathbf{\Delta k}|)|^2$ for different charge density functions: (i) uniform unit sphere; (ii) Saxon-Woods $\rho(r) \propto [1+\exp((r-R)/a)]^{-1}$ with $R = 1$, $a = 0.2$. The corresponding Saxon-Woods charge density [15] is shown in (iii).

a) By expanding in the position basis, and defining a new variable $\mathbf{X} = \mathbf{x}' - \mathbf{x}''$, show that the Born approximation to the scattering amplitude can be expressed in the form

$$f(\mathbf{k}', \mathbf{k}) = f(\mathbf{k}', \mathbf{k})_{\text{point}} \times F_{\text{nucl}}(\boldsymbol{\Delta}\mathbf{k})$$

where $f(\mathbf{k}', \mathbf{k})_{\text{point}}$ is the scattering amplitude from a point charge,the *nuclear form factor*

$$F_{\text{nucl}}(\boldsymbol{\Delta}\mathbf{k}) = \int d^3x' \, e^{-i\boldsymbol{\Delta}\mathbf{k}\cdot\mathbf{x}'} N(|\mathbf{x}'|)$$

is the 3D Fourier transform of the charge density distribution, and $\boldsymbol{\Delta}\mathbf{k}$ is the change in momentum of the projectile.

Hence show that

$$\frac{d\sigma}{d\Omega} = \left(\frac{d\sigma}{d\Omega}\right)_{\text{Rutherford}} |F_{\text{nucl}}(\boldsymbol{\Delta}\mathbf{k})|^2.$$

b) Consider the example form factors in Figure 9.1 (i) and (ii). How would these form factors scale along the Δk-axis if the radius r of the corresponding sphere of charge was doubled? By relating the momentum transfer to the scattering angle, use the data to estimate the size of the silver nucleus. Compare to the expectation for an incompressible nucleus, $r = r_0 A^{\frac{1}{3}}$ with $r_0 = 1.25\,\text{fm}$.

c) How might one accelerate protons to kinetic energy of $17\,\text{MeV}$, and subsequently detect the scattered protons experimentally?

2.8. The cross section for the production of γ-rays by neutrons incident on a certain nucleus (N, Z) is dominated by a resonance and given by the Breit-Wigner formula,

$$\sigma(n, \gamma) = \frac{\pi}{k^2} \frac{\Gamma_n \Gamma_\gamma}{(E - E_0)^2 + \Gamma^2/4}. \tag{9.3}$$

a) Define the symbols in this formula and explain the physical principles that underlie it, and the conditions under which it applies.

b) What are the mass and lifetime of the resonant state?

c) All spin effects have been ignored in (9.3). How would the formula differ if spins are included?

d) On the same plot draw how the inelastic (n, γ) and elastic (n, n) cross sections would behave close to the resonance, when $\Gamma_\gamma = 4\Gamma_n$, labeling important quantities including the peak cross section values.

[In (d) you may assume that resonant scattering dominates both cross-sections, and that decays other than to n and γ are negligible.]

2.9. The cross section for the reaction $\pi^- p \to \pi^0 n$ shows a prominent peak when measured as a function of the π^- energy. The peak corresponds to the Δ resonance which has a mass of 1232 MeV, with $\Gamma = 120\,\text{MeV}$. The partial widths for the incoming and outgoing states are $\Gamma_i = 40\,\text{MeV}$, and $\Gamma_f = 80\,\text{MeV}$ respectively for this reaction.

At what pion beam energy will the cross section be maximal for a stationary proton?

Describe and explain the similarities and differences you would expect between the cross section for $\pi^- p \to \pi^0 n$ and the one for $\pi^- p \to \pi^- p$, for centre-of-mass energies not far from 1.2 GeV. Giving values for the variables in the Breit-Wigner formula where possible. Use quark-flow diagrams to explain what is happening.

By considering the quark content of the intermediate states, discuss whether you would expect similar peaks in the cross sections for the reactions (a) $K^- p \to$ products and (b) $K^+ p \to$ products.

Optional questions

2.10. Consider the Hamiltonian $H = H_0 + V$, where H_0 is the free-particle Hamiltonian, and V is some localised potential. Let the ket $|\phi\rangle$ represent an eigenstate of H_0, and the ket $|\psi\rangle$ represent an eigenstate of H which shares the same energy eigenvalue as the $|\phi\rangle$ in the limit $\epsilon \to 0$.

Show that the Lippmann-Schwinger equation

$$|\psi^{(\pm)}\rangle = |\phi\rangle + \frac{1}{E - H_0 \pm i\epsilon} V |\psi^{(\pm)}\rangle.$$

is consistent with the states defined above by multiplying it by the operator $(E - H_0 \pm i\epsilon)$ and taking the limit $\epsilon \to 0$.

2.11. Show that the Green's function

$$G_\pm(\mathbf{x}, \mathbf{x}') \equiv \frac{\hbar^2}{2m} \left\langle \mathbf{x} \right| \frac{1}{E - H_0 \pm i\epsilon} \left| \mathbf{x}' \right\rangle$$

can be written

$$G_\pm(\mathbf{x}, \mathbf{x}') = \frac{i}{4\pi^2 \Delta} \int_0^\infty dq\, q \frac{e^{iq\Delta} - e^{-iq\Delta}}{q^2 - k^2 \mp i\epsilon} \tag{9.4}$$

where $E = \frac{\hbar^2 k^2}{2m}$ and $\Delta = |\mathbf{x} - \mathbf{x}'|$.

[Hint: start by inserting identity operators $\int d^3p' |\mathbf{p}'\rangle\langle\mathbf{p}'|$ and $\int d^3p'' |\mathbf{p}''\rangle\langle\mathbf{p}''|$ on each side of the operator, and changing $\hat{H}_0 \to \hat{\mathbf{p}}^2/2m$.]

2.12. If you have done the course on functions of a complex variable, finish the integral in (9.4) using appropriate contour integrals to obtain

$$G_\pm(\mathbf{x}, \mathbf{x}') = -\frac{1}{4\pi} \frac{e^{\pm ik\Delta}}{\Delta}.$$

2.13. The pions can be represented in an isospin triplet ($I = 1$) while the nucleons form an isospin doublet ($I = \frac{1}{2}$),

$$\begin{pmatrix} \pi^+ \\ \pi^0 \\ \pi^- \end{pmatrix} \quad \text{and} \quad \begin{pmatrix} p \\ n \end{pmatrix}$$

while the Δ series of resonances have $I = \frac{3}{2}$.

By assuming that the isospin operators I, I_3, $I_\pm$ obey the same alegbra as the quantum mechanical angular momentum operators J, J_z, $J_\pm$, explain why the ratio of $\Gamma_i/\Gamma_f \approx \frac{1}{2}$ was found in a previous question.

[Hint: you will need the Clebsch-Gordon coefficients for $\langle j_1 j_2 m_1 m_2 | j_1 j_2 J M\rangle$ for $J = \frac{3}{2}$, $j_1 = 1$, $j_2 = \frac{1}{2}$, $M = -\frac{1}{2}$.]

2.14. A proton is travelling through a material and scattering the electrons in the material.

a) Express the scattering angle in terms of the impact parameter b, the reduced mass μ, the relative speed v, and the scattering angle in the ZMF. Hence show that the momentum transfer is

$$q = \frac{2\mu v}{\sqrt{1+z^2}}.$$

where $z = b\mu v^2/\alpha$.

b) Write down the energy given to an electron for a collision for a given impact parameter b. Integrate this up with area element $2\pi b\, db$ to show that the average energy lost by the projectile per distance travelled is

$$-\left\langle \frac{dE}{dx} \right\rangle = \frac{4\pi n_e \alpha^2}{m_e v^2} \int_{z_{\min}}^{z_{\max}} \frac{z\, dz}{1+z^2},$$

where n_e is the number density of electrons.

[Hint: recycle results from the Rutherford scattering question.]

2.15. a) A projectile travels through a medium of thickness x with n targets per unit volume. Show that the fraction absorbed or deflected by the medium is

$$P_{\text{absorb}}(x) = 1 - e^{-n\sigma x},$$

where σ is the absorption cross section.

b) Estimate, stating any assumptions you make, the thickness of lead that would be required to have a 50% chance of stopping a 2.3 MeV neutrino coming from a solar nuclear fusion reaction.

The cross section for the scattering of a neutrino from a stationary target is approximately

$$\sigma_{\text{tot}} = 2\pi G_F^2 \frac{4\pi\, p_{\text{CM}}^2}{(2\pi)^3} \frac{dp_{CM}}{dE_{\text{CM}}}$$

where E_{CM} is the centre-of-mass energy of the system, and p_{CM} is the momentum of the neutrino in the centre-of-mass frame.

c) Justify the form of this expression.

d) Explain how Figure 9.2 supports a model in which the proton contains point-like constituents.

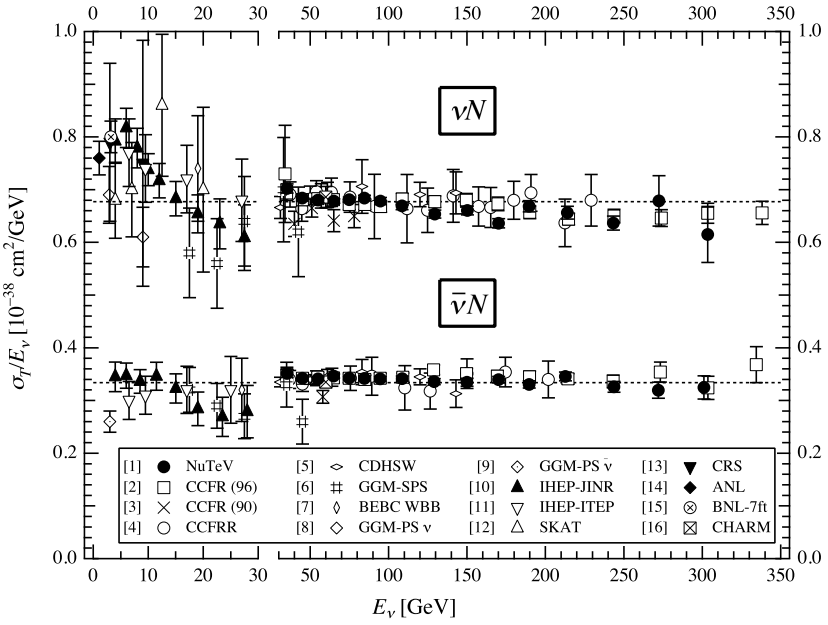

Figure 9.2: $\sigma_{\rm tot}/E_\nu$ for neutrino-nucleon νN (and anti-neutrino–nucleon $\bar{\nu}N$) interactions as a function of neutrino energy. From [12].

[The density of lead is about $11.3\,\mathrm{g\,cm^{-3}}$. Some data for the cross section of neutrinos ν scattering from nucleons – meaning protons or neutrons – are shown in Figure 9.2.]

2.16. The figure shows the fraction N/N_0 transmitted when protons of kinetic energy $E = 140\,\mathrm{MeV}$ impinge as a collimated beam on sheets of copper of various thicknesses x. By considering the 2-body kinematics of proton–electron collisions and proton–nucleus collisions, account for the attenuation for values of x between 0 and 20 mm, and for the sudden change in behaviour around the value of x marked $R(E)$.

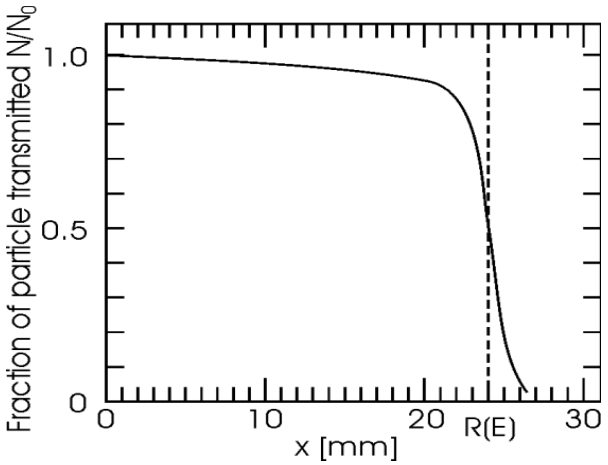

Results similar to the figure were obtained for protons of $E = 100\,\mathrm{MeV}$, except that in this case a value of $R(E) = 14\,\mathrm{mm}$ was obtained. Offer a brief explanation for the change in $R(E)$. What is the relative size of the nuclear scattering cross section σ_{Nucl} in copper compared to the geometric cross section?

[The density of copper is $8.9\,\mathrm{g\,cm^{-3}}$, and it has relative atomic mass 63.5. You may assume that the nuclear radius is given by $r = r_0\,A^{1/3}$ with $r_0 = 1.25\,\mathrm{fm}$]

9.3 Problems 3

Core questions

3.1. The Klein-Gordon equation,

$$\left(\frac{\partial^2}{\partial t^2} - \nabla^2 + m^2\right)\varphi(\mathbf{r}, t) = 0. \tag{9.5}$$

is the relativistic wave equation for spin-0 particles.

a) Show that

$$\varphi = \frac{e^{-\mu r}}{r}$$

is a valid static-field solution.

b) Show that another possible solution to the Klein-Gordon equation is:

$$\phi(\mathsf{X}) = A \exp\left[i\mathsf{P} \cdot X\right]$$

Where P and X are the momentum and position four-vectors respectively. What restrictions does (9.5) place on the components of P?

What are the physical interpretation of these solutions?

3.2. Draw all the lowest order electromagnetic Feynman diagram(s) for the following processes:

a) $e^- + e^+ \longrightarrow e^- + e^+$
b) $e^- + e^- \longrightarrow e^- + e^-$
c) $e^- + e^- \longrightarrow e^- + e^- + \mu^+ + \mu^-$
d) $\gamma \longrightarrow e^+e^-$ in the presence of matter
d) $\gamma + \gamma \longrightarrow \gamma + \gamma$

3.3. Why does the ratio

$$\frac{\sigma(e^+ + e^- \to \mu^+ + \mu^-)}{\sigma(e^+ + e^- \to \tau^+ + \tau^-)}$$

tend to unity at high energies? Would you expect the same to be true for

$$\frac{\sigma(e^+ + e^- \to \mu^+ + \mu^-)}{\sigma(e^+ + e^- \to e^+ + e^-)} \ ?$$

3.4. Draw leading order electromagnetic Feynman diagrams for the processes

$$e^+ + e^- \to \mu^+ + \mu^- \quad \text{and} \quad e^+ + e^- \to q + \bar{q}.$$

How do the vertex and propagator factors compare?

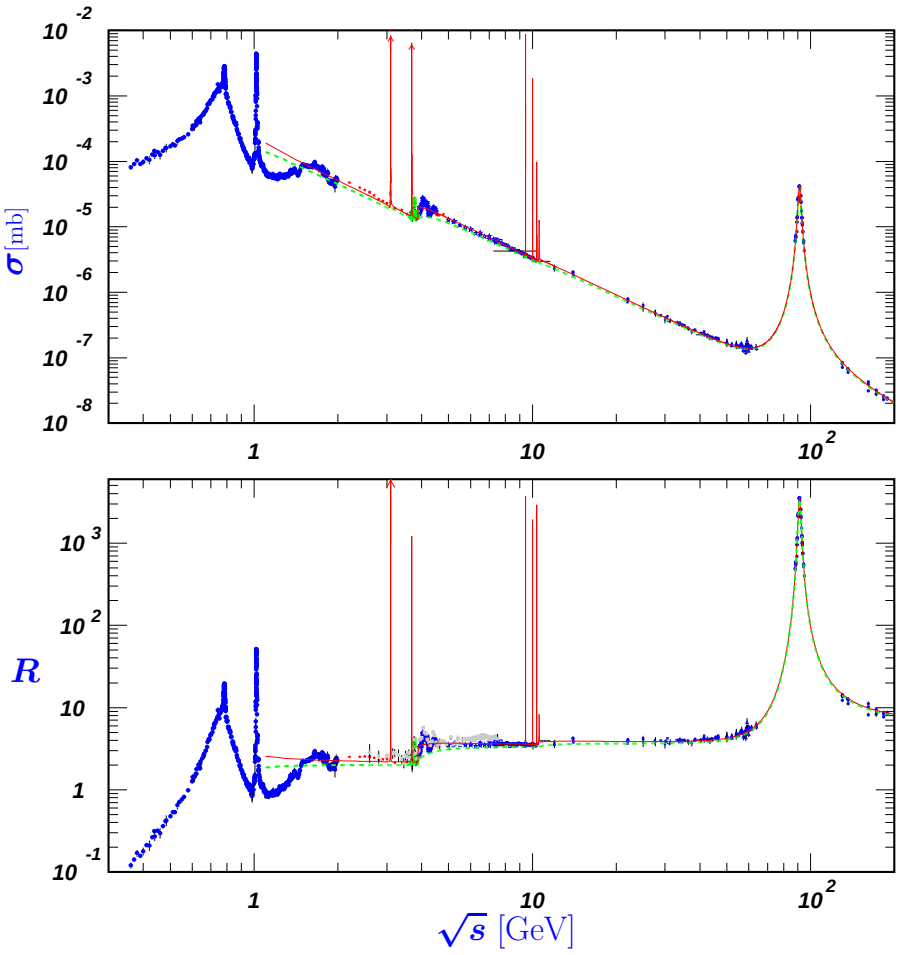

Figure 9.3: The cross section $\sigma(e^+e^- \to \text{hadrons})$ and the ratio of cross sections $R = \frac{\sigma(e^+e^- \to \text{hadrons})}{\sigma(e^+e^- \to \mu^+\mu^-)}$ as a function of the center of mass energy $\sqrt{s}$.

Figure 9.3 shows the ratio of the cross sections for the process of electron–positron annihilation to hadrons, and the corresponding cross section to the muon–antimuon final state as a function of $\sqrt{s}$, the centre-of-mass energy.

Considering the number of quarks that can be created at particular centre-of-mass energy, what values of R would you expect for centre-of-mass energy in the range $2\,\text{GeV} < \sqrt{s} < 20$ GeV? How do your predictions match the data? How do these measurements support the existence of quark colour?

What is causing the sharp peaks in σ and R at centre-of-mass energy of ≈ 3 GeV, 10 GeV, and 100 GeV?

3.5. At the HERA collider 27 GeV positrons collided with 920 GeV protons. Why can these collisions can be considered to be due to positrons scattering off the quarks in the protons?

For these collisions draw **one** example of a Feynman diagram for **each** of the cases of weak charged-current, weak neutral-current and electromagnetic interaction.

Calculate the center-of-mass energy of the quark–positron system assuming that the 4-momentum of the quark P_q can be represented as a fixed fraction f of the proton 4-momentum P_p, in the approximation where both particles are massless.

What is the highest-mass particle that can be produced in such a collision in the approximation that a quark carries about $\frac{1}{3}$ of the proton momentum?

How does the propagator for the weak charged current and electromagnetic interactions vary with 4-momentum transfer P^2? Hence explain the fact that at low values of the momentum transfer it is found that the ratio of weak interactions to electromagnetic interactions is very small whereas at very high values it is found that the ratio is of the order of unity.

3.6. The J/Ψ has mass 3097 MeV, width 87 keV and equal branching ratios of 6% to $e^+ + e^-$ and $\mu^+ + \mu^-$ final states. What would you expect for these branching ratios if the J/Ψ decayed only electromagnetically? What does this tell you about the "strength" of the strong interaction in this decay? For comparison, the Ψ'' has mass 3770 MeV, width 24 MeV, but branching ratio to $e^+ + e^-$ of 10^{-5}.

Draw diagrams for the decays $D^0 \to K^- + \pi^+$ and $D^0 \to K^- + e^+ + \nu_e$. Disregarding the differences in the 2-body and 3-body density of states factors, what do you expect for the relative rates of these decays?

Optional questions

3.7. By conserving momentum at each vertex in the centre-of-mass frame (or otherwise) determine whether the propagator momentum is space-like ($\mathrm{P}^2 < m^2$) or time-like ($\mathrm{P}^2 > m^2$) for (i) $e^- + \mu^- \to e^- + \mu^-$ and for (ii) $e^+e^- \to \mu^+ + \mu^-$.

3.8. Draw Feynman diagrams showing a significant decay mode of each of the following particles:

a) π^0 meson
b) π^+ meson
c) μ^-
d) τ^- to a final state containing hadrons
e) K^0
f) top quark

9.4 Problems 4

Core questions

4.1. a) Draw Feynman diagrams for the the production of $W^{\pm}$ bosons being produced in a $p\bar{p}$ collider. If the W^+ boson is close to its Breit-Wigner peak, what possible decays may it have? (Which final states are kinematically accessible?)

b) What fraction of W^+ decays would you expect to produce positrons?

c) Suggest why the W was discovered in the leptonic rather than hadronic decay channels.

d) How could the outgoing (anti-)electron momentum be determined? How might the components of the neutrino momentum perpendicular to the beam be determined?

4.2. Write down Feynman diagrams for the decays of the muon and the tau lepton. Are hadronic decays possible? By considering the propagator factor in each case explain why one might expect on dimensional grounds that lifetimes should be in the ratio

$$\frac{\Gamma(\tau^- \to e^- + \nu + \bar{\nu})}{\Gamma(\mu^- \to e^- + \nu + \bar{\nu})} = \left(\frac{m_\tau}{m_\mu}\right)^5.$$

Using the following data

$$m_\tau = 1777.0\,\text{MeV} \qquad \tau_\tau = 2.91 \times 10^{-13}\,\text{s}$$
$$m_\mu = 105.66\,\text{MeV} \qquad \tau_\mu = 2.197 \times 10^{-6}\,\text{s}$$
$$BR(\tau^- \to e^- \nu + \bar{+}\nu) = 17.8\%$$

test this prediction.

4.3. Which of the Standard Model fermions couple to the Z^0 boson? To which final states may a Z^0 boson decay?

Explain why for the Z^0 the sum of the partial widths to the observed states (e^+e^-, $\mu^+\mu^-$, $\tau^+\tau^-$, hadrons) does not equal the FWHM of the Breit-Wigner.

By referring to the properties of the Breit-Wigner forumla, suggest how the LEP e^+e^- collider operating at centre-of-mass energies in the range $80\,\text{GeV}$ to $100\,\text{GeV}$ could have inferred that there are three neutrino species with $m_\nu < m_Z/2$, even though the detectors were unable to detect those neutrinos.

4.4. Consider a model with two neutrino mass eigenstates ν_2 and ν_3 with masses m_2 and m_3 and energies E_2 and E_3, mixed so that

$$|\nu_\mu\rangle = |\nu_2\rangle \cos\theta + |\nu_3\rangle \sin\theta$$
$$|\nu_\tau\rangle = -|\nu_2\rangle \sin\theta + |\nu_3\rangle \cos\theta.$$

Consider a beam of neutrinos created from from $\pi^- \to \mu^- \nu$ decays. Show that the observed flux of muon neutrinos observed at a distance L from such a source is

$$J(L) = J(L=0) \times \left[1 - \sin^2(2\theta) \sin^2 \left\{ \left(\frac{E_3 - E_2}{2\hbar} \right) \frac{L}{c} \right\} \right].$$

If m_2 and m_3 are much less than the neutrino momentum, $|\mathbf{p}|$, show that

$$|\nu_\mu(L)|^2 \approx |\nu_\mu(0)|^2 \times \left[1 - \sin^2(2\theta) \sin^2 \left\{ A \left(m_2^2 - m_3^2 \right) \frac{L}{|\mathbf{p}|} \right\} \right].$$

What is the first length L^* at which the ν_μ detection rate is at a minimum?

If a range of neutrino energies are present what will be the ratio of the rate (per neutrino) of $\nu + n \to \mu^- + p$ for $L \ll L^*$ and $L \gg L^*$.

What would be the corresponding ratio for neutral-current scattering?

Solar neutrinos emitted in p–p fusion have been detected via the processes

$$\begin{aligned} \nu_e + d &\to p + p + e^- \quad \text{and,} \\ \nu_x + d &\to p + n + \nu_x. \end{aligned}$$

Suggest why the charged-current reaction showed only a third of the neutrino flux of the neutral-current reaction.

4.5. Draw all leading Feynman diagrams for the following processes:

a) $\nu_\mu + n \to p + \mu^-$

b) $\nu_\mu + e^- \to \nu_\mu + e^-$

c) $\bar{\nu}_e + e^- \to \bar{\nu}_e + e^-$

d) $\bar{\nu}_e + p \to e^+ + n$

For d) the cross section takes the form

$$\sigma = \frac{2\pi}{\hbar} \frac{1}{c} G_F^2 \frac{4\pi}{(2\pi\hbar)^3} \frac{E_\nu^2}{c^3}$$

Justify this expression in terms of the Golden rule and the Fermi four-fermion theory.

Antineutrinos are incident on a stationary proton target. At what $\bar{\nu}_e$ energy would you expect the above formula to break down?

4.6. Write brief notes on:
a) The evidence that there are three and only three families of quarks and leptons.
b) The Cabibbo angle and quark mixing.
c) The evidence for confinement of quarks in hadrons.

4.7. How does helicity of a state change on application of the parity operator (which reverses the coordinate axes: $\mathbf{x} \overset{\mathbb{P}}{\mapsto} -\mathbf{x}$)?

If $|\Phi\rangle$ is an eigenstate of the parity operator, what can be said about the parity of the state $(1 + a\,\mathbf{S}\cdot\mathbf{p})|\Phi\rangle$?

$^{60}\mathrm{Co}$ nuclei ($J^P = 5^+$) are polarised by immersing them at low temperature in a magnetic field. When these nuclei β decay to $^{60}\mathrm{Ni}$ (4^+) more electrons are emitted opposite to the aligning B field than along it[1]. Explain carefully why this demonstrates parity violation in the weak interaction.

Justify the direction of the parity-violating effect.

4.8. Neutrino and anti-neutrino states have only ever been observed with the following eigenvalues of the helicity operator respectively:

$$\nu : -\tfrac{1}{2}\hbar \qquad \bar{\nu} : +\tfrac{1}{2}\hbar$$

What values of the projection operators

$$\mathcal{P}_{\pm} = \frac{1}{2}\left(1 \pm \boldsymbol{\sigma}\cdot\frac{\mathbf{p}}{|\mathbf{p}|}\right)$$

must be present in weak processes for (anti-)neutrinos reactions?

What is the implication for parity in the weak interaction?

4.9. Write down Feynman diagrams and for the processes $\pi^+ \to e^+\nu_e$ and $\pi^+ \to \mu^+\nu_\mu$. By considering the helicities of the final state particles, suggest why the π^+ ($J^P = 0^-$) decays dominantly to $\mu^+\nu_\mu$.

Optional questions

4.10. The Large Hadron Collider has been designed to accelerate counter-rotating beams of protons to energies of 7 TeV, and to collide those beams at a small number of interaction points.

a) Use dimensional analysis to estimate the smallest length scale which this machine could be used to resolve. How does this compare to the size of e.g. atoms, nuclei and protons?

b) The LHC beam pipe is evacuated to reduce loss of beam from collisions with gas moleceules. If less than 5% of the beam protons are to be lost from collisions with gas nuclei over a ten hour run, estimate the maximum permissible number density of H gas atoms in the beam pipe.

c) The machine collides counter-rotating bunches of protons, each bunch having circular cross section with radius 17 μm (in the direction perpendicular to travel). How many protons are required in a bunch to have an average of ten interactions per bunch crossing?

[1] Reported in [16].

d) If such bunches collide every $25\,\mathrm{ns}$, what is the *luminosity* of the machine? (Express your answer in units of $\mathrm{cm}^{-2}\,\mathrm{s}^{-1}$.)

e) If the cross section for producing a Higgs Boson is $50\,\mathrm{pb}$, how many will be made each second?

f) What is the kinetic energy of each bunch of protons in the LHC?

[Some data for proton-proton cross sections can be found in Figure 9.4.]

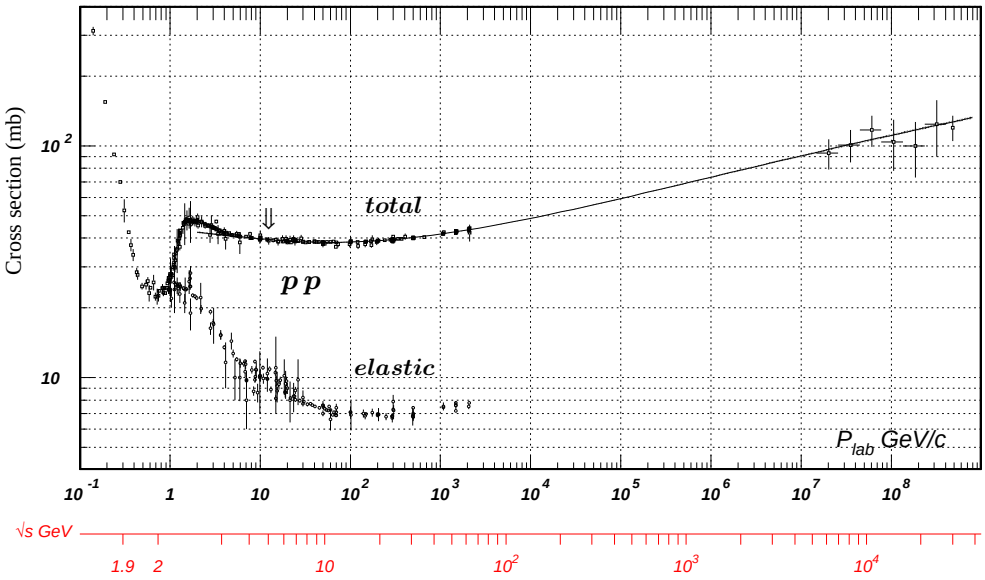

Figure 9.4: Proton–proton scattering cross section data as a function of laboratory momentum (upper scale) and of the centre-of-mass energy (lower scale). From [12].

9.5 Problems 5

Core questions

5.1. a) Why does $^{235}\mathrm{U}$ fission with thermal neutrons whereas $^{238}\mathrm{U}$ requires neutrons with energies of order MeV?

b) The fission of $^{235}\mathrm{U}$ by thermal neutrons is asymmetric, the most probable mass numbers of fission fragments being 93 and 140. Use the semi-empirical mass formula to estimate the energy released in fission of $^{235}_{92}\mathrm{U}$ and hence the mass of $^{235}_{92}\mathrm{U}$ consumed each second in a 1 GW reactor.

c) In almost all uranium ores, the proportion of $^{235}\mathrm{U}$ to $^{238}\mathrm{U}$ is 0.0072. However, in certain samples from Oklo in the Gabon the proportion is 0.0044. Assuming that a natural fission reactor operated in the Gabon 2×10^9 years ago, estimate the total energy released from 1 kg of the then naturally occurring uranium. How might the hypothesis that $^{235}\mathrm{U}$ was depleted by fission be tested?

[$t_{1/2}(^{238}\mathrm{U}) = 4.5 \times 10^9$ years, $t_{1/2}(^{235}\mathrm{U}) = 7.0 \times 10^8$ years.]

5.2. Write down the semi empirical mass formula. Which terms are responsible for the existence of a viable chain reaction of thermal-neutron-induced uranium fission? What distinguishes the isotopes of uranium that support such a reaction?

In the construction of a nuclear fission reactor an important role is often played by water, heavy water or graphite. Describe this role and explain why are these materials are suitable.

Why is the fissile material not completely mixed up with the moderator?

5.3. A neutron produced in a fission reaction is emitted with considerable energy. Discuss how the design of the reactor determines the competition between i) neutron absorption by sharp resonances; ii) neutron decay; iii) neutron energy transfer to the reactor media (and thence to turbines); iv) neutron absorption by resonances with high branching ratios to further fission. Most of these processes happen very fast indeed. How is it possible to control the reactor flux with a response time of seconds to minutes, or even longer?

5.4. a) Draw a diagram showing how the fusion process

$$p + p \rightarrow d + e^+ + \nu$$

is related to the Fermi theory of beta decay.

b) Find the approximate height $\mathcal{B}$ of the Coulomb barrier for pp fusion. To approximately what temperature would one need to heat hydrogen for pp fusion to overcome the Coulomb barrier?

c) If plasma at this temperature is to be magnetically confined what will be a typical Larmor radius (gyro-radius) for the duterium ions in the magnetic field?

d) Given the following reactions and energy release (in MeV)

$$\begin{aligned} d + d &\to {}^3\mathrm{He} + n \quad Q = 3.27, \\ d + d &\to t + p \quad\quad Q = 4.04, \\ d + t &\to {}^4\mathrm{He} + n \quad Q = 17.6, \end{aligned}$$

suggest *two* reasons why the artificial fusion reactors depend largely on the $d + t$ reaction.

e) Tritium has a half-life of about 12 years, and must be generated through reactions with both ${}^6\mathrm{Li}$ and ${}^7\mathrm{Li}$. Write down the form of these reactions, and explain why the ${}^7\mathrm{Li}$ reaction is helpful even though it is endothermic.

[d means ${}^2\mathrm{H}$ and t means ${}^3\mathrm{H}$. You may assume the magnetic field strength is 13.5 Tesla, which is what has been proposed for the ITER Tokamak.]

5.5. Show that for a star in a state of hydrostatic equilibrium (with pressure balancing gravity), the pressure gradient is given by

$$\frac{dP}{dr} = -\rho \frac{Gm}{r^2}$$

where m is the mass contained within the sphere of radius r. Hence show that the pressure at the center of a star satisfies

$$P_c = \int_0^M \frac{Gm\,dm}{4\pi r^4} > \int_0^M \frac{Gm\,dm}{4\pi R^4},$$

where R is the radius of the star.

Estimate the pressure and temperature at the the center of the sun.

5.6. The rate of thermonuclear fusion reactions is approximately proportional to

$$\exp\left(-\frac{2\pi Z_1 Z_2 \alpha c}{v}\right) \exp\left(-\frac{mv^2}{2kT}\right).$$

Sketch the form of this curve and explain the origin of these two terms.

Find the value of v at which the rate is maximal. At what temperature should one run a Tokamak?

5.7. a) Assuming that the energy for the sun's luminosity is provided by the conversion of $4H \to {}^4\mathrm{He}$, and that the neutrinos carry off only about 3 percent of the energy liberated how many neutrinos are liberated each second from the sun?

b) What neutrino flux would you expect to find at the Earth?

c) By what sequence of reactions do the above conversions dominantly proceed?

d) Why might the alternative rare process

$$p + e^- + p \rightarrow d + \nu_e$$

be of interest when studying solar neutrinos from the earth?

[$4M(^1\mathrm{H}) - M(^4\mathrm{He}) = 26.73\,\mathrm{MeV}$. The earth is on average about 1.50×10^{11} m from the sun, and is subject to a radiation flux of about $1.3\,\mathrm{kW\,m^{-2}}$.]

5.8. Give brief accounts of the methods of synthesis of:

a) $^{12}\mathrm{C}$

b) $^{28}\mathrm{Si}$

c) $^{56}\mathrm{Fe}$

d) $^{238}\mathrm{U}$

Optional questions

5.9. The two figures show properties of the 'valley of stability' of nuclei in the N-Z plane and the binding energy per nucleon versus mass number A, for nuclei with lifetimes greater than 10^8 years.

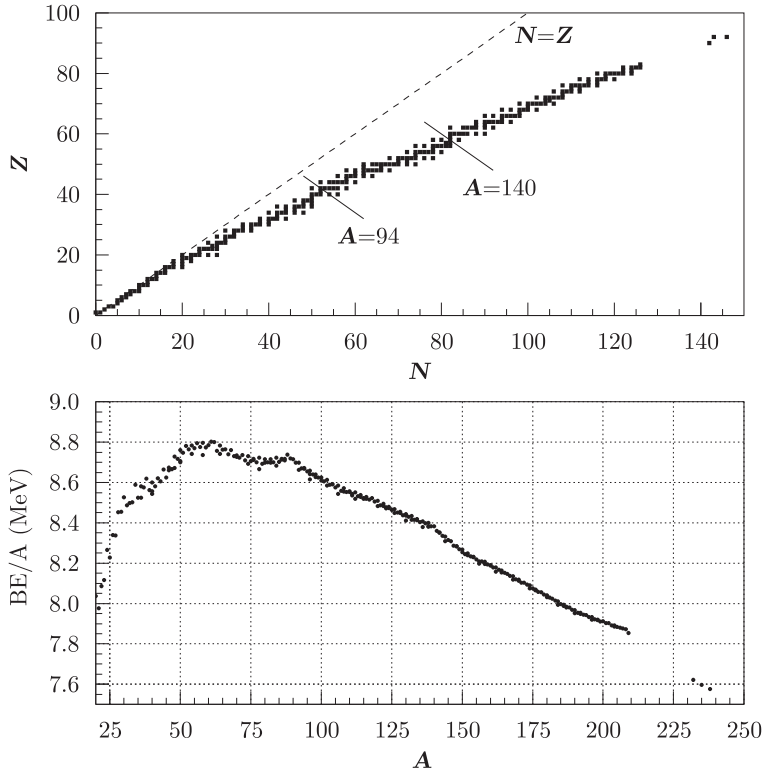

Using the data in the figures, estimate the energy released in the thermal-neutron induced fission of ^{235}U, given that the daughter nuclei tend to cluster asymmetrically around $A = 140$ and 94. Where are the daughter nuclei in relation to the valley of stability and what happens to them subsequently? Compare this with the $^{238}\mathrm{U}$ decay chain, which comprises eight α decays and six β decays to $^{206}\mathrm{Pb}$ with a total release of 48.6 MeV and a lifetime of $2 \times 10^{17}\,\mathrm{s}$.

There is a flow of heat from the Earth's interior amounting to a total of the order of $35\,\mathrm{TW}$. Much of this may be accounted for by decay of radioactive elements. Using the model above for a typical fission, estimate the rate of fissions needed to produce such a heat flow and the associated flux of neutrinos.

In a certain model of the Earth it is postulated that there is a self-sustaining fission reactor at the Earth's centre, fuelled by $^{235}\mathrm{U}$, contributing as much as $5\,\mathrm{TW}$ to the overall heat flow. If the 'geo-neutrino' flux could be measured, how might the 'core reactor' model be tested?

5.10. The CNO cycle proceeds in the following steps

			Q / MeV	rate	lifetime
$^{12}\mathrm{C} + p$	$\rightarrow$	$^{13}\mathrm{N} + \gamma$	1.944	r_{12}	
$^{13}\mathrm{N}$	$\rightarrow$	$^{13}\mathrm{C} + e^+ + \nu$	2.221		τ_N
$^{13}\mathrm{C} + p$	$\rightarrow$	$^{14}\mathrm{N} + \gamma$	7.550	r_{13}	
$^{14}\mathrm{N} + p$	$\rightarrow$	$^{15}\mathrm{O} + \gamma$	7.293	r_{14}	
$^{15}\mathrm{O}$	$\rightarrow$	$^{15}\mathrm{N} + e^+ + \nu$	2.761		τ_O
$^{15}\mathrm{N} + p$	$\rightarrow$	$^{12}\mathrm{C} + {}^4\mathrm{He}$	4.965	'fast'	

How much energy is released per cycle? Estimate the fraction of that energy in neutrinos.

The beta decay time constants are of the order of minutes. The shortest proton capture time is for $^{15}\mathrm{N}$ which is of the order of years, whereas the other capture timescales are significantly longer. Write the coupled linear differential equations of $(^{12}\mathrm{C}, {}^{13}\mathrm{C}, {}^{14}\mathrm{N})$ in the form

$$\frac{d}{dt}\mathbf{U} = \mathsf{M}\mathbf{U}$$

where M depends on the r_x but not the τ_x.

Show that this set of coupled differential equations admits a solution

$$\mathbf{U}(t) = \sum_{i=1,3} a_i e^{\lambda_i t}\mathbf{u}_i$$

with

$$\lambda_1 = 0 \quad \lambda_{2,3} = \frac{1}{2}(-\Sigma \pm \Delta)$$

and find Σ and Δ. Why must the elements of $\mathbf{u_{2,3}}$ sum to zero?

Express the relative equilibrium abundances of $^{12}\mathrm{C}$, $^{13}\mathrm{C}$ and $^{14}\mathrm{N}$ in terms of the r_x, and show that the equilibrium fractions of the beta decaying isotopes satisfy equations of the form

$$B = \tau_B r_A A.$$

Syllabus

Prerequisites You should make sure you are familiar with relativistic notation including four-vectors, and the Dirac formulation of quantum mechanics, including the Fermi Golden Rule.

Concept of a scattering cross section §2.4.1, Quantum mechanical scattering §4.1; The Born approximation §4.1.2. Feynman rules in quantum mechanics §5, Yukawa potential §4.3, propagator, virtual particle exchange §5.2.4. Resonance scattering, Breit-Wigner; decay widths §2.4.2. Fermi's golden rule §2.B.1. Use of invariants in relativistic particle decay and formation §5.

Elastic and inelastic scattering §2.3; form factors §2.4.3. Structure of the nucleus: nuclear mass & binding energies §2.2; stability, radioactivity §2.2.1, α §2.3.1 and β decay §2.3.2; measurement of radioactivity with semiconductor detectors §8.C.1; Fermi theory §2.3.2, the (A, Z) plane §2.2.1.

Energy production through fission (nuclear reactors) §7.1, fusion ($p - p$ and $D - T$) in the Sun and Tokamaks §7.2. The $p-p$ & CNO cycles §7.3. Solar neutrinos §7.3,§6.5. Stellar structure §7.3; formation of heavier elements §7.3.4.

Quark model of hadrons §3: the light meson §3.3.2 and baryon §3.3.1 multiplets; nucleons as bound states of quarks; §3.1 quarkonium §3.6; the ratio of cross-sections ($e^+ + e^-$ to hadrons) to ($e^+ + e^-$ to muons) §6.3.2; phenomenology of deep inelastic scattering §6.3.1.

The Standard Model: quark and lepton families §6.1, fundamental interactions and flavour mixing §6.3,§6.4. The strong interaction and qualitative discussion of confinement §3.4,§6.3. Weak interaction §6.4; decay of the neutron §6.4 and parity violation §6.4.3. Production, experimental detection, and decay of the W and Z bosons §6.4.2; the width of the Z and the number of neutrino types §6.4.2; neutrino oscillation §6.5.

Bibliography

[1] G. Aad et al. The ATLAS Experiment at the CERN Large Hadron Collider. *JINST*, 3:S08003, 2008.

[2] A. Abdesselam et al. The barrel modules of the ATLAS semiconductor tracker. *Nucl. Instrum. Meth.*, A568:642–671, 2006.

[3] Carl D. Anderson. The positive electron. *Phys. Rev.*, 43(6):491–494, Mar 1933.

[4] Tatsumi et al Aoyama. Tenth-Order QED Contribution to the Electron $g - 2$ and an Improved Value of the Fine Structure Constant. *Phys.Rev.Lett.*, 109:111807, 2012.

[5] G. Audi, A. H. Wapstra, and C. Thibault. The 2003 atomic mass evaluation: (ii). tables, graphs and references. *Nuclear Physics A*, 729(1):337 – 676, 2003. The 2003 NUBASE and Atomic Mass Evaluations.

[6] V. E. Barnes et al. Observation of a hyperon with strangeness minus three. *Phys. Rev. Lett.*, 12:204–206, Feb 1964.

[7] Jr. Davis, Raymond et al. Search for neutrinos from the sun. *Phys.Rev.Lett.*, 20:1205–1209, 1968.

[8] H. Geiger and E. Marsden. On a diffuse reflection of the α-particles. *Proceedings of the Royal Society of London. Series A*, 82(557):495–500, 1909.

[9] A. E. Glassgold. Nuclear density distributions from proton scattering. *Rev. Mod. Phys.*, 30(2):419–423, Apr 1958.

[10] D. et al Hanneke. New Measurement of the Electron Magnetic Moment and the Fine Structure Constant. *Phys.Rev.Lett.*, 100:120801, 2008.

[11] T. D. Lee and C. N. Yang. Question of parity conservation in weak interactions. *Phys. Rev.*, 104:254–258, Oct 1956.

[12] PDG. Review of particle physics. *Phys. Lett.*, B667:1, 2008.

[13] SNO. Direct evidence for neutrino flavor transformation from neutral current interactions in the Sudbury Neutrino Observatory. *Phys.Rev.Lett.*, 89:011301, 2002.

[14] M. Takeda et al. Extension of the cosmic-ray energy spectrum beyond the predicted Greisen-Zatsepin-Kuz'min cutoff. *Phys. Rev. Lett.*, 81(6):1163–1166, Aug 1998.

[15] Roger D. Woods and David S. Saxon. Diffuse surface optical model for nucleon-nuclei scattering. *Phys. Rev.*, 95(2):577–578, Jul 1954.

[16] C. S. Wu et al. Experimental test of parity conservation in beta decay. *Phys. Rev.*, 105:1413–1415, Feb 1957.